UNIVERSIDAD NACIONAL AUTÓNOMA DE MÉXICO

POSGRADO EN CIENCIA E INGENIERÍA DE MATERIALES

INSTITUTO DE CIENCIAS NUCLEARES

MODIFICATION OF POLY(VINYL CHLORIDE) URINARY CATHETERS WITH A SINGLE AND BINARY GRAFT OF ACRYLIC ACID AND POLY(ETHYLENE GLYCOL) METHACRYLATE TO PREVENT BACTERIAL ADHESION

T H E S I S

to obtain the degree of

DOCTOR of PHILOSOPHY in MATERIALS SCIENCE & ENGINEERING

b y

MsC. LUISA ERANDI ISLAS FLORES

THESIS DIRECTOR

Dr. Guillermina Burillo Amezcua

Instituto de Ciencias Nucleares, UNAM

THESIS COMMITTEE MEMBERS

Dr. Emilio Bucio Carrillo

Instituto de Ciencias Nucleares, UNAM

Dr. Humberto Vázquez Torres

Universidad Autónoma Metropolitana

México, D.F.   January, 2016

Thesis Jury

President - Dr. Rafael Herrera Nájera
Facultad de Química

First vocal - Dr. Guillermina Burillo Amezcua
Instituto de Ciencias Nucleares

Second vocal - Dr. Alberto Ruiz Treviño
Universidad Iberoamericana

Third vocal - Dr. Ernesto Rivera García
Instituto de Investigaciones en Materiales

Secretary - Dr. Alejandra Ortega Aramburu
Instituto de Ciencias Nucleares

Abstract

In this work, poly(vinyl chloride) urinary catheters were modified with a single and binary graft of acrylic acid and/or poly(ethylene glycol) methacrylate in order to prevent the growth and adhesion of bacteria to their surface, as well as to give them lubrication. The polymer graft was carried out using the pre-irradiation method, in the presence of oxygen, with a ^{60}Co γ-ray source. The grafting percentages obtained fell within 5-158% using doses of 5-60 kGy and aqueous (v/v) solutions of 10, 30, 50% AAc and 16% PEGMA. For the binary graft, the presence of either AAc or PEGMA on the catheter resulted in better grafting yields of the second compound. The catheters were characterized by IR and x-ray photoelectron spectroscopy, thermogravimetric analysis, water contact angle, scanning electron microscopy, mechanical analysis, and cytocompatibility tests. The modified catheters were able to swell in water and an artificial urine medium, with those that were grafted with AAc having the highest swelling percentages as well as showing a swelling response to changes in pH. In addition, AAc grafted catheters loaded higher quantities of ciprofloxacin and also sustained-released the drug for up to 6 h. All of the drug-loaded catheters were effective at preventing bacterial-growth after a first challenge against *Escherichi coli* and *Staphylococcus aureus*, while only PVC-*g*-AAc and PVC-*g*-PEGMA catheters were effective at preventing surface bacterial adhesion.

Resumen

En este trabajo se modificaron catéteres urinarios de poli(cloruro de vinilo) con un injerto individual y binario de ácido acrílico y/o poli(etilenglicol) metacrílato para verificar si era posible prevenir el crecimiento y la fijación de bacterias en su superficie, así como darles lubricación. El injerto se realizó con el método de pre-irradiación oxidativa a través de una fuente de rayos-γ de ^{60}Co. Los porcentajes de injerto obtenidos se encontraron en el rango de 5-158% cuando se uso una dosis de 5-60 kGy y concentraciones acuosas (v/v) de 10, 30, 50% de AAc y 16% de PEGMA. En cuanto al injerto binario, la presencia de AAc o PEGMA en el catéter produjo un mejor rendimiento de injerto del segundo compuesto. Las características de los catéteres se obtuvieron por espectroscopía de IR y fotoelectrónica de rayos-x, análisis termogravimétrico, ángulo de contacto, microscopía electrónica de barrido, análisis mecánico y citocompatibilidad. Los catéteres modificados fueron capaces de hincharse en agua y en un medio de orina artificial, donde se encontró que aquellos que contenían AAc mostraron los mejores porcentajes de hinchamiento, así como una respuesta de hinchamiento a cambios en el pH. Además, los catéteres con AAc mantuvieron mayores cantidades de ciprofloxacina y también pudieron ceder el fármaco de una forma controlada durante 6 h. Todos los catéteres cargados con fármaco pudieron prevenir el crecimiento bacteriano después de una primera prueba contra *Escherichia coli* y *Staphylococcus aureus*, mientras que sólo los sistemas de PVC-*g*-AAc y PVC-*g*-PEGMA fueron eficaces en la prevención de la fijación bacteriana en su superficie.

Acknowledgments

To my family

Thank you Rita, Alfredo, and Tamagos for being my second family.

Thank you **dad** for teaching me to be proud of my work, and for sacrificing a lot of things so that I could have a better and greater future. Thank you **mom** for being one of the strongest persons I have ever known. You were able to pick me up from all my stumbles and carry me without a scratch. You taught me to multiply, divide, and even about force, mass, and acceleration. Lastly, I want to thank my **sister** for keeping me with my feet on the ground and constantly reminding me of my weirdness.

"The important thing is not to stop questioning,
curiosity has its own reason for existing"

Albert Einstein

Contents

List of Tables

List of Figures

Chapter 1

Introduction

The role of materials science in the medical field, working alongside engineering and biology, has been insurmountable. The development of the first artificial heart, contact lenses, sutures, catheters, artificial tendons and ligaments, among others, has been brought about by the innovation of new materials such as polymers, composites, metals, and ceramics (Ratner *et al.,* 2012; Temenoff & Mikos, 2008). These materials, specifically designed to interact with biological systems to treat, evaluate, augment, or replace any tissue, organ, or function in the body are classified as biomaterials (Williams, 1999). Biomaterials, aside from meeting their intended purpose, must not trigger an adverse biological response, or in other words, they must be biocompatible.

Currently, one of the main problems with biomaterials is their susceptibility towards the development of biofilms, which can lead to serious infections in patients. In the United States, one of the leading causes of healthcare associated infections (HAIs) are urinary tract infections (Chenoweth *et al.,* 2014). Healthcare associated tract infections (HAUTIs) begin with the development of a biofilm on the surface of the catheter. Once the biofilm is present, it can travel to other parts of its surroundings and reach the bladder, causing further implications for the patients, which in severe cases, can mean death. Furthermore, the treatment of catheter-related urinary tract infections (CAUTIs) is not simple and it translates to higher costs for the healthcare system and the patient.

One approach to prevent CAUTIs is to impede the initial attachment of bacteria on the urological device, which can be managed by modifying its surface properties or by allowing it to release biocides. There are several methods to carry out the surface modification of a material, one of them is polymer grafting, which is an attractive choice because the new polymer, with its desired properties, is permanently attached to the surface of the device. One simple method to graft polymers is by using ionizing radiation, particularly gamma-radiation, where active sites suitable for grafting are created when homolytic breaks happen in the polymer backbone. Within this approach, polymers can be grafted to the surface of the material, endowing it with properties such as an inherent ability to prevent the adhesion of macromolecules. In addition, there are smart polymers that

can react to changes in their environment (e.g. changes in temperature or pH), allowing for a specific design of the biomaterial, such as giving it the ability to retain and release biocides, depending upon its specific purpose.

Overall goal

The overall goal of this work is to modify poly(vinyl chloride) (PVC) urinary catheters to improve upon their biocompatibility, which entails two specific goals: (1) preventing bacteria from adhering to the surface of the catheter, and (2) to give the catheter lubrication.

Hypothesis

The hypothesis of this thesis is that the PVC catheters grafted with acrylic acid (AAc) and poly(ethylene glycol) methacrylate (PEGMA) will be able to prevent the attachment of bacteria to their surface, which is the first step towards the development of a biofilm. These two compounds were chosen because PEG and its derivatives are considered highly biocompatible polymers that are known to prevent the adhesion of macromolecules to their surface; and because AAc is a smart polymer that can deprotonate at high pH values and allow the release of pre-loaded biocides. Furthermore, both polymers are hydrophilic and are thus expected to give lubrication to the device.

Specific goals

The specific goals of this work are to study the grafting conditions (e.g. reaction time, monomer concentration, irradiation dose) of the single and binary graft of PEGMA and AAc onto PVC through the use of ionizing gamma irradiation; to characterize the material through various methods including thermal analysis, equilibrium swelling time, critical pH, water contact angle, IR-spectroscopy, x-ray photoelectron spectroscopy, scanning electron spectroscopy, and cell viability studies; to study the load (in water) and release (in artificial urine) of ciprofloxacin, which is an antibiotic typically used to treat UTIs, onto and from the catheter, respectively; to study whether the modified drug-loaded catheters are able to inhibit the growth and attachment of bacteria (*E. coli* and *S. aureus*); and lastly, to measure the catheters' lubrication.

Chapter 2

Literature: modification of urinary catheters

The modification of urinary catheters to prevent bacterial colonization has been studied for some years. One of the most popular methods to make anti-bacterial catheters, which was adapted early on and has been implemented in some hospitals, is to coat the catheter with silver particles. Silver has been investigated to be a good antiseptic towards a variety of bacteria and fungi, with a minimum risk of these organisms developing a silver-resistance (Chopra, 2007); and the use of silver-containing catheters has been studied and proven to reduce the incidence of CAUTIs (Rupp *et al.,* 2004; Davenport & Keelye, 2005). However, knowing that CAUTIs remain one of the top HAIs, the efficacy of silver has been called into question.

Some clinical trials have shown that the use of silver-coated catheters does not prevent the presence of catheter-use associated bacteria in the patient's urine, with the concentration of some bacteria increasing for patients that used silver-coated catheters (Riley *et al.,* 1995), while other studies have shown that bacteria adhesion on silver containing catheters was only minimally diminished as compared to non-silver containing catheters (Desai *et al.,* 2010). Furthermore, although some make the argument that the reduction of CAUTIs overweights the cost of using silver-containing catheters, with a cost difference of \$4.86/device in the United States (Rupp *et al.,* 2004), a more recent study has found that the minimal reduction-risk of these catheters does not compensate for the higher costs (Kilonzo *et al.,* 2014). Other commercially available catheters include those coated with drugs, particularly Nitrofurazone. There have been studies that suggest Nitrofurazone is better at preventing CAUTIs than silver-containing catheters (Soshami-Regev *et al.,* 2011; Johnson *et al.,* 2010), and that catheters containing Nitrofurazone are cost-effective (Kilonzo *et al.,* 2014); however, these catheters have not been widely used and they are mainly recommended for short-term use only (Kilonzo *et al.,* 2014; Johnson *et al.,* 2010).

On the research side, catheters have been modified with antibiotic hydrogel coatings (DiTizio *et al.,* 1998) with relative success at inhibiting bacterial growth (up to 7 days). One problem with this approach is that the hydrogel coating is only done on the outer surface of the device, while it has been established that bacterial colonization of catheters can happen on their inner and outer surface. More recently, some of the works that could be potential candidates for long-term catheterisation include latex catheters that were first coated with heparin so that the Sparfloxacin antibiotic could then be covalently and non-covalently attached to the catheter; these catheters were able to inhibit the growth of bacteria (*S. aureus* and *E. coli*) for up to 30 days *in vitro* (Kowalczuk *et al.,* 2010). Nonetheless, the coating of these catheters was also only done on the outer surface of the device.

Another promising approach is to coat the catheter with polyurethane acrylate and give it the ability to control-release salicylic acid (Nowatzki *et al.,* 2012), which is a known biofilm inhibitor. These catheters were able to prevent the growth of biofilms *in vitro* and could release the salicylic acid for prolonged periods of time (more than 28 days). Unlike the previous studies, the catheters were coated on the inner surface as well.

Along the continuance of coatings, in another work silicon catheters were coated with dopamine so that in a second step the researchers would be able to immobilize a synthetic antimicrobial peptide (CWR11). The peptide modified catheters were able to retain their antimicrobial potency for up to 21 days, even after exposing the catheter to different environments (Lim *et al.,* 2015). Differently from coating, silicone catheters were modified by swelling them in an antimicrobial solution that contained rifampicin, triclosan, and sparfloxacin so that upon drying, they would be impregnated with the drugs; after 30 days, the catheters had only eluded about 30% of the drugs, also making them suitable for long-term catheterisation (Fisher *et al.,* 2015).

Overall, most of the works presented focused on coating the catheters, either by directly coating them with antibiotics, or by first coating them with compounds that had the right functional groups to later immobilize the active antimicrobial component. One of the potential problems with the coating approach is that it is not a permanent attachment, and further tests would have to be done in order to see how well the catheters will withstand their regular use. In addition, the works only tackled the problem from one approach, whether it was preventing bacteria colonization through contact-killing or biocide leaching. In this work, by grafting the catheters with PEGMA and AAc they will be endowed with a dual ability to prevent bacteria colonization by giving them the ability to load and control-release biocides, and by making them inherently able to prevent bacteria from attaching to their surface.

Chapter 3

Background

3.1 Catheter related urinary tract infections

The modern design for urinary catheters - the latex Foley catheter - was first introduced by Dr. Frederick Foley in 1937 (Kimono *et al.,* 2001; Stickler & Feneley, 2013). Nowadays, the use of urinary catheters has been thoroughly implemented in hospitals (with about 100 million users worldwide at a given time) where they are used for different purposes, which include: monitoring the urinary output, facilitating urinary drainage, and to bypass obstructive processes in the urethra, prostate, or bladder. The catheterisation times are divided into short, medium, and long term catheterisation. For example, patients who have undergone routine surgery typically use a catheter between 1-7 days; critical care patients whose urine output needs to be measured will be catheterised between 7-30 days; the longest catheterisation times are for patients that have acute or chronic urinary retention, with catheterisation times that can surpass 30 days. There is a variety of materials that are utilized for the fabrication of catheters, such as latex, rubber, silicone, poly(vinyl chloride), and polytetrafluoroethylene. Aside from the different designs that have emerged for the catheters (e.g. three-way Foley, Robinson, Coudé etc.), the urinary catheter has not changed much since its introduction (Stickler & Feneley, 2013; Tenke *et al.,* 2008; Dehn & Asprey, 2013).

In the United States, around 20% of patients use a urinary catheter while they are in a hospital, which is an alarming figure noting that as early as the 1950s, clinicians were warned that the decision to use catheters should be done knowing that it involves the risk of producing serious diseases that are difficult to treat (Stickler & Feneley, 2013). One of the main concerns regarding urinary catheters is that their use weakens the natural defense mechanism of the bladder, which prevents bacteria from reaching it by flushing the bacteria through the lower urinary tract through its filling and emptying cycle. Once a patient has been exposed to outside bacteria, which can come from the local pathogens already present in the patient's own skin's bacterial flora, the bacteria can

quickly gain access to the bladder, where urine serves as a good replenishable growth medium, and lead to the development of a urinary tract infection (UTI). Once the bacteria is in the bladder, it quickly multiplies and can reach populations of 10^7 cfu/ml (Stickler & Feneley, 2013).

Due to their wide use, it is not surprising that presently about 70% of UTIs are caused by the use of a urinary catheter; this statistic increases to 90% for patients in intensive care units. Overall, catheter-associated urinary tract infections (CAUTIs) account for 40% of all healthcare related infections (Saint & Chenoweth, 2013). The risk of developing a CAUTI increases with longer catheterisation times: while around 10-25% of short-term catheterisation patients develop a UTI, long-term catheterisation patients will inevitably acquire an infection (Stickler & Feneley, 2013). Although most CAUTIs manifest themselves mostly through fever and pain localized in the infected area, and some can even be asymptomatic, they can also cause severe problems for the patients. For example, in rare instances when the infection reaches the bloodstream, the mortality rate of the patient is of 32.8% (Chenoweth & Saint, 2013). Furthermore, CAUTIs are also a costly burden for the healthcare system, in the United States about $3 to $4 billion dollars are spent annually to treat them. Because CAUTIs are difficulty to treat and they are often recurrent, it had been suspected that *biofilms* formed on the surface of catheters; however, this was not officially established until 1985 after a Foley catheter, that had been removed from a woman who suffered from recurring CAUTIs, was studied using electron microscopy (Nickel *et al.,* 1985).

3.1.1 Biofilms

A bacterial biofilm is defined as a community of microorganisms (bacteria, fungi, or algae) that are irreversibly attached to the surface of a material, this latter one can be abiotic or live tissue. In the particular case of urinary catheters, this bacterial attachment can occur on the inner and outer surface of the catheter. There are four key steps that lead to the development and maturation of a biofilm (Fig. 3.1). First, when bacteria comes into contact with the catheter, it *reversibly* attaches to the surface of the device. This initial attachment is governed by the physiochemical properties of the biomaterial and the bacterial cell surface (e.g. flagella, motility, protein ligands). Once it has attached, the bacteria go through a change in their gene and protein expressions that favours the *irreversible attachment* to the surface. Afterwards, the bacteria proliferates, forming aggregates until communal clusters develop. When the clusters are formed, the bacteria are able to communicate with each other, through the secretion of chemical signals, and influence their growth. The next step in the biofilm development is the production of an extracellular polymeric substance (EPS), which is a polymer matrix made up of proteins and polysaccharides, that can encapsulate the bacteria clusters and thus provide structural integrity. After some time, the biofilm develops into a three-

dimensional structure. Once the biofilm has matured, parts of it can detach and form a new biofilm in the surroundings, thus spreading the infection (Brooks *et al.,* 2013; Soto, 2014; Stoodley *et al.,* 2004).

(a)   **(b)**   **(c)**   **(d)**
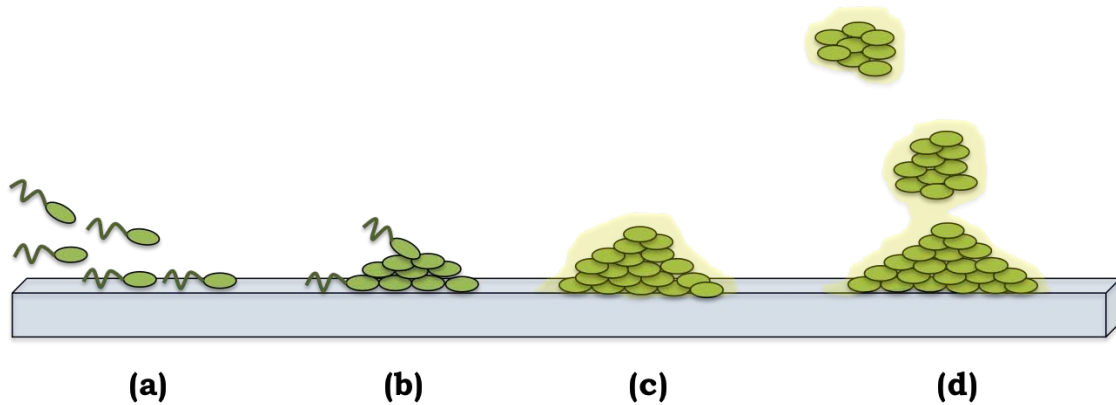
Figure 3.1: The four key stages towards the development of a biofilm are: a) bacteria reversibly adhere to the surface; b) irreversible adherence of bacteria to the surface with proliferation and the formation of communal clumps; c) the biofilm is established and an extracellular polymer matrix (EPS) is produced; d) the biofilm matures and travels to its surroundings.

Biofilms can be composed of one single organism or diverse bacteria. For urinary catheters, the principal bacteria species associated with CAUTIs are *Escherichia coli*, *Proteus mirabilis*, *Klebsiella pneumoniae*, *Pseudomonas aeruginosa*, *Staphylococcus epidermis*, *Enterococcus faecalis*, and *Staphylococcus aureus* (Cadieux & Carriveaue, 2009). Furthermore, in long-term catheterisation, blockage of the catheter tends to occur due to the presence of some bacteria, principally *Proteus mirabilis*, which produces an excess of urease, an enzyme that catalyses the hydrolysis of urea in the urine and increases the pH (Mobley & Warren, 1987). An increase in the urinary system's pH results in the precipitation of minerals such as strivite and carbonate-apatite, which aside from causing catheter encrustation, can also lead to the formation of renal calculi (Griffith *et al.,* 2014). Overall, in order to improve upon the design of the urinary catheter, the prevention of the formation of a biofilm on its surface must be addressed.

Bacteria in a biofilm can become more virulent, with most organisms in a biofilm's phenotype exhibiting more than 1,000 times greater minimum inhibitory concentrations (MIC) than their non-biofilm counterpart strains (Brooks *et al.,* 2013). This resistance to antibiotics has been explained because of the slow diffusion and penetration of antibiotics into the biofilm's polymer matrix. Furthermore, the low metabolic activity, due to the biofilm's oxygen-poor environment, and the physiological changes that the biofilm's bacteria undergo, allow for the biofilm to survive any antibiotic treatment. In addition to antibiotic-mediated killing, the biofilms are also resistant to physicochemical treatments such as UV-light, heavy metals, acidity, changes in hydration or salinity, and phagocytosis (Brooks *et al.,* 2013; Lebeax *et al.,* 2014). Therefore, the typical treatment for any

biomaterial associated infection (BAI) is to remove the infected device and then to treat the patient with parenteral antibiotic therapy, which can result in a longer hospital stay and it exposes the patient to the risk of recurrence (Brooks *et al.,* 2013). Overall, in order to improve upon the original design of the urinary catheter, it is necessary to prevent the formation of a biofilm on its surface.

3.1.2 Biofilm prevention

There are several approaches in the literature aimed at preventing the growth of a biofilm, which include: the inhibition of bacterial adhesion to the surface of the bio-material; using molecules (e.g. FimH bacteria lectin inhibitors) that are known to stop bacteria from developing adhesins; and other strategies that target specific process when a biofilm has already formed, such as stoping the biofilm from reaching maturation through the use of quorum-sensing quenchers, which disrupt the ability of bacteria to communicate with each other, and degrading the biofilm's EPS through the use of compounds such as DNaseI or Dispersin B (Beloin *et al.,* 2014). Nonetheless, because the first step in the development of a biofilm is the initial attachment of bacteria to the material's surface, it is strategically crucial to modify urinary catheters to prevent this attachment. The factors that affect this initial interaction are diverse, making its prevention a difficult goal to achieve; however, in the literature there are three main approaches towards preventing bacterial adhesion from happening: 1) endowing the material with the ability to resist bacterial adhesion (antibiofouling), 2) giving the material the ability to *contact-kill* any bacteria that come into contact with its surface, and 3) loading the material with biocides that will later leach and diffuse, causing the death of any nearby bacterium and preventing it from reaching its surface (Lichter *et al.,* 2009; Danese, 2002). All of these approaches could be implemented on a material through its surface modification.

3.2 Biomaterial surface modification

The surface properties of a material will determine the interaction between the material and the surrounding tissue. Because at the surface/surroundings interface there is an increased surface tension, one way materials lower this surface tension is through the adsorption of atoms or other molecules, which in the case of biomaterials it means ions, water, proteins, and other macromolecules (sometimes classified as a conditioning film). Overall, there are four main driving forces identified as having an effect on the surface adsorption of proteins and other macromolecules: the hydrophobic nature of the material, the surface charge of the material, its surface roughness, and steric hindrance. There are different approaches to modify the surface of a material, either through chemical, biological, or physical methods.

The physical surface modification methods usually revolve around surface patterning, where well defined regions are created on the surface by using methods such as micro-contact printing and microfluidics, among others. These regions could sometimes have different properties than the substrate, allowing the surface to be multi-functional (Temenoff & Mikos, 2008). Nonetheless, although for example, nano and micro-structured surfaces have been proven to decrease the degree of bacterial adhesion due to the lower surface area available for bacteria to initiate the adhesion process (Seddiki *et al.,* 2014), there have also been instances when the opposite has happened (Mitik-Dineva *et al.,* 2008), or even when the surface roughness does not impact bacterial adhesion at all (Hilbert *et al.,* 2003). Overall, although it is accepted the the surface roughness of a material at the micro and nano-scale plays a critical role in the attachment of bacteria to the surface, there are many factors such as the type and size of bacteria, the orientation of the cells with respect to to the patterned indentations, and even the type of material, that influence the way bacteria respond to the modified patterned surface (Hsu *et al.,* 2013). In order to to fully understand and exploit the influence of surface roughness on bacterial adhesion, there remains further research to be done.

The biological surface modification is slightly more complicated because active molecules have to be attached to the surface. These molecules (which include enzymes, lipids, DNA probes, peptides, bacteriophages etc.) are then free to interact with the specified organisms (Glinel *et al.,* 2012). However, whereas it is often the case with antibiotics that only small quantities are needed to have an effect on bacteria, sometimes larger quantities of the bioactive compound have to be utilized (Goddard & Hotchkiss, 2007). Furthermore, there have to be other considerations and factors that must be taken into account. For example, in the case of bacteriophages, one of the challenges is to find a good way to immobilize the phages and also to understand how they will interact in the presence of proteins and other bodily fluids (Hosseinidoust *et al.,* 2014). Nonetheless, because most biomaterials do not have the functional groups needed to immobilize the bioactive components, the first step needed is the the functionalization of the material's surface, which is achieved through chemical paths.

The surface chemical modification centers around covalent and non-covalent coatings, which are implemented through the use of plasma discharge, chemical and physical vapor deposition, sputtering, polymer grafting, self-assembled monolayers, solution coatings, Langmuir-Blodgett films, and surface modifying additives (Temenoff & Mikos, 2008). Specifically, chemical surface modification is done so that antimicrobial agents can be attached to the surface of the catheter (antibiotics or bioactive components); or to attach other materials, usually polymers, that can change the surface properties of the material to make it harder for bacteria to adhere (Danese, 2002). This latter one is more complicated because although in the literature there are several studies that propose different surface properties that could affect the first step in the adhesion process (such

as the charge, hydrophobicity, ability to hydrogen bond, and even mechanical stiffness of the material among others), there remains a lack of a good understanding of the principal characteristics that govern the adhesion process, with some works contradicting the findings of others (Lichter *et al.,* 2009).

The following figure (Fig. 3.2) summarizes the different approaches to prevent bacterial colonization, which is the first step towards biofilm formation, and the different methods of surface modification that have been used to meet those goals.

Attaching bioactive compounds or biocides to the surface of the material

Loading the material with biocides (whether it be through swelling or other methods) so that they can later be released. A controlled-release could be accomplished if the material is given the right functional groups.

Contact killing

Strategies to prevent bacterial colonization

Resist bacterial adhesion

Biocide leaching

Changing the surface properties of the material (e.g. hydrophobicity, roughness, steric hindrance) through physical methods or covalent/non-covalent coatings.

Figure 3.2: Strategies to prevent bacterial colonization (Lichter *et al.,* 2009) and the different methods of surface modification to accomplish them.

To accomplish the overall goal of this project, we propose the covalent surface modification, through polymer grafting, of PVC urinary catheters with materials that will allow it to prevent bacterial adhesion on two fronts: (1) attaching a polymer with the inherent ability to repel the colonization of bacteria, and (2) to give the catheter the ability to load and release biocides. Polymer grafting is an attractive method because the polymers are permanently anchored to the surface of the material, avoiding problems such as leaching or the disintegration of the coating due to interactions with living tissue or simple wear.

3.2.1 Smart and biocompatible polymers

Polymers are an alluring choice for surface modification because of their flexible synthesis methods, their ability to be made into different morphologies, and the biodegradability that some of them exhibit. However, one of the disadvantages of using any synthetic material is that it is less predictable to determine whether it will prompt a toxic or inflammatory biological response by the host (Bank & Brown, 2014). Therefore, any modification to the surface of a biomaterial must not compromise its biocompatibility. The term *biocompatibility* is defined as the material's ability to perform its function with an appropriate host response in a specific application; however, there is no precise measurement of this parameter (Ratner *et al.*, 2012). Generally to ensure biocompatibility, biomaterials are evaluated to determine if they will cause adverse effects (blood clotting, bacterial colonization, complicated healing, carcinogenic effects, etc.) whether it be through direct contact or through the leaching of chemicals (Ratner *et al.*, 2012).

One group of polymers that has been proven to be highly biocompatible is poly(ethylene glycol) (PEG) and its derivatives (Fig. 3.3). PEG is a nontoxic, immunogenic, non-antigenic polymer that does not harm active proteins or cells when it comes into contact with them, it can attach to surfaces without affecting their chemistry too much, and it is soluble in water and most organic solvents (Alcantar *et al.*, 2000). Furthermore, and the reason why PEG has been singled out in this work, plenty of literature has demonstrated that PEG has the ability to prevent proteins and other biomolecules from reaching the surface of a material. This inherent ability is explained by PEG's conformation in aqueous solutions, where it exposes its uncharged hydrophilic groups to increase the surface mobility. When a protein or other biomolecule approaches a PEG coated surface, the PEG chains experience a loss of conformational freedom and a repulsive force is created. In addition, there is also the compression and interpenetration of the protein in the PEG chains, leading to an osmotic repulsive force between the surface and the protein. Because PEG can serve as a shield, it has often been used to coat drugs, implants, and other medical instruments (Alcantar *et al.*, 2000).
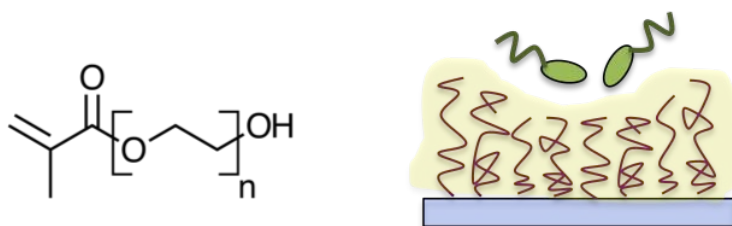
Figure 3.3: Structure of poly(ethylene glycol) methacrylate (left side), one of PEG's derivatives. PEG and its derivates are said to have a "stealth" behaviour (right side) because they can prevent the adhesion of macromolecules to the surface of a material.

In addition to polymers that inherently prevent the adhesions of proteins and other

biomolecules, there has also been thorough research regarding a group of polymers that are stimuli-responsive to very small changes in their environment, these polymers are termed "smart" or "intelligent" polymers. One interesting aspect of smart polymers is that their stimuli-response is reversed when the environmental stimuli is removed. Some of the stimuli-responses of smart polymers include changes in their shape, surface characteristics, solubility, and sol-gel transition, among others (Kumar *et al.,* 2007). The trigger for these responses varies for each polymer, but most often it involves changes in the environment's pH and temperature, although other factors could also have an effect as resumed in Table 3.1. These smart polymers have been widely used in the area of medicine and biology for purposes such as specific drug delivery, improving cell culture surfaces, and to run diagnostics (Kumar *et al.,* 2007; Honey *et al.,* 2014; Hoffman, 2013).

Table 3.1: Different environmental stimuli of smart polymers

Environmental stimuli	
Physical	*Chemical*
Temperature	pH
Ionic force	Specific ions
Solvents	Chemical agents
Radiation (UV, visible)	
High pressures	
Magnetic fields	

In the specific case of pH-responsive polymers, or polyelectrolytes, the process is governed by the protonation and deprotonation of their ionisable functional groups. The pH-responsive polymers typically used for biomedical applications tend to have weak acids and bases allowing for the protonation/deprotonation process to occur in the 4-8 pH range, making them ideal to use in the human body. The transition point for the protonation and deprotonation process is known as the pKa. When the pH of the environment approaches the pKa of the pendant functional group the degree of ionization will change quickly. Some of the most common pH-responsive polymer groups are carboxylic acids, whose pKa is often found in the 4-5 range (Kuckling *et al.,* 2012). When the pH of the environment is below the pKa value of the carboxylic acid group, the functional group is protonated and uncharged. As the pH increases and reaches the pKa value, the carboxylic acid group will deprotonate and go through a conformational change where, due to an ionic repulsion of the charged groups, there will be greater spaces in between the polymer chains (Fig. 3.4). The process is the same but reversed for weak bases like ammonia (Ortega-Reyes, 2014).
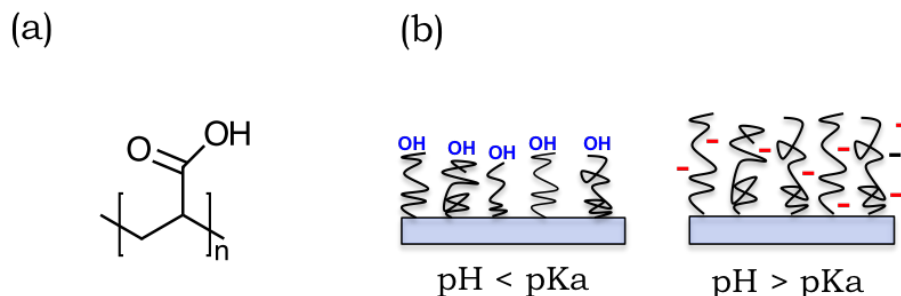
Figure 3.4: (a) Structure of poly(acrylic acid), a well known polyelectrolyte; (b) polymers with carboxylic acid groups can deprotonate when the pH of the environment is greater than the pKa.

3.2.2 Polymer grafting

Polymer grafting provides a means to incorporate new properties into a bulk material. The difference between grafted polymers and simple block-copolymers is that the graft copolymer is the covalent attachment of a polymer or monomer (type A), to a polymer backbone of a different chemical nature (type B), where the final copolymer structure resembles a comb. Customarily, polymer grafting follows one key initial step, which is the creation of active sites in the polymer backbone. These active sites can be present in the bulk polymer surface, a method known as *grafting-from*, or be a part of the polymer chains that will be grafted, which is the *grafting-to* method (Fig. 3.5). Although this latter method, *grafting-to*, can provide a better control of the chain structure that will be grafted, it is often not employed because it involves more complicated procedures that will be harder to implement in industrial processes (Kato *et al.*, 2003). Another disadvantage of the *grafting-to* methods is that it does not yield high grafting densities due to the steric repulsion between the grafted chains. The opposite is observed for the *grafting-from* method, where because the graft happens *in situ*, higher grafting densities are obtained (Yu *et al.*, 2015).
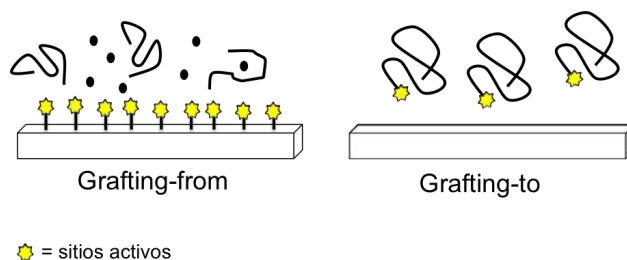
Figure 3.5: *grafting-from* and *grafting-to* methods.

There are different means by which the active sites for *grafting-from* can be created. Chemically, the reactions usually involved are free-radical grafting involving reduction-oxidation reactions, grafting through living polymerization reactions such as atomic transfer radical polymerization (ATRP) or controlled radical polymerization, and ionic

grafting (Bhattacharya & Misra, 2004). One of the disadvantages of these chemical methods is that they require the use of various initiators and catalysts. A different method to *graft-from* materials makes use of high energies, such as ionizing radiation, that are able to produce homolytic breaks on the polymer backbone and thus create active sites suitable for grafting. This method of grafting is attractive because it circumvents the use of other chemicals, it can be done in different mediums and materials, and it can be done in the solid, liquid, or gaseous state. The energy sources for ionizing radiation are diverse and they include the use of plasma discharges, electron-beams, UV, and gamma radiation. In particular, the advantages of using gamma-radiation include a minimal rise in the temperature of the material while it is being irradiated, a high penetration depth, it is a precise and reproducible process, it is easy to regulate because only the dose must be controlled, and the materials can be used immediately after being irradiated (Drobny, 2013).

3.3   Gamma radiation

Ionizing radiation is on the high end of the electromagnetic spectrum and it encompasses electron beams, x-rays, and gamma radiation. In the particular case of gamma radiation, gamma-rays are emitted from excited atomic nucleus of unstable atoms through a process known as radioactive decay. The energies that gamma rays carry allow them to penetrate farther than alpha or beta particles, thus ionizing their path. When exposed to living cells, the energy of gamma rays can disrupt the DNA or other cellular structures, leading to death or serious diseases such as cancer. Gamma-rays are able to ionize materials because the photons that go through the material lose energy, a process known as attenuation, based on an interaction probability of unit length of travel, where the energy can be absorbed leading to the disappearance of the photon, or scattered with a change in the photon's direction of travel and an energy loss. Overall, there are three main interactions between the incident photon and the irradiated material that will contribute to the attenuation process: the photoelectric effect, Compton scattering, and pair production (Biggin, 1991).

The photoelectric effect happens when a photon loses all of its energy (E_o) to one of the inner electrons of the atom. This electron is then ejected with an energy (E_e) equal to the difference between the photon's energy and the electron's binding energy (E_s), as depicted in Equation 3.1.

$$E_o - E_s = E_e \tag{3.1}$$

The atom that remains, now an ion, seeks to regain stability through the release of energy, which is achieved by one of its outer electrons falling to the lower energy vacancy. This energy released can manifest as characteristic x-rays, or it can be used

to eject an outer shell electron, a process known as the Auger effect. The photoelectric effect is more typical for atoms with high atomic numbers and low energy photons, with the electric absorption varying from atom to atom as Z^3, where Z is the atomic number (Spinks & Woods, 1990).

Compton scattering (Fig. 3.6) occurs when the incident photon interacts with a free electron, or one from the outer shell of an atom, by giving it enough energy to be ejected from the atom, the photon then scatters as a new gamma-photon of lower energy and with a diminishing penetrating power. The amount of energy transferred to the electron by the photon is given by Equation 3.2, where $_e\sigma_s$ is the *Compton scattering coefficient*, which is the fraction of the energy that is retained by the photon after interacting with the electron, and $_e\sigma$ is the total *electronic Compton absorption coefficient*, which gives the fraction of the photons of energy E_o that will participate in the Compton process.

$$_e\sigma_a =_e \sigma -_e \sigma_s \qquad (3.2)$$

The Compton interactions are more predominant for photon energies between 1 - 5 MeV for high atomic number materials, with this energy range widening as the atomic number decreases.

The pair production is slightly more complicated and it occurs when an incident photon has greater energy than two electron rest mass energies (1.022 MeV), and is completely absorbed by an atomic nucleus (and sometimes an electron) which leads to the creation of an electron-positron pair with some kinetic energy. The end result of the pair production is annihilation radiation (0.51 MeV), brought about by the interaction between the electron and its antiparticle. Out of these three interactions, the Compton effect is the main energy absorption mechanism (Biggin, 1991). The energy absorption is measured in grays (Gy; 1 J/kg).
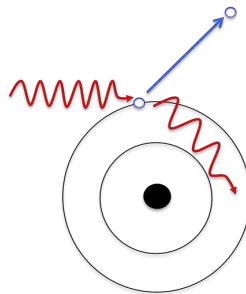
Figure 3.6: Compton effect

3.3.1 Sources and uses of gamma-radiation

Some of the most commonly used sources of gamma-rays are cobalt-60, cesium-137, and iridium-192. However, cobalt-60 (^{60}Co) is one of the most popular radiation sources

because it is easy to produce, and it is insoluble in water. The decay mechanism of ^{60}Co is the following: first, ^{60}Co decays into excited ^{60}Ni through beta decay, emitting an electron of 0.31 MeV; secondly, ^{60}Ni drops down to its ground state by emitting two gamma rays (1.17 and 1.33 MeV) which are responsible for the radiation processes of ^{60}Co in industries (Biggin, 1991) (Fig. 3.7). Because of its high energy, ionizing radiation is used in industries to sterilize healthcare instruments; to irradiate food to disinfect and control pests, among other things; and to modify materials through polymerization and cross-linking processes.
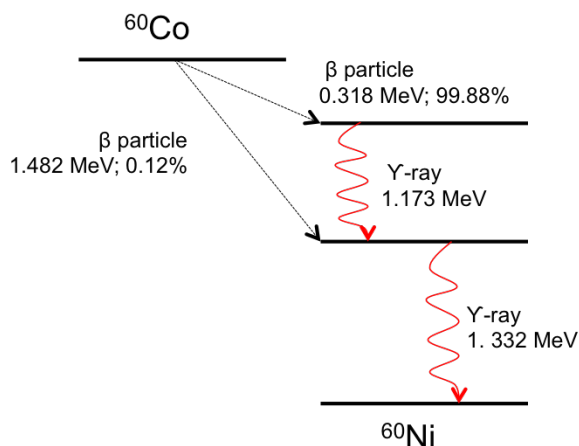
Figure 3.7: Decay mechanism of ^{60}Co.

3.3.2 Irradiation of polymers

When a polymer is first exposed to γ-rays, ionized and excited species are produced through the Compton effect, where the ejected electrons lose energy until reaching thermal energy equilibrium, and they can either recombine with cations that are created, or interact with polar groups in the molecule as a solvated species or an anion radical. The exited molecule can then create free radicals through the homolytic scission of the backbone polymer chain or dissociation of the bonds (e.g. C-H) (free radical reactions), or it can form two reactive ions (ion-molecule reaction) (Fig. 3.8). Out of these two possible process, the reaction of radicals is the preferable one, given that the ion-molecule processes have been found to occur less frequently in higher homologues of CH_4 (Chapiro, 1962).
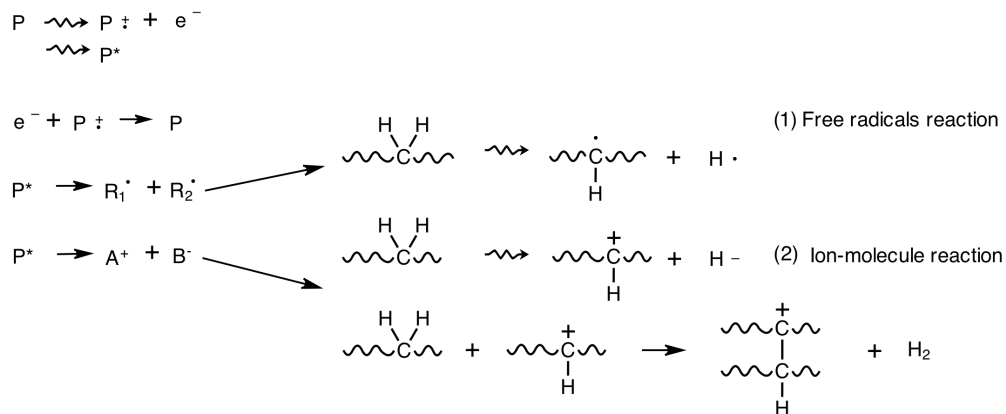
Figure 3.8: Radical formation in a polymer due to gamma-radiation

Depending on the type, a polymer can undergo cross-linking, where its chains join to create a 3D network; long-chain branching, where the polymer chains join together without forming a network; chain scission, where the polymer loses molecular weight most likely from a degradation process; polymerization, which occurs via free-radical polymerization; and grafting, which is a chemical reaction that happens when a new monomer/polymer attaches to the main chain of the backbone polymer. The radiation chemical-yield of radicals, known as the G-value, is used to predict whether a polymer will have a tendency to degrade or crosslink, and it is a measure of the number of molecules that that will be transformed per 100 eV of energy lost by the charged particle (photons) (Drobny, 2013).

Irradiation of PVC, PAAc, and PEGMA

The creation of radicals and the degradation of PVC due to gamma-radiation has been thoroughly studied (Costa *et al.,* 2004; Baccaro *et al.,* 2003; Miller, 1959). Upon exposure to radiation, PVC will tend towards crosslinking rather than chain scission, where the cleavage of an H or Cl atom from the backbone chain leads to the creation of three possible radicals (Fig.3.9):
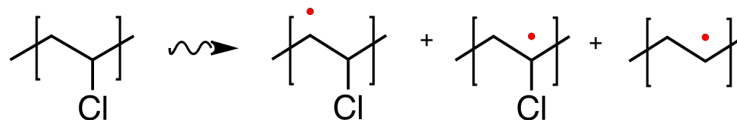
Figure 3.9: PVC radicals formed due to gamma-radiation.

However, because the bond dissociation energy of C-Cl is smaller than that required for C-H bonds, the cleavage of the C-Cl bond is preferred. The incision of a C-C bond can also happen; nevertheless, because PVC is a material more likely to crosslink than to degrade, if any C-C bonds break they are more inclined to recombine. Once the bond has

cleaved and the free radicals have been created, conjugated unsaturation could happen after heating the PVC, leading to a change in color to an orange and sometimes brown material.

In the case of poly(acrylic acid), the irradiation will most likely lead to the cleavage of C-H bonds, because the bond dissociation energy of the carboxylic group is much greater. The same is expected for the PEGMA chain, where the most likely cleavage will be that of the C-H bonds. This is not to say that other cleavages will not happen, but rather will be less frequent.

In the literature, there are studies where radiation grafting has been used to graft PEGMA onto chitosan nanoparticles to improve their hydrophilicity (Pasanphan *et al.,* 2014), onto cellulose films to make them less prone to thrombus formations (Nho & Kwon, 2003), and there is a study dealing with the radiation-graft kinetics of PEGMA onto PVC tubes (Arenas *et al.,* 2007). For acrylic acid, the number of studies where radiation has been used as the grafting method is higher, as well as the type of materials where it has been grafted, with some studies grafting AAc to increase the hydrophilicity of the materials (Fugaru *et al.,* 2012; Yang *et al.,* 2014), to take advantage of the intelligent-response of acrylic acid towards changes in pH (Ferraz *et al.,* 2014; Ortega *et al.,* 2015; Gupta *et al.,* 2008b; Ramirez-Fuentes *et al.,* 2007), to improve upon the bioactivity of the material (Hidzir *et al.,* 2012), and to bequeath the material with the ability to interact with metal ions (Gupta *et al.,* 2008a; Hien *et al.,* 2005; Benarmer *et al.,* 2011; Gonzales-Gomez *et al.,* 2014). The most recent literature review did not yield results of urinary catheters that had been modified through grafting of PEGMA or AAc.

3.3.3 Radiation grafting

There are two methods to initiate grafting via radiation: the direct and the indirect method. Depending upon the grafting system, one method is preferable to the other. For example, when grafting monomers that have a high radiation radical chemical yield (G_r) value, meaning they are sensitive towards radiation, in comparison to the substrate, it is better to chose the indirect method of grafting because otherwise there would be a greater formation of homopolymer than of grafted chains.

The direct method

In this method the substrate, polymer-A, is irradiated in the presence of the monomer-B (in a vacuum). One of the challenges that arise with this method is that monomer-B is also being irradiated and thus homopolymer-B can form. Nonetheless, there are methods to avoid the formation of homopolymer-B such as including ferrous salts in the process. Some of the parameters that can be controlled with this method include the irradiation dosis, the monomer concentration, and the reaction medium.

The indirect method

Within the indirect method there are two ways through which the process can be carried out, either in a vacuum or in the presence of oxygen. When the indirect method is carried out in a vacuum, the substrate, polymer A, is irradiated on its own to form radicals within itself. Once the radicals have been formed, it is placed in contact with monomer B. However, this second reaction must happen quickly to avoid the radicals of polymer-A to react within themselves and inhibit the grafting of monomer-B.

When the substrate is irradiated in the presence of oxygen or air, thermally unstable peroxide and hydroperoxide groups are created, as depicted in Figure 3.10. The irradiated polymer-A is then placed in contact with monomer-B and heated in order to initiate grafting. The advantage of this method is that the peroxide and hydroperoxide groups have a relatively long shelf-life if properly stored (refrigerated), so grafting can be initiated at a later time. Furthermore, there are other parameters that can be easily controlled, in addition to the ones previously mentioned, such as reaction time and temperature.
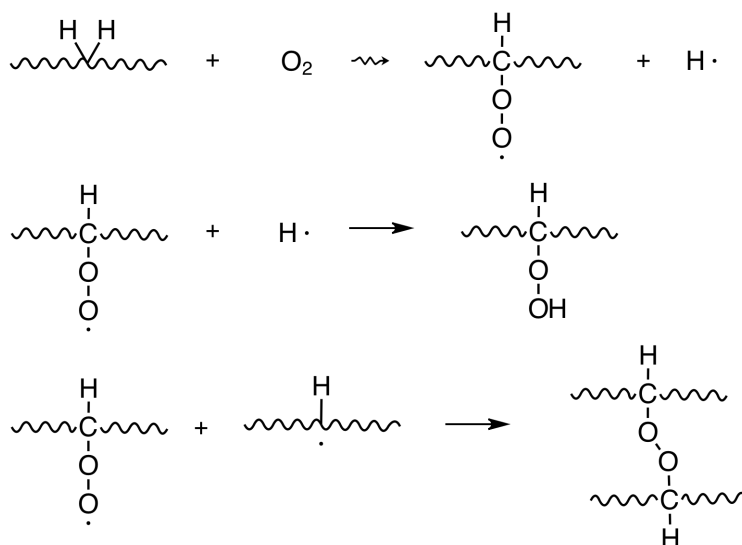
Figure 3.10: Formation of radicals formed after being irradiated in the presence of oxygen.

In this work, the graft will be carried out using the oxidative pre-irradiation method due to AAc's susceptibility towards homopolymerization.

Chapter 4

Materials & Methods

4.1 Graft of AAc or PEGMA onto PVC catheters (PVC-*g*-AAc o PVC-*g*-PEGMA)

Materials

PVC urinary catheters (diameter 3 mm, thickness 0.5 mm; Bicakcilar, Turkey) were cut into 2 cm pieces and washed in methanol for 24 h, changing the medium after 3, 6, and 18 h. The catheter pieces were then dried in a vacuum desiccator at room temperature for 24 h and in a vacuum oven at 38 °C for 6 h. Acrylic acid (AAc) and poly(ethylene glycol) methacrylate (PEGMA, Mn 360) were from Sigma Aldrich (St. Louis, MO, USA) and distilled before using.

Method

Pieces of PVC catheters (2 cm) were placed inside an open glass-ampoule and irradiated with a ^{60}Co gamma-ray ionizing radiation source (GammaBeam 651 PT from Nordion Co., Canada). Then, an AAc (10, 30 or 50% v/v) or PEGMA (14% v/v) aqueous solution (5 mL) was added to the glass ampoules. The ampoules were bubbled with argon for 10 minutes and then sealed. In the particular case of AAc, the glass ampoule was placed in a water bath (5 °C) while it was being bubbled to prevent any hompolymerization. The sealed ampoules were placed in a hot water bath at a set temperature for time periods ranging from 1 - 5 h. After the grafting reaction, the catheters were washed with distilled water (minimum 48 h) to remove any non-grafted homopolymers and unreacted monomer. The catheters were then dried under vacuum at 38 °C. The grafting percentage was calculated using Eq. 4.1,

$$G(\%) = \frac{W_f - W_o}{W_o} \times 100 \qquad (4.1)$$

where W_f is the weight of the grafted catheter and W_o is the initial weight of the unmodified catheter.

Surface area change

The surface area (SA) of the catheters was calculated by measuring the length (ℓ) and diameter (d) of a 2 cm long piece of catheter before and after grafting, and multiplying those values togetheter. Thereafter, the surface area change was calculated using Eq. 4.2, where A and A_o are the initial and final surface area of the catheter, respectively.

$$SA(\%) = \frac{A - A_o}{A_o} \times 100 \qquad (4.2)$$

4.2 Graft of AAc onto PVC-*g*-PEGMA, and PEGMA onto PVC-*g*-AAc

For the binary graft, the aforementioned process was repeated by exposing the PVC-g-AAc and PVC-*g*-PEGMA modified catheters to gamma-radiation, followed by immersion into an aqueous PEGMA or AAc solution, respectively, bubbled with argon and then heated. The grafting percentage was calculated using Eq. 4.1, W_o being the weight of the formerly grafted PVC-*g*-AAc or PVC-*g*-PEGMA catheter. It is important to note that water was the only solvent used for the grafting process because it is known that plasticizers leach in the presence of other organic compounds (Zygoura *et al.,* 2011)

4.3 Equilibrium swelling time and critical pH

Materials

For the artificial urine medium the urea, creatinine, ammonium chloride, and sodium citrate were from Sigma Aldrich (Madrid, Spain); calcium chloride from Scharlau (Barcelona, Spain); potassium chloride, magnesium sulphate heptahydrate, and sodium chloride from Pareac (Barcelona, Spain); and sodium phosphate mono basic hydrate and sodium phosphate dibasic dehydrate were from Merck (Madrid, Spain). The agar technical was from Biolife (Milano, Italy).

Methods

Dried grafted catheters were immersed in distilled water at 18 °C for 15 min and then removed, gently padded with a paper towel, weighed and placed back in water. The process was repeated every 15 min up to an hour and then every 30 min, until a constant swelling weight was obtained. The percent swelling was calculated using Eq. 4.3,

$$S(\%) = \frac{W_s - W_d}{W_d} \times 100 \tag{4.3}$$

where W_d and W_o represent the weight of the dried and swollen catheter, respectively. The same protocol was used to measure the swelling in urine. The artificial urine (AU) was prepared by adapting two different AU formulas (Brooks & Keevil, 1996; Chutipongtanate & Thongboonkerd, 2010) as follows: 170 mM urea, 7 mM creatinina, 2 mM $Na_3C_6H_5O_7$, 90 mM NaCl, 2 mM $MgSO_4$, 2 mM $NaHCO_3$, 10 mM Na_2SO_4, 3.6 mM NaH_2PO_4, 0.4 mM Na_2HPO_4, 15 mM NH_4Cl y 2.5 mM CaCl dissolved in purified water (MilliQ, Millipore, Madrid, Spain). The pH was adjusted to 6 with a 0.1 M HCl solution.

The critical pH point was determined by placing the catheters in buffer solutions of a pH ranging from 2.5 to 12, for a period of 24 h at 20 °C. The buffer solutions were prepared by mixing a 0.2 M boric acid/0.05 M citric acid aqueous solution with a 0.1 M trisodium phosphate dodecahydrate aqueous solutions, at various proportions.

4.4 Lubricity

Materials

The lubricity of 6-cm long catheters (previously wetted for 30 s or swollen for 4 h in water) was measured using a texture analyzer (TA.XT plus, Stable Micro Systems, Surrey, UK).

Methods

Each catheter piece was screwed to a bolt fixed to a cylindrical aluminum probe (Ref. P/20) and lowered at 5 mm/s into agar (1% w/v in purified water) to a depth of 20 mm (Fig.5.28). The sample remained inside the agar for 120 s and then it was removed at 5 mm/s. The forces required to insert and to withdraw each catheter into/from agar were recorded. All the experiments were carried out in triplicate at 20 °C. The agar medium was prepared by dissolving 10 g of agar in 1 L of boiled water, which was maintained under mechanical stirring (300 rpm) at 60 °C for 60 min, and then poured in to 125 mL plastic containers. The agar was then stored for 48 h at 5 °C. The agar containers were removed from the fridge 2 h before the texture tests.
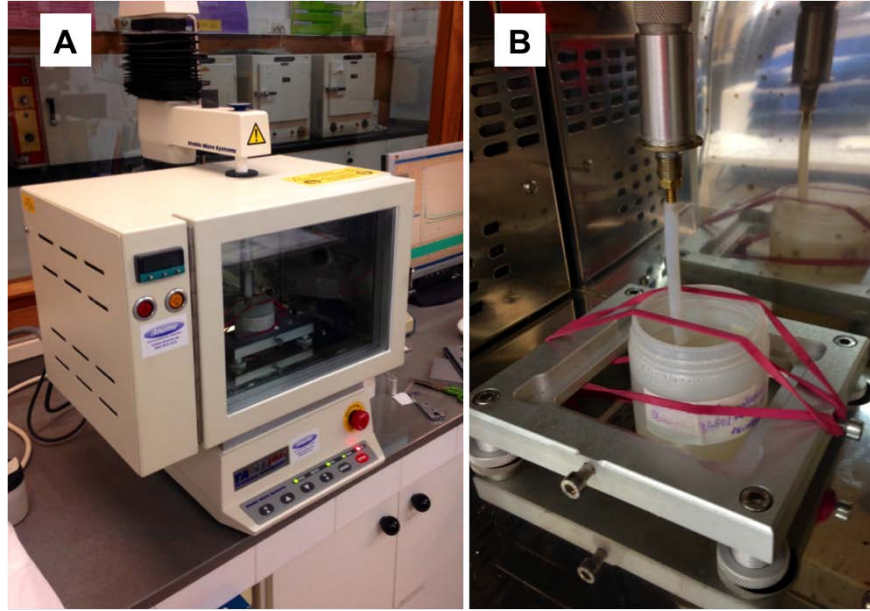
Figure 4.1: (A) Texture analyzer (TA.XT plus, Stable Micro Systems, Surrey, UK); (B) The catheter pieces were screwed to a bolt fixed to a cylindrical aluminum probe and lowered at a speed of 5 mm/s into agar as a way to simulate the force required to insert and remove the catheter from the urethra.

4.5 Cytocompatibility

Materials

For the cytocompatibility assays, the fetal bovine serum (FBS), Dulbecco's Modified Eagle Medium F12 Ham (DMEM F12 Ham) and the antibiotic solution (penicillin 10,000 units/mL and streptomycin 10.00 ug/mL) were from Invitrogen Corporation (Carlsbad, CA, USA).

Methods

The tests were conducted in vitro using BALB 3T3 mouse fibroblast clone A31 cells (ATCC(R) CCl-163(TM); Manassas, VA, USA). The catheters (3 x 1 mm rectangular strips) were previously washed for 48 h in 20 mL of a sterile phosphate buffer saline solution pH 7.4, then in purified water for 24 h, and finally dried for 30 h at 40 °C. Afterwards, the strips were UV irradiated for 2 min and left in 300 μL of culture medium (DMEM F12 Ham supplemented with 10% FBS and 1% of the antibiotic solution) at 37 °C for 24 h. 100 μL of the medium that had been in contact with the samples were poured onto 100 μL of a BALB/3T3 cell suspension (200,000 cells/mL) in DMEM F12 Ham, supplemented with 10% FBS and 1% of an antibiotic solution, then seeded in 96-well plates. The plates were incubated during 24 or 48 h (37 °C, 5% CO_2, 90% RH). Afterwards, the culture

medium was replaced with 100 μL of fresh medium, and 10 μL of the reagent 1 of the MTT kit were added. The cell viability estimation was calculated using Eq. 4.4,

$$Viability(\%) = \frac{A_m - A_b}{A_c - A_b} \times 100 \tag{4.4}$$

where A_m, A_b and A_c are the absorbances of the sample, blank, and negative control, respectively. The absorbances were measured at 550 nm with an ELISA plate reader (BIORAD Model 680 Microplane Reader, USA).

4.6   Ciprofloxacin loading

Pristine pieces and grafted catheters (1 cm long) were placed in 5 mL of a ciprofloxacin aqueous solution (0.012 mg/mL; protected from light), and the absorbance at 271 nm was monitored for 48 h. The amount of drug loaded was calculated from the difference between the initial and final concentrations of ciprofloxacin in the loading medium. The experiments were carried out in triplicate.

4.7   Ciprofloxacin release

Ciprofloxacin-loaded catheter pieces were taken out of the drug solution and gently padded with adsorbing paper to remove any excess solution. They were then placed in 5 mL of artificial urine at 37 °C under constant magnetic agitation and protected from light for 48 h. Samples of the release medium were taken at regular time intervals to measure the absorbance at 273 nm, and immediately returned to the corresponding vials.

4.8   Microbiological tests

Non-loaded and ciprofloxacin-loaded catheters were challenged against *Staphylococcus aureus* (ATCC 25923) and *Escherichia coli* (ATCC 11229), and inhibition zones and bacteria adhesion were recorded. For the inhibition growth tests, the sample piece (1 cm in length) was placed in a Petri dish containing Mueller-Hinton agar that had been seeded with either *Staphylococcus aureus* or *Escherichia coli*. The plates were kept at 37 °C for 24 h and then assessed for inhibition zones. The samples that displayed activity against the bacteria were then transferred to a new plate (with freshly seeded bacteria), and the process was repeated again for a third time if the samples continued to exhibit antimicrobial activity.

For the bacterial adhesion tests, 1-cm long catheter pieces were immersed in either water or a ciprofloxacin aqueous solution (0.012 mg/mL) and autoclaved for 20 min at

120 °C. The catheters were then left in their respective medium until tested (maximum for 5 ays). *Escherichia coli* was cultured in trypticase soy agar (TSA) at 37 °C for 24 h. The catheter pieces were then transferred to vials containing 2 mL of *Escherichia coli* solution in trypticase soy broth (TSB; 8 x 10^8 CFU/mL) and cultured with phosphate buffer (PBS) solution to remove any non-adhered bacteria, and then placed in 2 mL of a sterile PBS and sonicated with a Bronson Sonifier 250 for 5 min to suspend adhered bacteria. The suspensions were then spread on TSA plates, and the CFUs were measured after 24 h of incubation at 37 °C.

4.9   Physicochemical and mechanical characterization

A perking-Elmer Spectrum 100 spectrometer (Perking-Elmer Cetus Instruments, Norwalk, CT) was used to record the FTIR-ATR spectra of the pristine and modified catheters.

The thermal decomposition was evaluated in a TGA Q50 (TA Instruments, New Castle, DE, USA) under a nitrogen atmosphere for a temperature range between 35 and 800 °C.

A drop shape analyzer, DSA 100 (Kruss GmbH, Hamburg, Germany), was used to measure the surface water contact angle. The opened catheters were flattened by placing them in-between two clean glass slides (clamped) and dried in a vacuum oven for 8 h at 40 °C. The contact angle was measured immediately after the water droplet touched the surface of the catheter and 30 s later. All the measurements were repeated 3 times at different surface points.

The mechanical properties of the pristine and grafted catheters (flattened as previously described; 3 x 1 cm) were analyzed using a DMA Q800 (TA Instruments, New Castle, DE, USA) in air at 28 °C.

The surface roughness of the samples was analysed using an ambient scanning electron microscope (Zeiss EVOL515, Madrid, Spain) at magnifications of 100, 300, 500, and 1000x.

The XPS analyses were carried out using a RIBER LDM-32 spectrometer. The apparatus uses a vacuum generated by an ionic pump in the pressure range of 8^{-10} Torr, and a non-monochromatic Al Kα radiation source (hν 1486.6 eV). The elemental wide scan spectra were obtained using a pass energy of 3 eV and energy steps of 1 eV, with a time interval of 0.1 s. For each spectra 10 scans were run in the energy range of 0 to 1400 eV. For the high-resolution spectra the pass energy was lowered to 0.8 eV and the energy steps to 0.2 eV for C1s, Cl2p and O1s. There were 10 cycles per analysis and 10 scans per cycle. All binding energies (BE) were shifted to the aliphatic C1s peak at 285 eV to correct for the sample charging. The high-resolution and broad-scan data was processed and fitted using the CASAXPS software (Neal Fairley, UK), version 2.13.14dev38, using a linear-type background. The C1s spectra of the pristine and modified PVC catheter was de-convoluted using 70% Lorentian/30% Gaussian peak shapes.

Chapter 5

Results and Discussion

5.1 Modification of catheters through radiation grafting

5.1.1 Grafting AAc onto PVC

The proposed grafting mechanism is depicted in Fig. 5.1. Because the process is carried out in the presence of oxygen, the first step after the catheter is irradiated is the formation of peroxides and hydroperoxides as was previously shown in Fig. 3.10. When heat is applied, these thermally unstable peroxides break to form the radicals that will participate in the grafting process (2). In the case of the PVC-*g*-AAc graft, these radicals attack the alpha carbons of the AAc (3) and then propagate (4), making the PAAc chain grow until termination, which can happen either with other peroxide radicals, hydride anions, or through recombination with other PAAc chains (5).
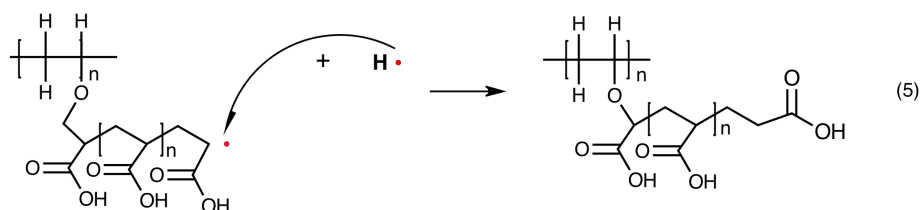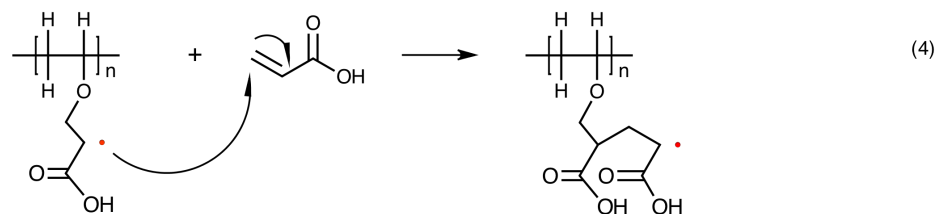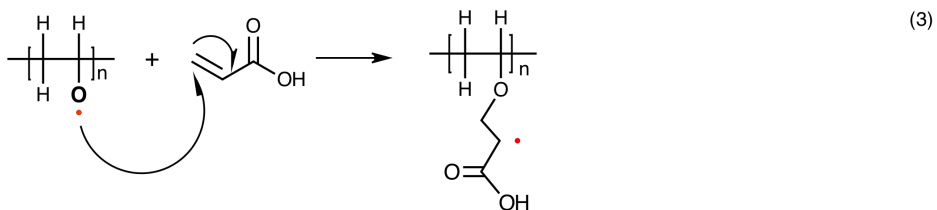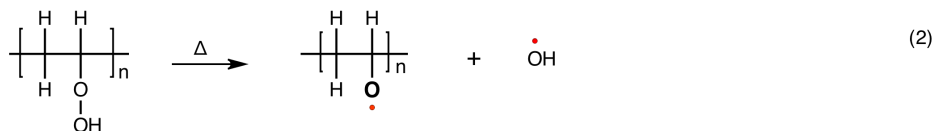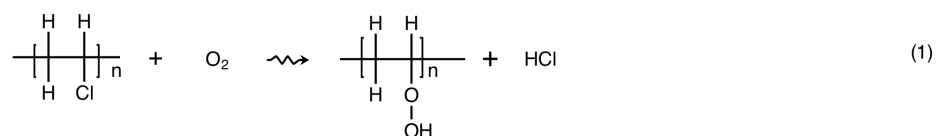
Figure 5.1: Proposed grafting scheme of AAc onto PVC.

As the radiation dose decreased, the grafting percentage of AAc upon PVC decreased due to a lower number of active sites created in the catheter (Fig. 5.2). With pre-irradiation doses of 10 and 15 kGy, more than 50% AAc was grafted in an hour for a 50% (v/v) aqueous monomer solution and a reaction temperature of 80 °C. After 4 h, 116 and 158% AAc had been grafted for 10 and 15 kGy, respectively. It is interesting to note that for 10 kGy, the curve seemed to reach an asymptote after 2 h, remaining within a 50% AAc grafting percentage; however, it spiked up to 116% after 4 h. This could possibly be explained by the fact that once the catheter has been grafted with AAc, it can swell in the aqueous reaction medium and thus allow for the AAc, and at this point PAAc chains, to diffuse within the polymer matrix; therefore, it is likely that both grafting mechanisms, *grafting-from* and *grafting-to*, are happening at the same time. Lowering the irradiation dose to 5 kGy, aside from the advantage of exposing the catheter to shorter irradiation times and thus reducing the risk of the material degrading, yielded

27

a linear array of grafting percentages ranging from 5 - 50% in the 1-4 h reaction times.
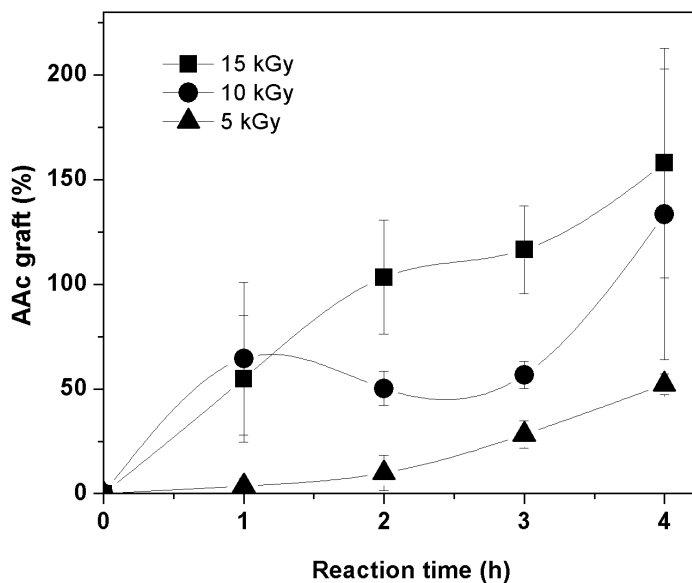
Figure 5.2: Graft of AA onto PVC as a function of reaction time for a 50% (v/v) aqueous AAc solution and a reaction temperature of 80 °C.

The grafting of AAc was not only achieved on the surface of the catheter, but in bulk, as quantified by the increase in the catheters' surface area (Fig. 5.3). As the grafting percentage increased, the catheters were visibly grown, the edges were deformed, and the material was hardened. Furthermore, AAc can rapidly polymerize, which makes it more difficult to control the grafting process even for the low irradiation doses of 15 and 10 kGy, as it is illustrated by the higher standard of deviations in Fig. 5.2. Due to the aforementioned reasons, further grafting studies were conducted with catheters that had grafting percentages lower than 30% AAc, as those catheters would still be able to serve their intended purpose, and using a 5 kGy dose.
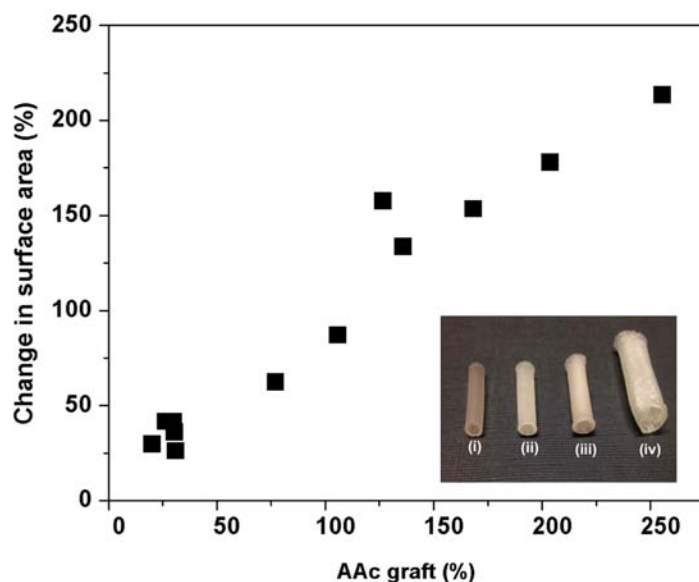
Figure 5.3: Surface area change (%) of PVC-*g*-AAc catheters as a function of AAc grafting percentage; the insert image shows catheters of (i) PVC, (ii) PVC-*g*-AAc(30%), (iii) PVC-*g*-AAc(55%), and (iv) PVC-*g*-AAc(250%).

5.1.2 Grafting of PEGMA onto PVC

Because there is an existing previous work that studies in detail the grafting conditions of PEGMA onto PVC tubes (Arenas *et al.,* 2007), for the purpose of this work we reproduced those results using a radiation dose of 60 kGy (Fig. 5.4), which was the dosis that yielded some of the highest PEGMA grafting percentages. After 25 h, the maximum PEGMA grafted was 25%, which is in agreement with the literature (Arenas *et al.,* 2007).
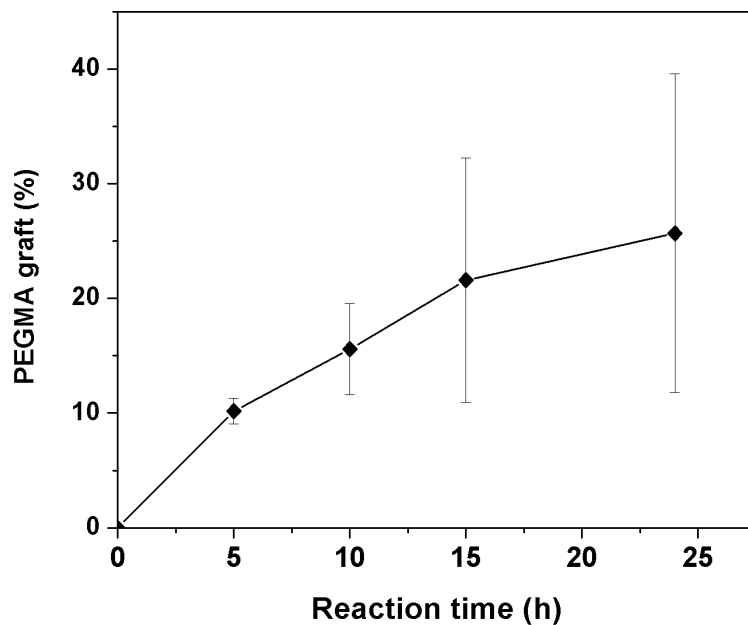
Figure 5.4: PEGMA grafted onto PVC as a function of reaction time for a 16% (v/v) aqueous PEGMA solution, 60 kGy dose, and T = 70 °C.

One important observation is that after heating, the catheter changes color to a light orange (Fig. 5.5), which is a sign that the material has begun to degrade (due to the loss of Cl) and conjugated bonds, as well as HCl, are forming in the polymer backbone. This change in color is typical of PVC and it begins to happen when the material is exposed to radiation doses of 25 kGy or higher (Sastri, 2010).

Figure 5.5: PVC-g-PEGMA(25%) catheter grafted using a16% (v/v) aqueous PEGMA solution, 60 kGy dose, and T = 70 °C.

The grafting scheme depicted in Fig. 5.6 picks up after the PVC was irradiated in the presence of oxygen and heated so that peroxide radicals have formed (Steps 1 and 2 in Fig. 5.1). The mechanism shows the initiation step where the radical on PVC attacks the PEGMA alpha carbon (1); the propagation step follows (2), and the process ends either through a termination with other radicals, as depicted with a hydrogen atom (3), or recombination. In the figure it is appreciated that PEGMA grafts in a "comb-like"

manner upon the PVC.
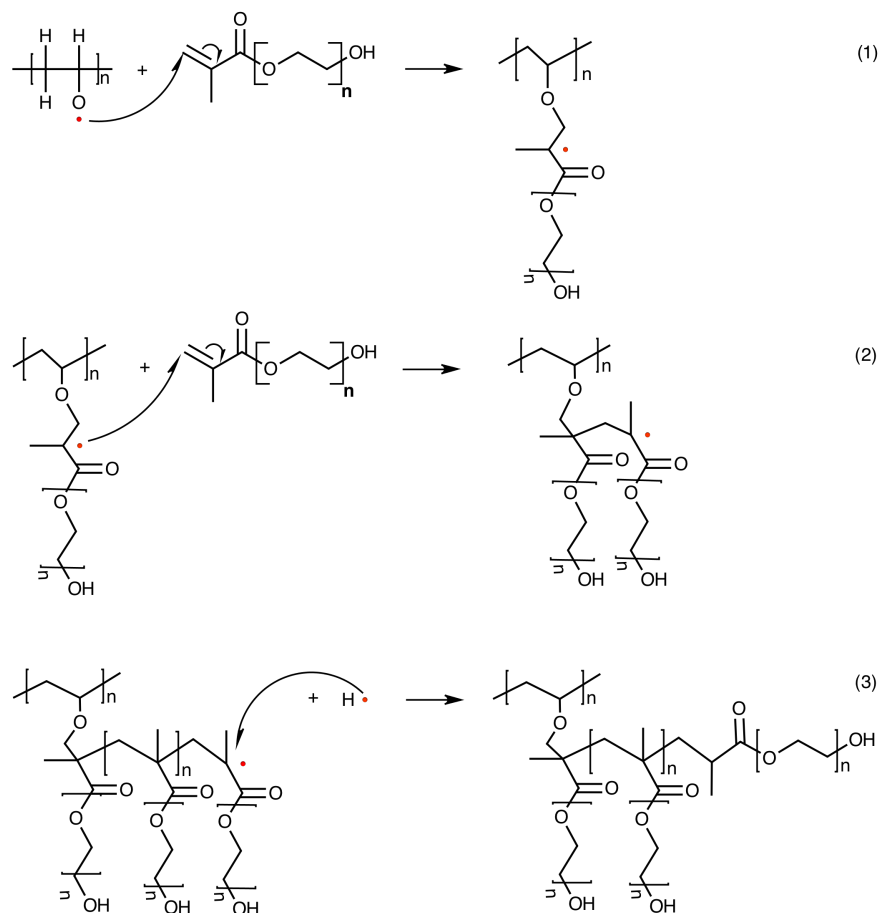
Figure 5.6: Proposed grafting scheme of PEGMA onto PVC

5.1.3   Grafting of PEGMA onto PVC-*g*-AAc

The grafting scheme of PEGMA onto PVC-*g*-AAc is depicted in Fig. 5.7. Because the radiation affects the entire catheter (the PVC backbone as well as the grafted AAc chain) it also probable that some PEGMA will graft upon the PVC backbone, although to a lesser extent. When the PAAc is irradiated, there are a couple of possibilities where grafting can be initiated: a radical will form in the alpha carbon or the beta carbon; however, the radical in the alpha carbon would be a tertiary radical and thus more stable than the secondary radical in the beta carbon. Again, when heat is added the peroxide/hydroperoxide radicals break and in the presence of PEGMA, grafting is initiated (1 and 2). The grafted chain propagates (3) until termination or recombination (4).
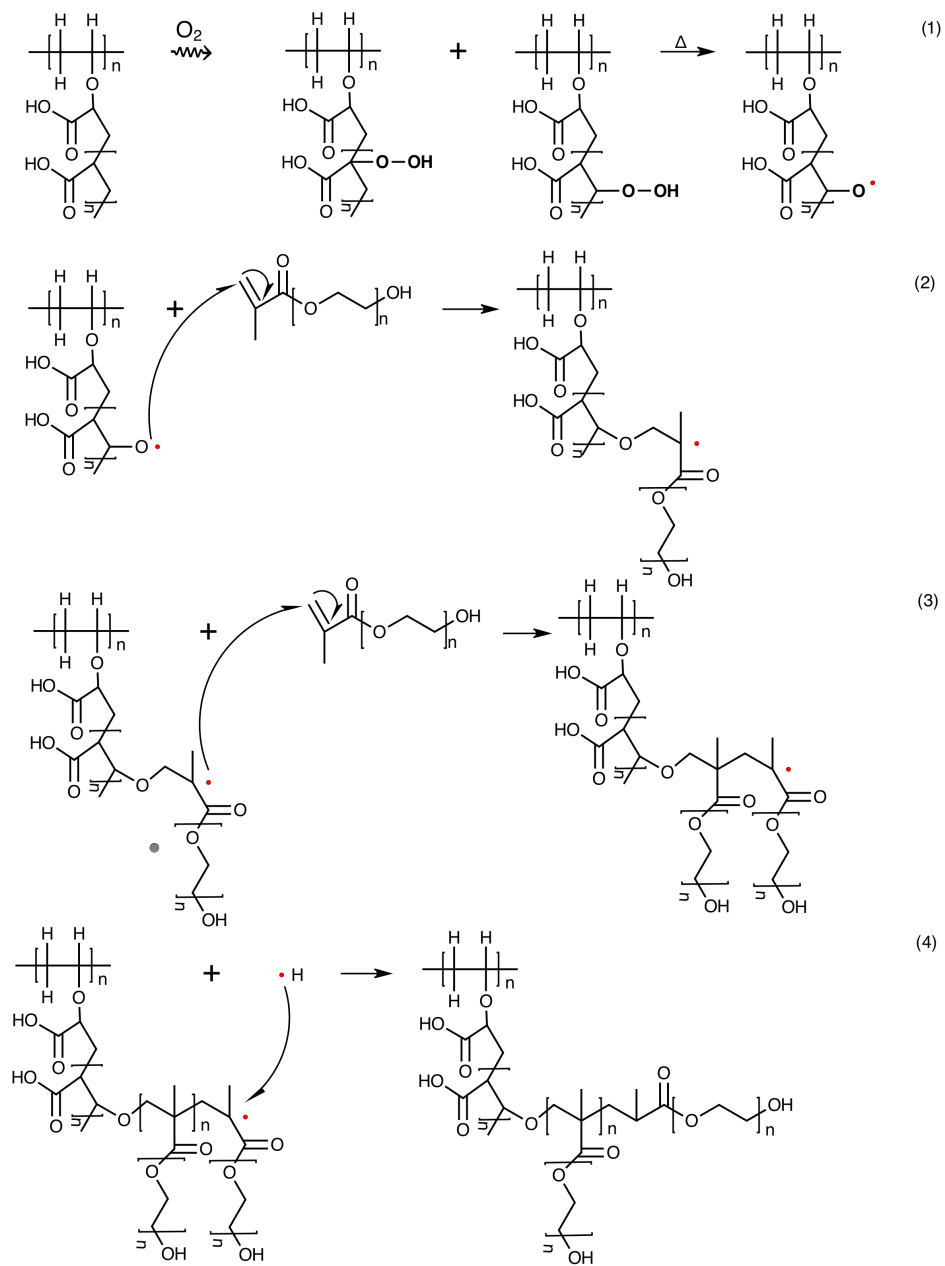
Figure 5.7: Proposed grafting scheme of PEGMA onto PVC-*g*-AAc

The presence of AAc on the catheter improved upon the amount of PEGMA that could be grafted (Fig. 5.8a). In 5 h, 44% PEGMA had been grafted onto PVC-*g*-AAc(27%), in comparison to 13% grafted onto PVC under the same conditions (60 kGy, T = 70 °C). The maximum amount of PEGMA grafted was 57%, which was obtained in a little more than 15 h for PVC-*g*-AAc(27%). This improvement upon the PEGMA grafting yield is explained by the sensitivity of AAc towards radiation (G_r value of 3.6) in comparison to PVC (G_r value of 1.7) (Perera & Hill, 1989). Furthermore, the structure of this block copolymer is expected to be a combed-comb graft (Fig. 5.8b).
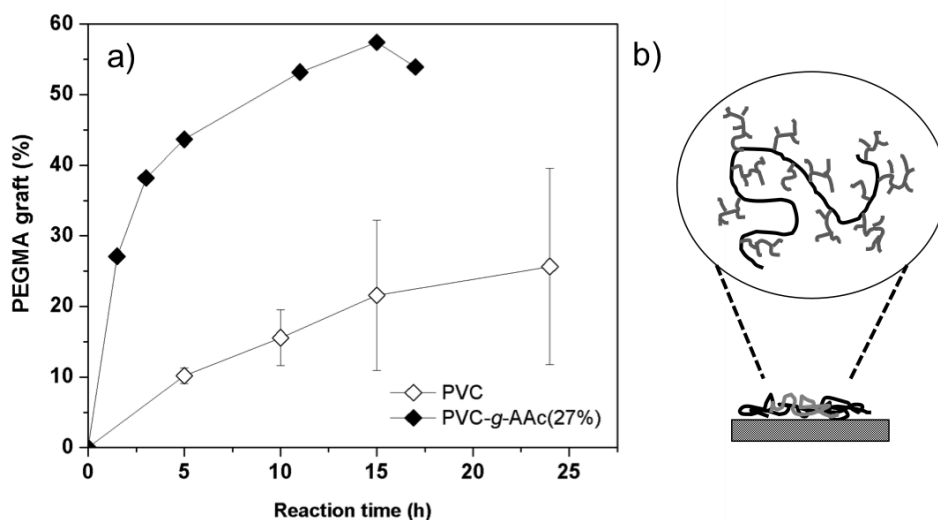
Figure 5.8: a) Graft of PEGMA onto PVC-*g*-AAc(27%) as a function of reaction time using a 16% (v/v) aqueous PEGMA solution, 60 kGy dose, and T = 70 °C; b) Structure of a combed-comb copolymer.

As the amount of AAc grafted increased, there was not a proportional increment in the amount of PEGMA that could be grafted, increasing from 37% to 53% for 8% and 50% AAc grafted, respectively (Fig. 5.9). This is an interesting result because catheters with a higher content of AAc swell more in the aqueous medium, which would perhaps make it easier for the PEGMA to diffuse deeper within the polymer matrix. However, the fact that there was not a big increase in PEGMA grafted suggests that the grafting process is predominantly happening at the surface and not within the polymer matrix. This could be because as it is illustrated in Fig. 5.7, although an increased presence of AAc could also mean a greater concentration of grafting radicals, as PEGMA begins to graft onto the PAAc, its own grafted chain could prevent other polymer chains in the reaction medium from reaching active sites closer to the PVC backbone.
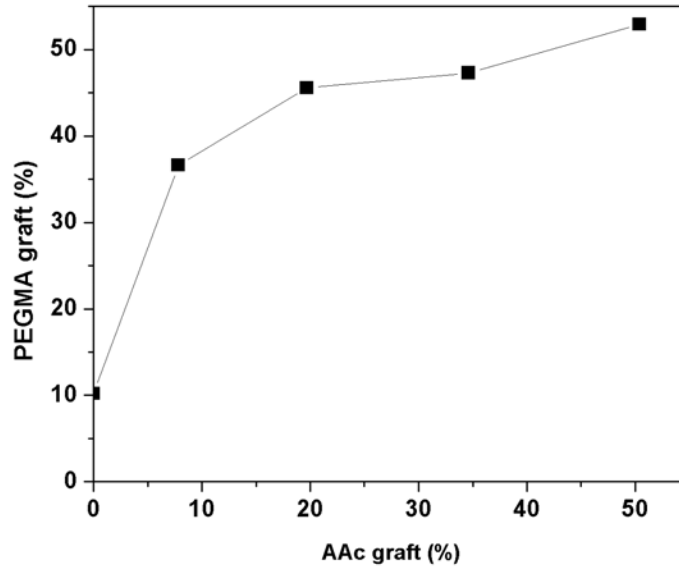
Figure 5.9: Graft of PEGMA upon PVC-*g*-AAc as a function of AAc grafted using a 16% (v/v) aqueous PEGMA solution, 60 kGy dose, 5 h reaction time, and T = 70 °C.

As it was the case for the PVC-*g*-PEGMA grafts, the [PVC-*g*-AAc]-*g*-PEGMA catheters turned an orange color. To lower the catheter's exposure to radiation, the grafting process was repeated but with lower doses of 40, 20, and 10 kGy (Fig. 5.10) and with catheters that had about 10% AAc, as it was discovered that higher amounts of AAc did not significantly improve upon the PEGMA grafting yield, and that higher amounts of AAc lead to a bigger catheter surface area change.
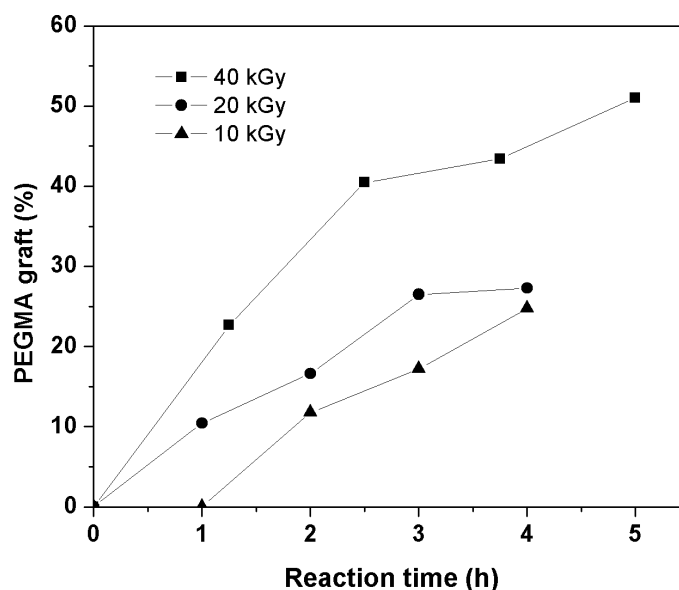
Figure 5.10: Graft of PEGMA upon PVC-*g*-AAc(10%) as a function of reaction time for 40, 20, and 10 kGy using a 16% (v/v) aqueous PEGMA solution and T = 70 °C.

As expected, lowering the irradiation dose lead to a decrease in the grafting percentage due to a lower number of active radicals formed. However, even with doses of 10 kGy, relatively good amounts of PEGMA (25%) were grafted in 4 h. The maximum grafting percentage obtained was of 50% for a dosis of 40 kGy (in 5 h). The grafting percentages for 60 and 40 kGy did not differ much, suggesting that at 40 kGy there is already a saturation of radicals. The catheters that were irradiated with 10 kGy still changed color, however to a much lesser extent than those exposed to higher radiation doses (Fig. 5.11). This color change at such a low dosis of radiation can be explain by the fact that the catheter is irradiated and heated twice (the first time to graft AAc) and thus some degradation of the polymer matrix cannot be avoided.

Figure 5.11: Color differences between (A) PVC, (B) PVC-*g*-PEGMA(15%), and (C) [PVC-*g*-AAc(12%)]-*g*-PEGMA(19%)

35

5.1.4 Grafting of AAc onto PVC-*g*-PEGMA

The grafting scheme of AAc onto PVC-*g*-PEGMA is depicted in Fig. 5.12, where it is appreciated that there are several sites where the radicals can form (1). However, because the poly(oxyethylene) chain has an oxygen with two lone pairs, the radicals created on either of its two carbons are very stable, and therefore the radials that will have a bigger role in the grafting process are the primary and secondary radicals that form in the poly(PEGMA) chain. In the diagram (Fig. 5.12) the grafting process is illustrated using the secondary radical (2), although the primary one is more reactive. After heating and in the presence of the AAc monomer, the radicals initiate the grafting process; the grafted chains grow during the propagation step (3), and finally the process ends when the chains terminate or recombine (4).
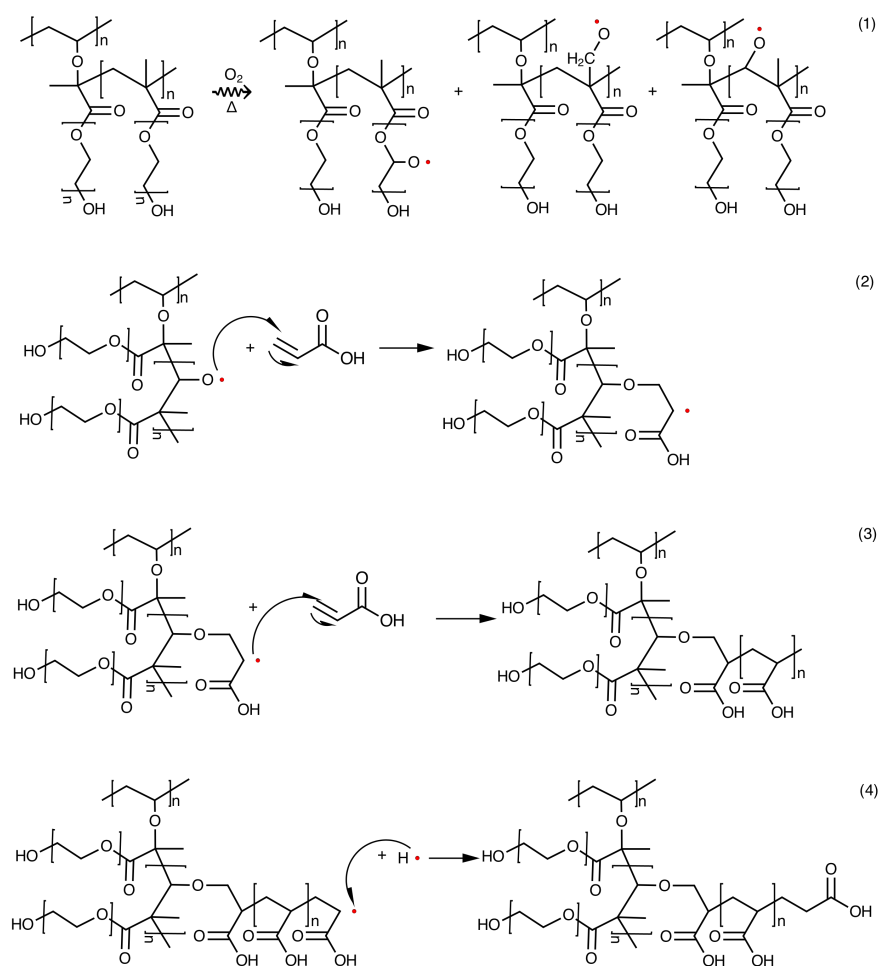
Figure 5.12: Proposed grafting scheme of AAc onto PVC-*g*-PEGMA

The presence of PEGMA had a positive effect on the amount of AAc that was grafted. Using an irradiation dose of 5 kGy and a reaction temperature of 80 °C, with as little as 12% PEGMA present, in 1 h about 80% AAc had been grafted, in comparison to the

8% grafted onto pristine PVC (Fig. 5.14). This dramatic increase implies that there is a greater number of active sites suitable for grafting created in the PVC-*g*-PEGMA polymer matrix, which is not surprising given that Fig. 5.12 shows that there are three main radicals (from two different polymer chains) that can equally participate in the grafting process. After an hour, the PVC-*g*-PEGMA system seems to have reached its saturation point as longer reaction times led to grafting percentages between 80-100%. As previously mentioned, catheters with such graft percentages tend to have drastic changes in their bulk properties such as hardening and increased visible rugosity.
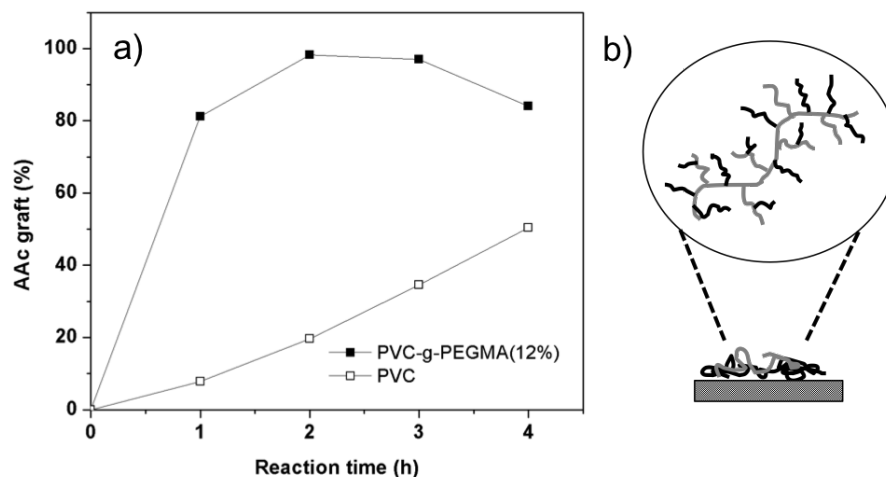
Figure 5.13: Grafting of AAc onto PVC-*g*-PEGMA(12%) and PVC using a dose of 5 kGy, a monomer concentration of 50% v/v aqueaous AAc, and a reaction temperature of 80 °C.

Because 5 kGy is already a low dose, to try an lower the grafting percentage further studies were conducted by lowering the monomer concentration in an aqueous solution to 30% and 10% AAc (Fig. 5.14). The lower concentration of 30% AAc led to a higher percentage of AAc grafted, with a maximum of 169% AAc grafted after 4 h. This can be explained because as there is less monomer present, the degree of homopolymerization is probably decreasing and grafting is favoured. Lowering the monomer concentration to 10% lead to a decrease in the grafting percentage, reaching a value of 12% AAc grafted after 1 h and staying within that range. This dramatic decrease in grafting percentage could be due because all of the homopolymer is consumed within the first hour of the reaction.
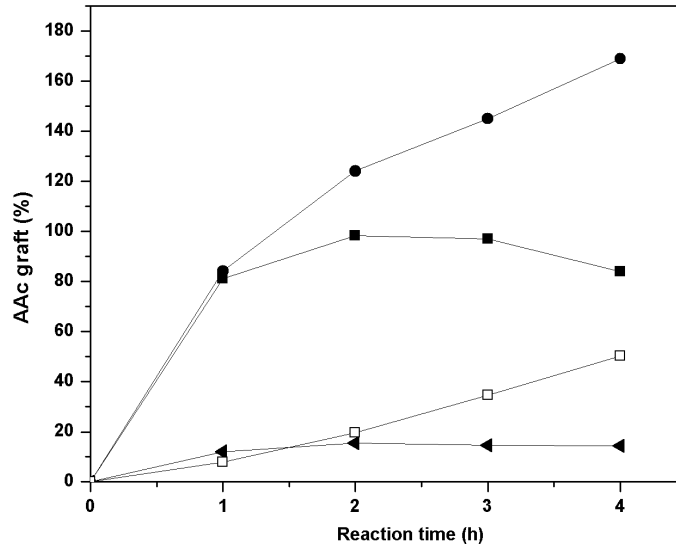
Figure 5.14: Grafting of AAc onto PVC-*g*-PEGMA(12%) (closed symbols) and PVC (open symbols) using a dose of 5 kGy, a monomer concentration of (■)50%, (●)30% and (▲)10% v/v aqueaous AAc, and a reaction temperature of 80 °C.

5.2 Physicochemical characterization

5.2.1 Infrared spectroscopy

The FTIR spectra (Fig. 5.15) of the pristine PVC catheter shows the typical C-H stretching peaks, symmetric and asymmetric, of an sp$_3$ hybridised carbon (2962, 2932, 2875, 2862 cm^{-1}). Knowing that most plasticizers used are phthalates, the peak at 1724 cm^{-1} is attributed to a C=O ester stretch, as well as the strong peak at 1260 cm^{-1} attributed to a C-O acyl stretch. The PVC-*g*-AAc catheter shows a broad peak in the range of 2400-3500 cm^{-1} attributed to the O-H stretch, which is typical of acids, and that overlaps the C-H stretching peaks (2922 and 2850 cm^{-1}). The C=O stretch of the carboxylic acid is identified by the 1700 cm^{-1} peak. Other peaks include the C-OH bending (1452 cm^{-1}) and C-O acyl stretch (1246 cm^{-1}). In the PVC-*g*-PEGMA spectrum there's a broad peak in the 3400-3500 cm^{-1} stretch typical of an OH alcohol stretch, the C-H stretches at 2912 and 2862 cm^{-1}, a peak at 1726 cm^{-1} attributed to the C=O ester stretch, and a peak at around 1106 cm^{-1} from the C-O stretch. With these results it can be established that at the surface of the grafted catheters PAAc and PEGMA are present.

For the binary grafted catheters, in the case of [PVC-*g*-PEGMA]-*g*-AAc there is the characteristic broad peak from 2400-3500 cm^{-1} from an OH stretch that overshadows the CH stretches (2952 and 2912 cm^{-1}). One sharp difference between the [PVC-*g*-

PEGMA]-*g*-AAc and PVC-*g*-AAc catheter is that there is also a broad peak at 1702 cm^{-1}, which is attributed to the C=O from the acid and ester groups that belong to the PAAc and PEGMA, respectively. For [PVC-*g*-AAc]-g-PEGMA, the spectrum strongly resembles that of PVC-*g*-PEGMA. There is the broad OH alcohol peak at around 3450 cm^{-1}, the CH stretches, the C=O ester stretch at 1726 cm^{-1}, the C-O stretch at around 1106 cm^{-1}. One distinct difference in this spectrum is the broadening of the peak at 1437 cm^{-1} previously attributed to the C-OH bending of the PAAc. The appearance of this peak suggest that there is a strong interaction of the -OH terminal group of the carboxylic acid with the PEGMA. Overall, for the binary grafted catheters it can be derived that, at least to the depth of the apparatus, the polymer that can be observed at the surface is the one that was grafted during the second step, suggesting that the grafting density of the latter polymer is high, thus confirming that the second graft is happening predominantly on the first graft, and not upon the PVC.
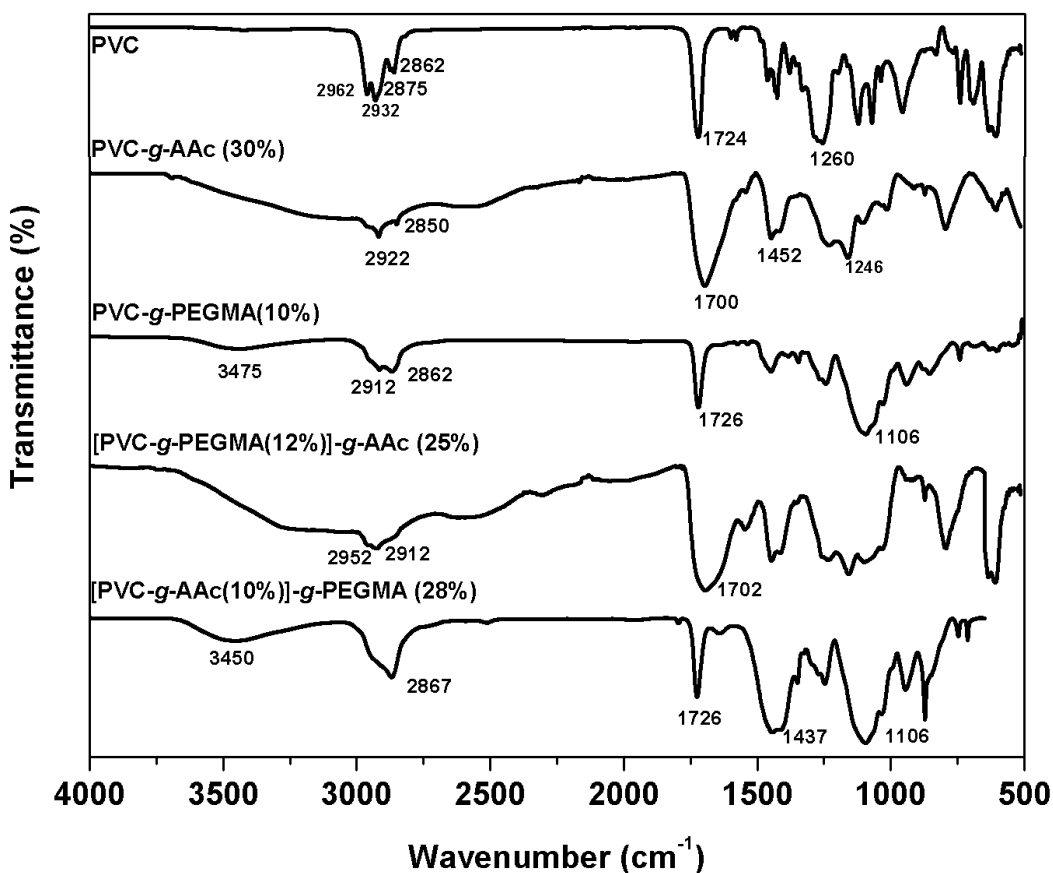
Figure 5.15: ATR-FTIR spectrum of pristine and modified catheters

5.2.2 Thermal analysis

The thermal analysis of the PVC, AAc, and poly(PEGMA) are shown in Fig. 5.16. The TGA of PVC shows a first weight drop, from 160 °C until around 400 °C, due to the dechlorination process. During this first weight drop, around 73% of the original mass is lost, which is a value 9% above the one typically found in the literature (Matuschek *et al.,* 2000) and could be because there is a loss of other components (aside from HCl) present in the catheter, perhaps from the different additives and fillers utilised during the manufacturing process, such as plasticizers. The subsequent weight loss steps are due to the the decomposition of the residual conjugated polymer backbone, which tends to happen through chain-stripping processes. At 800 °C there is no char residue. In the case of PAAc, one of the first weight drops happens at 132 °C and falls within the range where anhydride formation and loss of water begins to happen (Maurer *et al.,* 1987). The second decomposition step is attributed to the loss of CO_2. The remaining polymer backbone decomposes in the final weight drop. The final char residue at 800 °C of the PAAc is of 4%. The thermal decomposition of irradiated poly(PEGMA) (60 kGy) is distinguished by a single step weight drop (where the main products are formic acid and its derivatives (Glastrup, 1996) which begins at 100 °C and continues until 434 °C, with a 1% char residue at 800 °C.
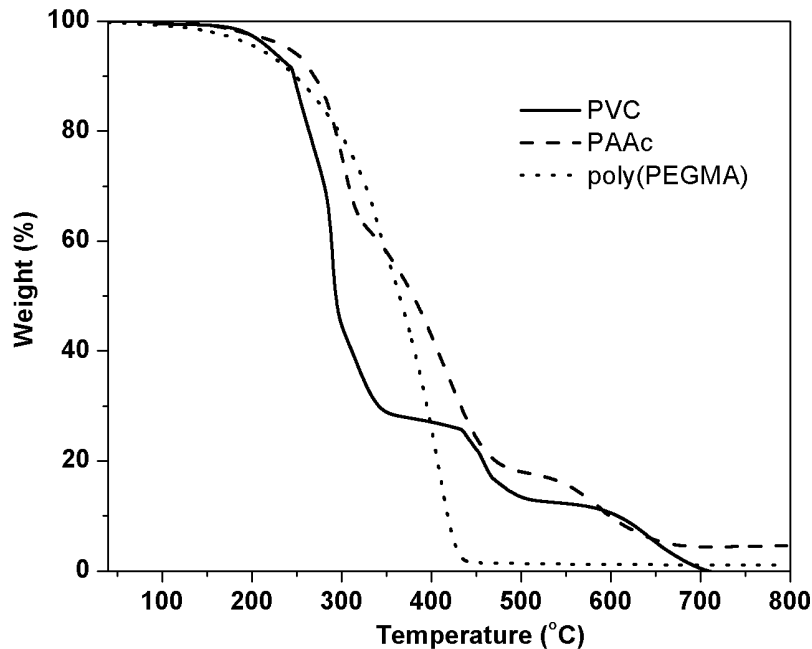
Figure 5.16: TGA of PVC, PAAc and PEGMA

For the modified catheters, we can see that as the percentage of AAc increases so

does the thermal stability of the polymers (Fig. 5.17, right), with the 10% weight-loss temperature for PVC at 253 °C, that of PVC-*g*-AAc(231%) at 337 °C, and values in-between for lesser AAc grafting percentages (Table 5.1). With as little as 8% AAc grafted there is already a decrease in the first weight drop percentage (down to 68% from 73%), signifying the loss of HCl. There was also an increase in the char residue percentage, increasing to 39% for PVC-*g*-AAc(258%). In the case of PVC-*g*-PEGMA, because none of the grafting percentages obtained were greater than 30%, only a PVC-*g*-PEGMA(27%) was analysed (Fig. 5.17, left). For this catheter, the 10% weight loss and the percent char residue increased to 254 °C and 6%, respectively. The first weight-loss of the PVC dechlorination process is also visible, although to a lesser degree, while the second decomposition step is completely lost. Overall, through the thermal analysis we can conclude that the grafted catheters are able to gain thermal stability as compared to the pristine PVC.
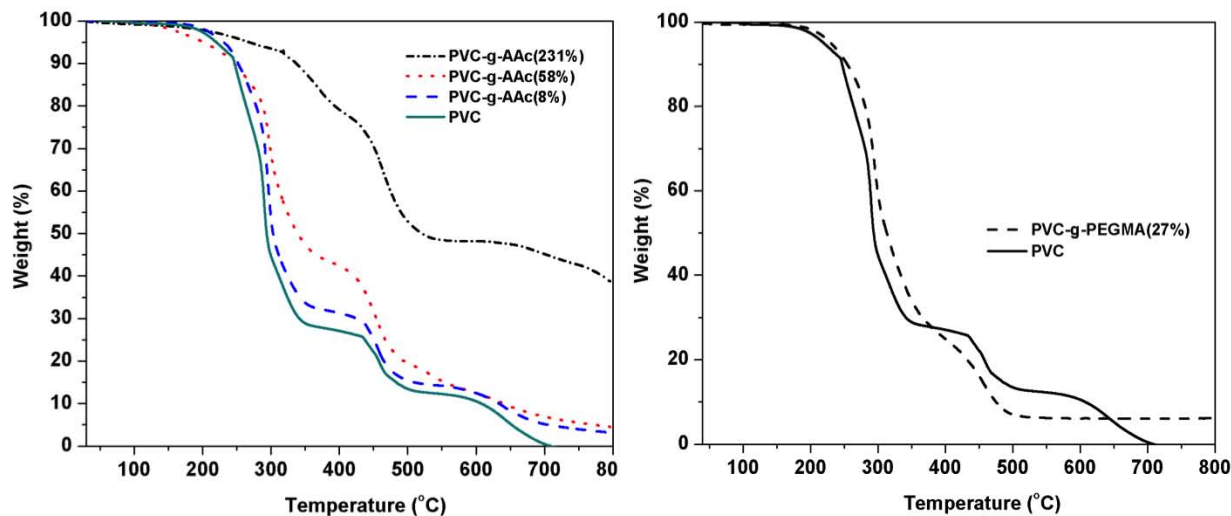
Figure 5.17: TGA of (right) PVC, PVC-*g*-AAc(8%), PVC-*g*-AAc(58%), and PVC-*g*-AAc(231%); and (left) PVC, and PVC-*g*-PEGMA(27%)

The binary grafted catheters were much more thermally stable than PVC. As the amount of AAc increased, so did the thermal stability of the catheter, with [PVC-*g*-AAc(46%)]-*g*-PEGMA(27%) showing a 10% weight loss at 298 °C, which is 20 degrees higher than that of [PVC-*g*-AAc(20%)]-*g*-PEGMA(93%). Furthermore, the char residue also increase with increasing AAc percentage, incrementing from 5 to 38% for PVC-*g*-AAc(20%)]-*g*-PEGMA(93%) and [PVC-*g*-AAc(46%)]-*g*-PEGMA(27%), respectively. From the figure it is gathered that the grafting percentage of AAc is more important in providing thermal stability to the PVC catheter, since it overshadowed the increase in the PEGMA grafting percentage. Furthermore, it is important to note that the dechlorination step of PVC's thermal decomposition was completely overshadowed for these binary grafted catheters, with [PVC-*g*-AAc(20%)]-*g*-PEGMA(93%) highly resembling the single-

41

step decomposition of poly(PEGMA) and [PVC-*g*-AAc(46%)]-*g*-PEGMA(27%) resembling the decomposition of PAAc.
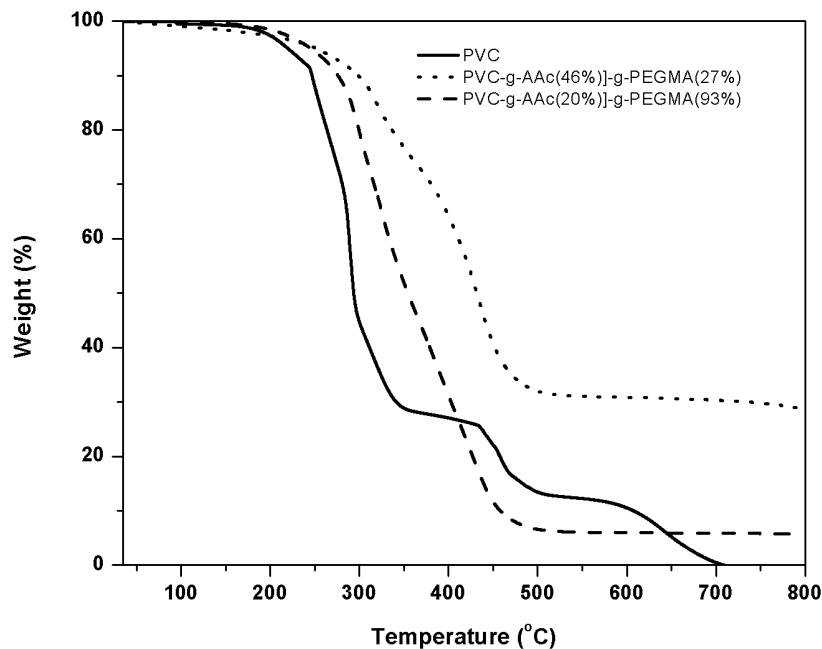
Figure 5.18: TGA of PVC and [PVC-*g*-AAc(46%)]-*g*-PEGMA(27%), [PVC-*g*-AAc(40%)]-*g*-PEGMA(93%)

The following table (Table 5.1) summarizes the 10% weight loss temperature and char residue for all the analyzed catheters.

Table 5.1: Temperature at which the 10% weight-loss occurs and percent char residue.

	10% weight loss temperature (°C)	*Char residue at 800°C* (%)
PVC	247	0
PAAc	269	5
poly(PEGMA)	249	1
PVC-*g*-AAc(8%)	252	3
PVC-*g*-AAc(58%)	246	5
PVC-*g*-AAc(231%)	337	39
PVC-*g*-PEGMA(27%)	254	6
[PVC-*g*-AAc(46%)]-*g*-PEGMA(27%)	298	29
[PVC-*g*-AAc(20%)]-*g*-PEGMA(93%)	276	6

5.2.3 Water contact angle analysis

The results of the water contact angle analysis, Table 5.2, show that PVC, with a contact angle of 99 ± 2°, which falls within the range reported in the literature (Li *et al.,* 2006), is not a hydrophilic material. For a PVC-*g*-AAc catheter with as little as 4% AAc grafted, the contact angle decreases to 91 ± 6°. As the content of AAc increases, the catheter loses hydrophobicity, reaching its lowest value of 82 ± 1° with 59% AAc grafted. These results were expected because PAAc is a hydrophilic polymer due to its pendant carboxylic acid functional group which is considered a super-absorbant. In the case of PVC-*g*-PEGMA, the surface water contact angle increased (up to a value of 114 ± 4° for a 41% PEGMA graft), which is a surprising result given that poly(ethylene glycol)s are considered hydrophilic polymers. The water contact angle was measured again once the water droplet had been in contact with the surface for 30 s, after which time the water contact angle for PEG grafted surfaces decreased between 20 and 30 degrees from the initial reading, reaching values in the range obtained for PVC-*g*-AAc catheters at 0 s. Because it is known that PEG polymer chain mobility increases with hydration (Ye & Zhou, 2015), it probably takes some time for the grafted PEGMA chains to rearrange their hydrophobic segments, which were initially exposed to the air, to allow for the hydrophilic regions to interact with the water and thus lower the surface tension. This dramatic decrease in water contact angle was not observed after 30 s for PVC-*g*-AAc catheters, suggesting that there is no rearrangement of the polymer chains, which is not surprising as PAAc chains are more rigid.

In the case of the binary grafted catheters, the results were not as expected. For both [PVC-*g*-AAc]-*g*-PEGMA and [PVC-*g*-PEGMA]-*g*-AAc the water contact angle remained above 90° at 0 s, and it even increased to 102 ± 5° for [PVC-*g*-AAc(46%)]-*g*-PEGMA(27%). Because both AAc and PEGMA are hydrophilic compounds, it was hypothesized that they would increase the hydrophilicity of the catheter. However, the increase in the water contact angle is explained by a complexation process driven by hydrogen bonding interactions between the carboxylic groups of PAAc and the oxygen groups of PEGMA (Holappa *et al.,* 2004). After 30 s the catheters that were grafted with PEGMA during the second step were able to lower the surface water contact angle, whilst the [PVC-*g*-PEGMA]-*g*-AAc catheters remained almost the same. This is further evidence that the polymer grafted during the second step is dominant at the surface because [PVC-*g*-AAc]-*g*-PEGMA was able to gain hydrophilicity after 30 s, meaning that the PEGMA chains at the surface were able to rearrange, which was not the case for [PVC-*g*-PEGMA]-*g*-AAc. Lastly, another factor that could explain the increase in the water contact angle is the visible roughness of the binary catheters, compared to pristine PVC, as it has been established that higher water contact angle measurements are observed for materials with rougher surfaces (Kubiak *et al.,* 2011).

Table 5.2: Water contact angle measured at 0 and 30 s after the water droplet touched the surface of pristine and modified PVC catheters

| | Water contact angle (°) | |
	0 s	*30 s*
PVC	99 ± 2	98 ± 3
PVC-*g*-AAc(4%)	91 ± 6	89 ± 4
PVC-*g*-AAc(20%)	87 ± 1	87 ± 1
PVC-*g*-AAc(59%)	82 ± 1	80 ± 2
PVC-*g*-PEGMA(16%)	107 ± 7	87 ± 9
PVC-*g*-PEGMA(41%)	114 ± 4	84 ± 2
PVC-*g*-AAc(5%)-*g*-PEGMA(21%)	94 ± 5	88 ± 3
PVC-*g*-AAc(11%)-*g*-PEGMA(40%)	102 ± 5	65 ± 4
PVC-*g*-PEGMA(13%)-*g*-AAc(12%)	99 ± 3	97 ± 2
PVC-*g*-PEGMA(15%)-*g*-AAc(84%)	94 ± 5	90 ± 3

5.2.4 Equilibrium swelling time and critical pH

The equilibrium swelling time was measured both in water and urine for PVC, PVC-*g*-AAc, and PVC-*g*-PEGMA catheters (Fig. 5.19).
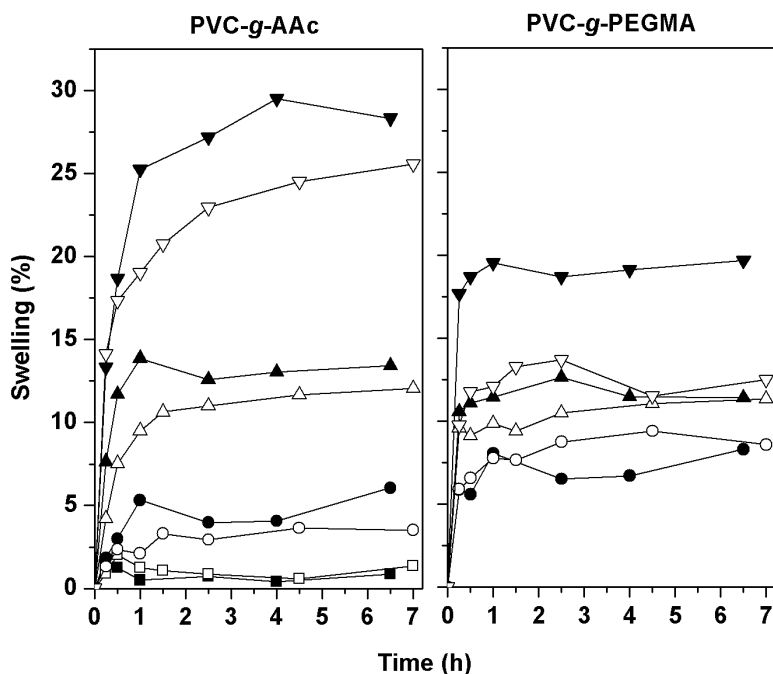
Figure 5.19: Swelling of a) PVC (■) and PVC-*g*-AAc with 36 (▼), 15 (▲), and 7 (●)% AAc; and b) PVC-*g*-PEGMA with 38 (▼), 20 (▲) and 11 (●)% PEGMA in water (closed symbols) and artificial urine (open symbols).

As was expected, PVC does not swell in water nor urine. As the AAc grafting content increased, PVC-*g*-AAc catheters swelled more with a maximum water swelling of 29% obtained in 4h for PVC-*g*-AAc(36%). Even catheters grafted with as little as 7% AAc were able improve the water uptake of the original catheter. PEGMA grafted catheters also exhibited swelling capabilities, although less than PVC-*g*-AAc catheters, with a maximum swelling of 20% observed for PVC-g-PEGMA(38%) in 1 h. The rapid water equilibrium time of PVC-*g*-PEGMA catheters suggests that the water molecules are being absorbed by PEGMA's hydrophilic regions, the poly(oxyethyelene) groups [-CH_2CH_2O-]n, which some models propose take a stiff coiled or helix shape in aqueous solutions (Tasaki, 1996), thus decreasing the space available for the water molecules to penetrate and resulting in a faster water uptake. This is in contrast to PVC-*g*-AAc catheters, where as the AAc content increased, the equilibrium swelling time was slightly longer, which was further confirmed by measuring the equilibrium swelling time of catheters with higher AAc contents (Fig. 5.20).
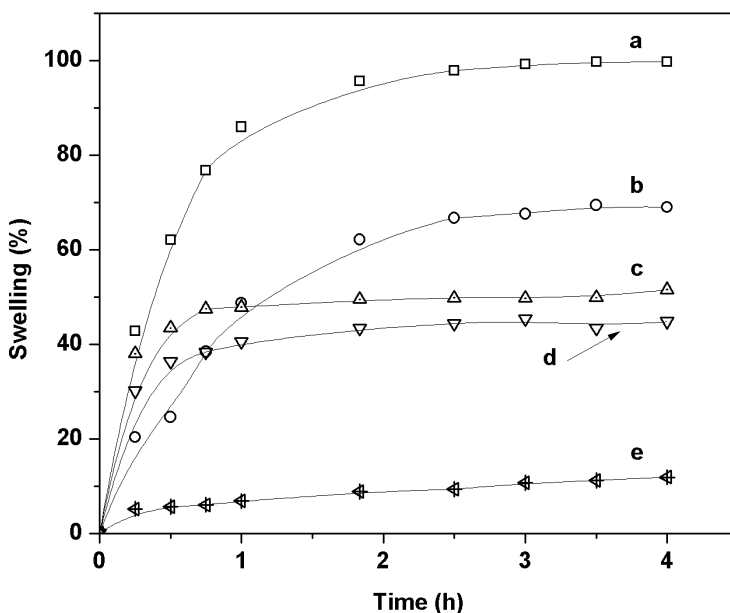
Figure 5.20: Water swelling equilibrium time for PVC-*g*-AAc with a) 257, b) 125, c) 49, d) 30 and e) 11% AAc grafted.

Catheters with 257 and 125% AAc content reached their water equilibrium in around 2.5 - 3 h, while catheters with lesser grafts had already reached equilibrium in 1 h. The longer water equilibrium times are an indication that the water molecules are diffusing at a slower rate in the polymer backbone as the grafting percentage increases because of two reasons: 1) there is a higher density of AAc chains grafted and/or 2) the grafted

AAc chains are longer. In all cases, once the catheter is submerged in water, the polyelectrolyte PAAc chains being to stretch and take more space, which slows down the flow of the water molecules into the catheter but at the same time opens up space for more water molecules to penetrate the grafted catheter, thus explaining the higher swelling percentages (Fig. 5.21). Both PVC-*g*-AAc and PVC-*g*-PEGMA also swelled in the artificial urine medium, albeit to a lesser extent. This could perhaps be explained by the presence of different ions in the artificial urine medium, which obstruct the water absorption process.
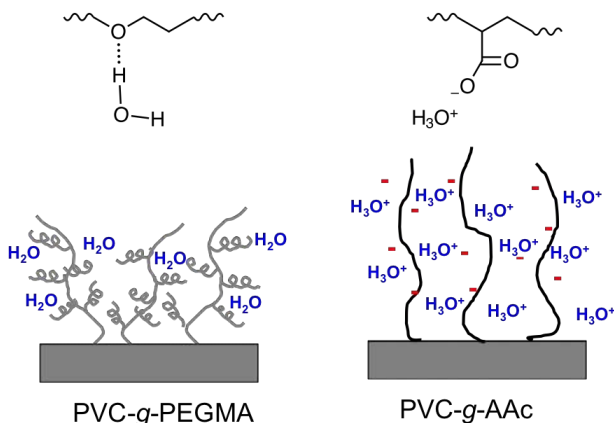
Figure 5.21: Interaction of PVC-*g*-PEGMA (left) and PVC-*g*-AAc (right) with water.

The water swelling equilibrium times of 1-3 h could help explain why increasing the AAc grafting percentage only led to a small increase in the PEGMA grafting yield (Fig. 5.9) for the reaction time of 5 h. It takes at least 1 h for water to fully diffuse within the PVC-*g*-AAc catheter, therefore, in the grafting process the PEGMA units will first interact with the outer layer of the grafted AAc chains. Although the PAAc will expand, the grafted PEGMA chains, which will also interact with water, will prevent the remaining PEGMA units from reaching any active sites deep within the polymer matrix, inadvertently leading to a gradient-brush-copolymer type of graft (Fig. 5.22).
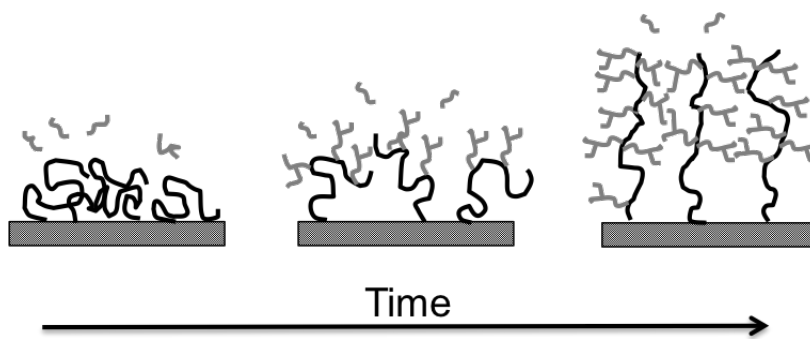
Figure 5.22: Gradient grafting of PEGMA onto PVC-*g*-AAc.

The swelling behaviour of [PVC-*g*-AAc]-*g*-PEGMA catheters was also studied to see if the presence of PEGMA on the surface of the catheter would have an effect on the water uptake (Fig. 5.23). Overall, increasing the amount of PEGMA only slightly increased the swelling percentage, incrementing from 52 to 57% for catheters that had 46% AAc but 27% and 63% PEGMA, respectively. This slight increase could be due because as figure 5.19 showed, PEGMA is able to interact with water. Furthermore, the "branched-brush" structure of the graft has an effect on the overall conformation of the chain, as it has been studied that heavily grafted brush copolymers tend to lose the random gaussian coil conformation, extending themselves and thus creating more space for the water molecules, as their grafting density increases (Ratgeber *et al.*, 2005). As expected, the factor that determined how much the catheter would swell remained the AAc percentage: lower AAc percentages led to faster equilibrium times and lower swelling percentages. The equilibrium swelling time for catheters with more AAc content was much longer (9 h) because it has been proven that the complexation of PEG with carboxylic acid groups slows down the water uptake of the system (Peppas *et al.*, 1999).
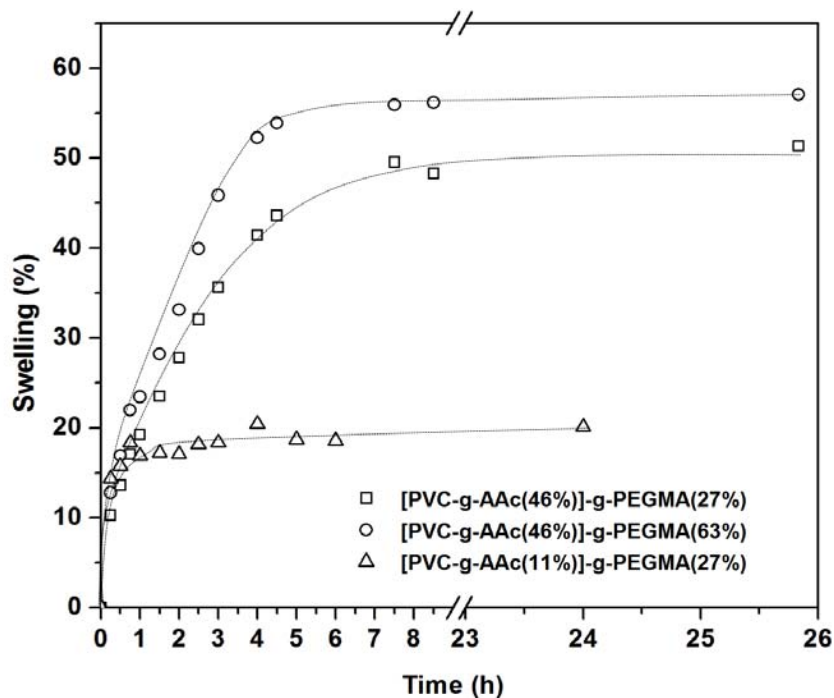
Figure 5.23: Water equilibrium swelling time of three different [PVC-*g*-AAc]-*g*-PEGMA catheters.

The binary system [PVC-*g*-PEGMA]-*g*-AAc reached water swelling equilibrium time in a manner similar to PVC-*g*-AAc (Fig. 5.24), where catheters with lower grafting percentages reached equilibrium in one hour while those with more AAc content took longer.

One important observation is that when the catheters were first immersed in water (particularly the catheter with 47% AAc), visible small air bubbles could be see on their surface. These bubbles remained even after the container was lightly shaken; however, by the time the first measurement for the swelling study was taken (15 minutes) the bubbles had disappeared. This observation could perhaps explain why the contact angle measurement of this binary system did not decrease from that of PVC at 0 and 30 s after the water droplet had touched the surface of the catheters. What is probably happening is that because the PAAc chains are stiffer, it takes longer for the complexation of PEGMA-PAAc to give way to the interaction between PAAc and water, thus exposing the hydrophobic parts of the chain for a longer period of time and enabling the material to entrap some water bubbles on its surface.
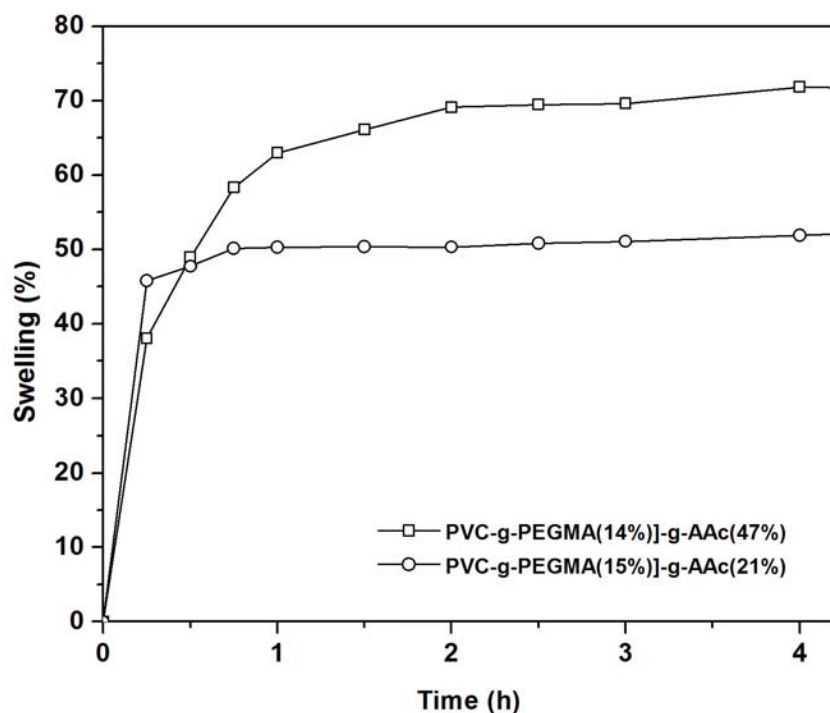
Figure 5.24: Water equilibrium swelling time of two different [PVC-*g*-AAc]-*g*-PEGMA catheters.

Because PAAc is a polyelectrolyte, it exhibits a critical swelling pH (Fig. 5.25). Catheters with a higher AAc grafting yield exhibited the biggest swelling response, going from a constant range of 55-60% swelling before a pH of 6, to more than 100% swelling in a pH greater than 9 for PVC-*g*-AAc(49%). This increment was not as dramatic for the lower grafted catheters, nonetheless, even catheters with as little as 11% grafted were able to increase their swelling ability in pHs above 7. The critical pH of the systems remained within the 7-8 range.
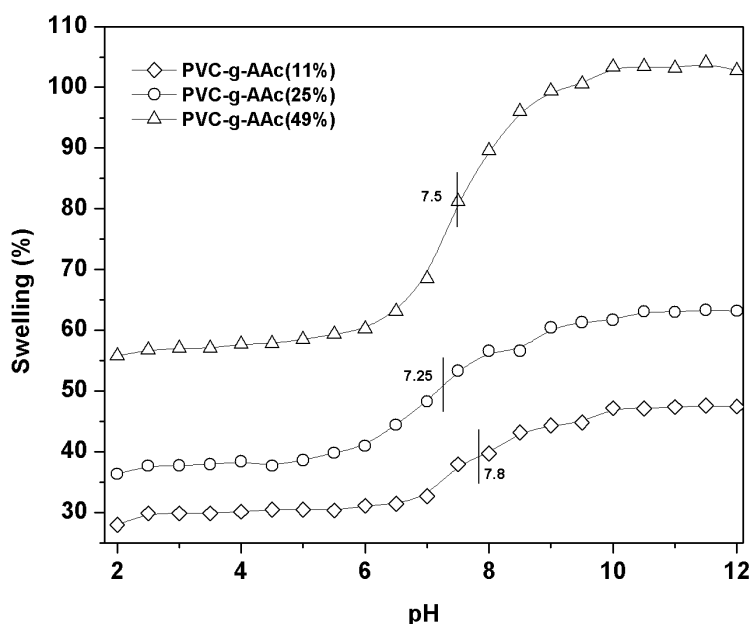
Figure 5.25: Critical swelling pH of PVC-*g*-AAc catheters with 11, 25, and 49% AAc grafted.

The critical swelling pH of the binary system was also studied and as it is seen in Fig. 5.26, the presence of PEGMA on the surface did not shift the critical pH of the catheter but it improved upon the final swelling percentage, increasing from 72% to 93% for PVC-*g*-AAc(25%) and PVC-*g*-AAc(27%)]-*g*-PEGMA(28%), respectively, at a pH of 12. This improvement could be a result that as the PAAc chains become ionized, they also start to repel the grafted PEGMA chains, opening up more space for the water molecules to penetrate and interact with the poly(oxyethylene) groups. At lower pH values, the binary system swelled slightly less than the PVC-*g*-AAc catheter, which is further indication of the hydrogen bonding between poly(oxyethylene) units and carboxylic acid.
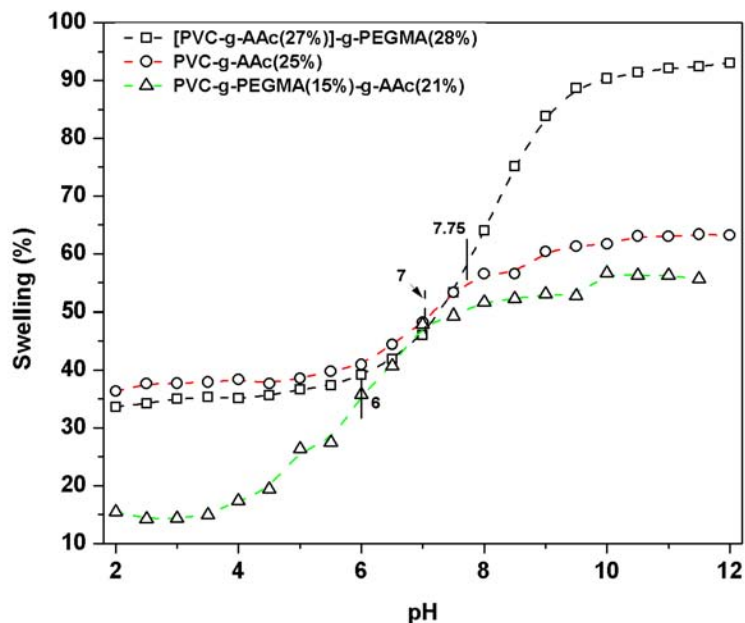
Figure 5.26: Comparison of the critical swelling pH between PVC-*g*-AAc(25%) and [PVC-*g*-AAc(27%)]-*g*-PEGMA(28%).

5.2.5 Mechanical analysis

The mechanical analysis shows that grafting PEGMA onto the catheter decreased the Young's modulus to a value of 12 MPa from 19 MPa for PVC, which is a value in agreement with published literature (Sastri, 2010). This result is not uncommon since PEG is known to be used as an internal plasticizer due to its below 0 ^{o}C glass transition temperature, which allows its chains to add space between the chains of the original polymer backbone. Grafting the catheter with acrylic acid made the material stiffer, with a PVC-*g*-AAc(25%) catheter having a Young's modulus of 64 MPa. This increase in stiffness is explained by the high Tg of PAAc (106 ^{o}C) (Chern, 2008). The binary graft shows that the polymer grafted in the second step dominates the mechanical behaviour, as the [PVC-*g*-AAc]-*g*-PEGMA catheter was still able to become more flexible with a Young's modulus of 12 MPa, a value in between that of PVC and PVC-*g*-PEGMA. This effect is due to the fact that the grafted PEGMA chains create space between the grafted PAAc chains, allowing them to easily slide past each other when stress is applied. However, the opposite happened for the [PVC-*g*-PEGMA]-*g*-AAc system, which displayed the highest Young's modulus recorded with a value of 150 MPa. Comparing the possible grafting structures of the grafted chains for the [PVC-*g*-PEGMA]-*g*-AAc and [PVC-*g*-AAc]-*g*-PEGMA systems, we can see that grafting AAc onto PEGMA does not make it easier for the grafted PEGMA chains to move, but instead through steric repulsions and lack

of PAAc chain mobility, these normally flexible poly(PEGMA) chains perhaps take stiffer extended positions (since increasing grafting density decreases chain gaussian recoil) making it much harder for the system to accommodate when stress is applied.
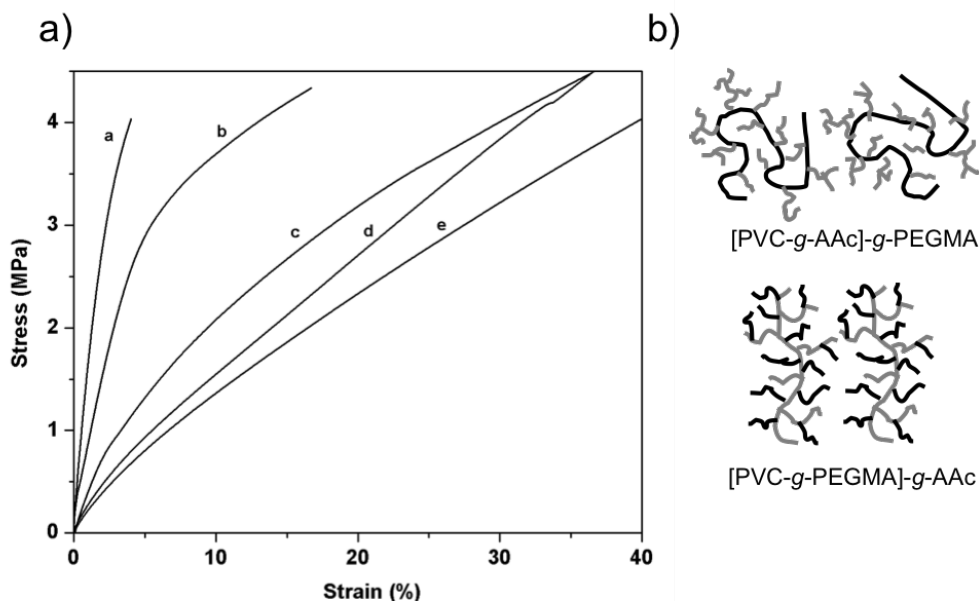
Figure 5.27: Stress (MPa) versus strain (%) curves for a) [PVC-*g*-PEGMA(12%)]-*g*-AAc(26%), b) PVC-*g*-AAc(25%), c) PVC, d) [PVC-*g*-AAc(12%)]-*g*-PEGMA(26%) and e) PVC-*g*-PEGMA(16%) catheters; and b) possible grafted chains structures of [PVC-*g*-AAc]-*g*-PEGMA and [PVC-*g*-PEGMA]-*g*-AAc.

5.2.6 Lubricity

The lubricity of the catheters was measured by registering the force required to insert and remove the catheters from agar (Fig. 5.28). For catheters that had been pre-lubricated for 30 s, the force required to insert them into agar decreased, with the lowest values of 0.117 ± 0.074 and 0.118 ± 0.008 N obtained for PVC-*g*-PEGMA(10%) and PVC-*g*-AAc(45%), respectively. Allowing the catheters to swell for 4 h in water before inserting them into agar increased the force required for insertion for all modified catheters, with the exception of PVC, where the force decreased. The greatest force recorded was of 0.152 ± 0.008 N for both catheters that had PAAc on their surface. This can perhaps be attributed to PAAc interactions with agar (hydrogen bonding) and also because after wetting, the PAAc can feel slightly *sticky* when touched.

For all the samples tested, the force required to remove the catheter from agar was lower than the one required to insert it; however, the force of removal of all the modified catheters was higher than that of PVC. There was not a clear pattern differentiating the force of removal between 30 s and 4 h wetted catheters, with some force-removal slightly decreasing or increasing. Nonetheless, as it was the case with the insertion, the

catheters that required the highest force to be removed were those that contained PAAc on their surface.
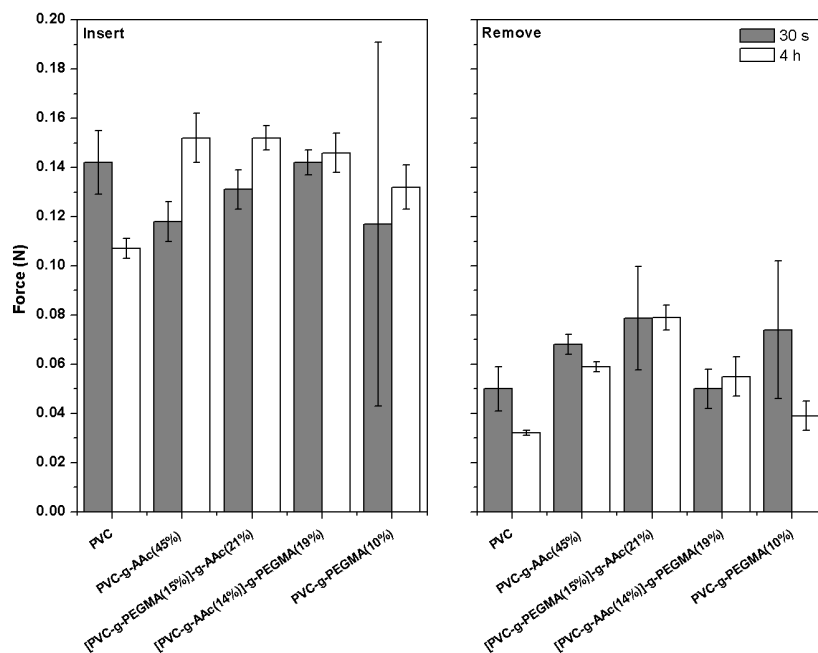
Figure 5.28: Force required to insert and remove the catheters from agar at a velocity of 5 mm/s for catheters that had been wetted for 30 s (shaded) and 4 h (white) prior to running the experiment.

5.2.7 X-Ray Photoelectron Spectroscopy (XPS)

The x-ray photoelectron spectroscopy (XPS) broad spectra of PVC, PVC-*g*-AAc(20%), and PVC-*g*-PEGMA(16%), Fig. 5.29, shows that for all the modified catheters there is an increment in the intensity of the O_{1s} peak, as well as the disappearance of the Cl_{2p} peak.
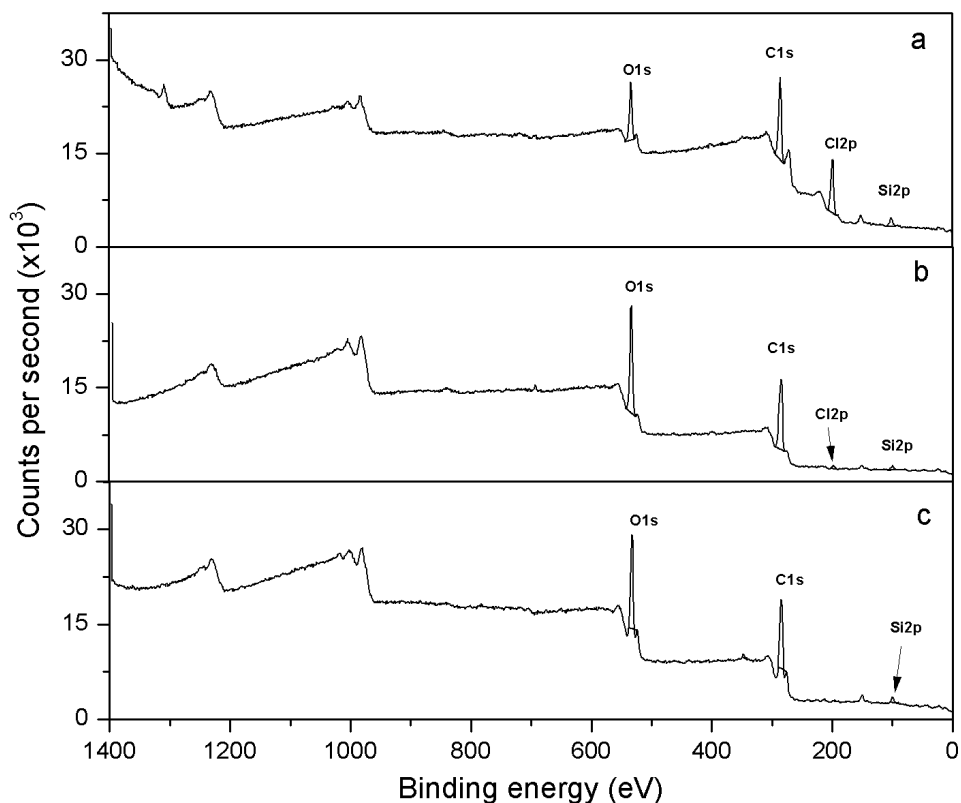
Figure 5.29: XPS survey spectra of a) PVC, b) PVC-*g*-AAc(20%), and c)PVC-*g*-PEGMA(16%). Element identification is shown (C_{1s}, O_{1s}, Cl_{2p}, and Si_{2p})

The results of the C_{1s}, O_{1s}, Cl_{2p}, and Si_{2p} percent composition of all the samples are presented in Table 5.3, where it can be observed that the PVC sample has a considerable oxygen percentage, 16.3%, present on its outer surface (the one exposed to the bodily tissue). Because the core structure of PVC lacks oxygen, this high oxygen percentage is attributed to the manufacturing process and the different additives, such as plasticizers, that give the catheter its flexibility. Alongside this, because Cl is characteristic of the PVC structure (in a 1: 2 ratio with carbon), the observed 16.4% Cl indicates that only about 30% of the carbon observed on the surface belongs to the PVC polymer matrix.

Table 5.3: XPS composition survey results for pristine and modified PVC.

	Element concentration (At. %)							
	Inner				Outer			
	C_{1s}	O_{1s}	Cl_{2p}	Si_{2p}	C_{1s}	O_{1s}	Cl_{2p}	Si_{2p}
PVC	60.0	16.3	16.4	7.3				
PVC-*g*-AAc(20%)	63.2	32.1	1.0	3.8	59.0	34.4	2.0	
[PVC-*g*-PEGMA(13%)]-*g*-AAc(12%)	58.4	34.0		4.8	65.5	28.6		4.3
PVC-*g*-PEGMA(16%)	62.8	30.5	0.5	5.7	65.8	30.6		3.7
[PVC-*g*-AAc(7%)]-*g*-PEGMA(20%)	62.4	29.0		6.0	65.0	28.0	0.9	5.5

Once AAc and PEGMA are grafted, hardly any Cl is visible on the catheter's surface, with PVC-*g*-AAc(20%) and PVC-*g*-PEGMA(16%) showing Cl percentages of 1 and 0.5%, respectively. The oxygen content of the grafted catheters almost doubled up to 32.1% and 30.5% for PVC-*g*-AAc(20%) and PVC-*g*-PEGMA(16%), respectively, from the initial 16.3% of the PVC. This was expected due to the presence of either the carboxylic group of the PAAc, and the esters and poly(oxyethlyene) chain of the grafted PEGMA. For both binary grafts, [PVC-*g*-PEGMA(13%)]-*g*-AAc(12%) and [PVC-*g*-AAc(7%)]-*g*-PEGMA(20%), the Cl peak disappears completely, and only C and O are observed in a ratio slightly close to what would be expected for pure PAAc and PEGMA (2 C:1 O). From the data it can be concluded that at the chosen grafting percentages, the surface of the catheters is completely covered with the new polymer chains, with the binary graft providing a better surface coverage. These results are not uncommon given the chosen grafting method, *grafting-from*, where a high grafting density is expected. Furthermore, the composition survey results of the inner surface of the character, the one in contact with urine, are similar to those of the outer surface, which was also expected due to the penetrating power of gamma-rays, where the same number of radicals are expected to form on the inner and outer surface of the catheter upon exposure to radiation. To better understand the surface composition, the high resolution spectra of C_{1s} was broken down and the peak energies were assigned in accordance to Table 5.4.

Table 5.4: HR-XPS peak assignment

Peak label	Possible chemical bond	Peak B.E. (eV)
C_1	$\underline{C}$-C	285
C_2	$\underline{C}$-C-Cl	285.5
C_3	$\underline{C}$-COOH	285.7
C_4	$\underline{C}$-Cl	287
C_5	$\underline{C}$-O	286.67 ± 0.06
C_6	$\underline{C}$=O	287.9
C_7	$\underline{C}$OOH	289.22 ± 0.03

Figure 5.30 shows the doconvoluted C_{1s} peaks of PVC, PVC-*g*-AAc(20%) and PVC-*g*-PEGMA(16%), alongside the O_{1s} and Cl_{2p} peaks; and Table 5.5 summarizes the composition percentages, for both inner and outer surface, of the deconvoluted C_{1s} peak of all the samples. Overall, although there are slight differences between the inner and outer surfaces, these differences are small (within 1-5%). Nonetheless, when comparing catheters of different grafts, the C_4 and C_7 carbons are particularly useful in differentiating which compound is being detected. Those catheters that had been grafted with AAc had C_7 (beta carbon of carboxylic acid; C-COOH) percentages in the 10-23% range, while those with PEGMA on their surface only presented percentages between 6.8 and 7.6%. A similar case, but reversed, is seen for C_4 (ether group; C-O): the catheters grafted with PEGMA had percentages of C_4 in the 42-56%, while those with AAc only showed percentages between 0-21%. For all the modified catheters, the presence of Cl was non-existent, with the exception of PVC-*g*-AAc(20%), where a hardly significant 1.5% Cl was detected on the outer surface.
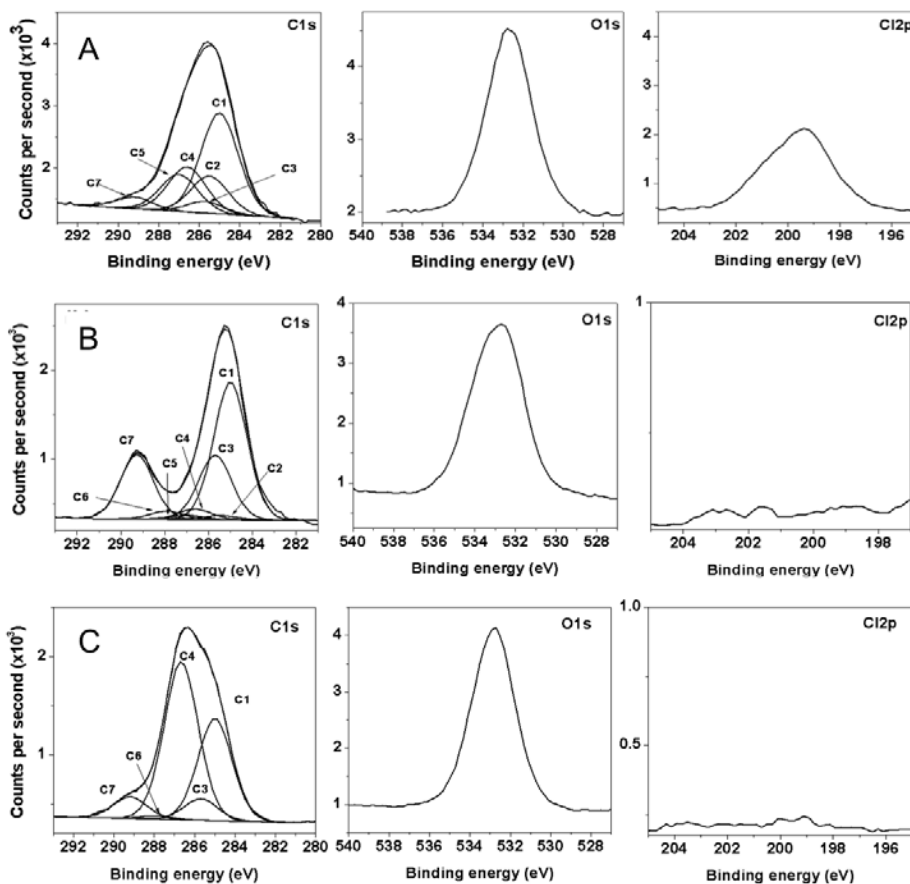
Figure 5.30: HR-XPS of a) PVC, b)PVC-*g*-AAc(20%), and c)PVC-*g*-PEGMA(16%)

Table 5.5: HR-XPS C1s breakdown

	PVC	PVC-*g*-AAc(20%)		[PVC-*g*-PEGMA(13%)]-*g*-AAc(12%)		PVC-*g*-PEGMA(16%)		[PVC-*g*-AAc(7%)]-*g*-PEGMA(20%)	
		C_{1s} concentrations (%)							
		Inner	*Outer*	*Inner*	*Outer*	*Inner*	*Outer*	*Inner*	*Outer*
C_1	41.3	55.1	46.7	57.0	58.4	28.3	33.3	33.3	41.6
C_2	13.3		1.5						
C_3	4.7	22.4	21.8	10.9	11.8	7.1	7.1	6.8	7.6
C_4	15.3		1.5						
C_5	18.6		3.6	21.1	14.5	55.9	51.5	48.6	42.1
C_6			2.8		3.5	1.7	1.1	4.5	1.1
C_7	4.7	22.5	21.9	11.0	11.9	7.1	7.1	6.8	7.6

Taking into consideration the differences between the percentages of C_4 and C_7 depending on whether PEGMA or AAc is grafted on the surface of the catheter, an iteration-based calculation was made to better understand the presence of each polymer on the surface. For these iterations, the C_4/C_7 ratio was first calculated for all the analysed samples and then an arbitrary fractional composition, x_{PAAc}, was assigned to calculate the contribution of PAAc towards the overall $(C_4/C_7)_{binary}$ ratio (Eq. 5.1),

$$x_{PAAc}((\frac{C_4}{C_7})_{binary}) = (\frac{C_4}{C_7})_{xPAAc} \qquad (5.1)$$

The expected contribution to the $(C_4/C_7)_{binary}$ ratio from PEGMA was then calculated using Eq. 5.2,

$$(\frac{C_4}{C_7})_{binary} - (\frac{C_4}{C_7})_{xPAAc} = (\frac{C_4}{C_7})_{xPEGMA} \qquad (5.2)$$

Then, the $(\frac{C_4}{C_7})_{xPEGMA}$ ratio was calculated again but this time using the corresponding compositional fraction of PEGMA (x_{PEGMA}; x_{PEGMA} = 1 - x_{PAAc}) and repeating the calculations from Eq. 5.1, but this time using the values from PEGMA,

$$x_{PEGMA}((\frac{C_4}{C_7})_{binary}) = (\frac{C_4}{C_7})_{xPEGMA} \qquad (5.3)$$

Then, the x_{PAAc} value was varied until $(\frac{C_4}{C_7})_{xPEGMA}$ calculated from Eq. 5.2 and Eq. 5.3 were equal, where the compositional fraction was converted to a composition percent. The results of these calculations are summarized in Table 5.6, where it is observed that although the compound that was grafted during the second step predominates at the surface, some of the initially grafted compound will also interact with the bodily tissue, albeit to a lesser extent, with [PVC-*g*-PEGMA(13%)]-*g*-AAc(12%) showing 85 and 77% AAc on the outer and inner surface, respectively; while [PVC-*g*-AAc(7%)]-*g*-PEGMA(20%) only had 25 and 2%.

Table 5.6: XPS breakdown analysis

Surface grafting composition analysis and atomic ratio for singly and binary grafted PVC catheters					
	PVC-*g*-AAc(20%)	PVC-*g*-PEGMA(16%)	[PVC-*g*-PEGMA(13%)]-*g*-AAc(12%)	[PVC-*g*-AAc(7%)]-*g*-PEGMA(20%)	
Ratio (%) of grafted PAAc (or PEGMA) to PVC suface	63	68	-	-	
Atomic ratio (C_5/C_7)	1/6	7.9/1	1/1.9	7.1/1	*Inner*
	1/6	7.3/1	1.2/1	1/5.5	*Outer*
Grafting ratio of AAc and PEGMA (%) — PAAc / PEGMA	-	-	77 / 23	2 / 98	*Inner*
Grafting ratio of AAc and PEGMA (%) — PAAc / PEGMA	-	-	85 / 15	25 / 75	*Outer*

It is important to mention that for these calculations it was assumed that there is not a significant difference among the grafting percentages used for the iterations.

5.2.8 SEM and AFM

The morphological surface roughness of PVC and various modified catheters is shown in the SEM images in Fig. 5.31. The surface of PVC and PVC-*g*-AAc(37%) is smooth, with the presence of AAc appearing to have made the material smoother because the AAc is grafting in bulk, thus providing a more homogenous coating. However, the PVC-*g*-PEGMA, [PVC-*g*-PEGMA]-*g*-AAc and [PVC-*g*-AAc]-*g*-PEGMA catheters all have a similarly rough surface with visible inter-twisted grooves. Therefore, the presence of PEGMA alone, because it predominantly grafts at the surface, gives the catheter a rougher surface. The catheter with the widest grooves is [PVC-*g*-AAc(16%)]-*g*-PEGMA(23%) (Fig. 5.31e). This type of surface could prove disadvantageous because the "empty" space between the grooves is big enough to allow bacteria, for example E. *coli* with dimensions of 2.5 x .8 μm (Howard, 2003), to penetrate those spaces.
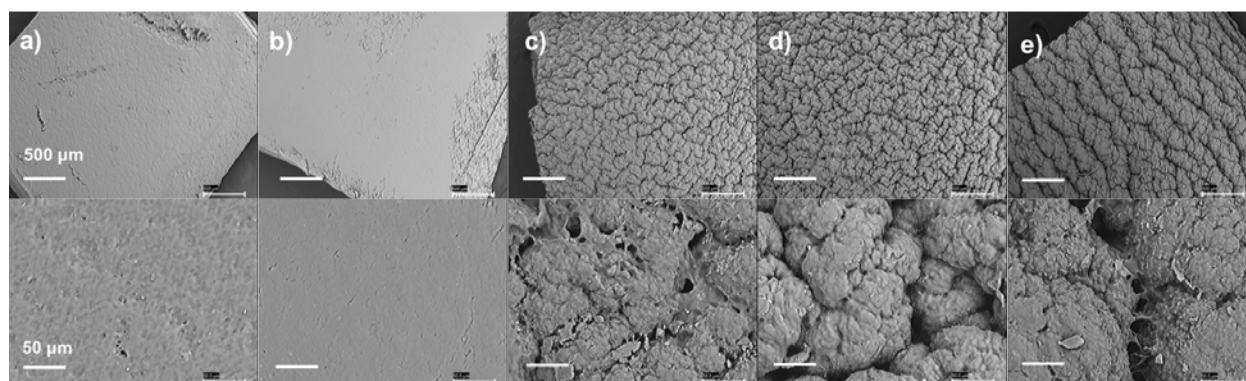
Figure 5.31: SEM images of a) PVC, b) PVC-*g*-AAc(37%), c) PVC-*g*-PEGMA(21%), d) [PVC-*g*-PEGMA(20%)]-*g*-AAc(14%) and e) [PVC-*g*-AAc(16%)]-*g*-PEGMA(23%) at 500 (top) and 50 (bottom) μm magnification.

5.3 Cytocompatibility

The cytocompatibility results (Table 5.7) show that after 24 h of exposure, the original PVC has 94 $\pm$ 7% cell viability, which is a value in accord with previous literature (Sastri, 2010). As the percentage of PEGMA grafted increases, so does the cell viability, with PVC-*g*-PEGMA(41%) reaching a value of 99 $\pm$ 1%. In the case of AAc grafted catheters, the cell viability remained within the range of the original PVC, even showing a considerable improvement for PVC-*g*-AAc(23%) with a 107 $\pm$ 6% cell viability, for low grafting percentages; however, the catheter with the highest amount of grafted AAc (44%) had a 67 $\pm$ 5% cell viability, which is incidentally the lowest value observed. This is perhaps not uncommon, as it has been studied that in certain instances high molecular weight PAAc could incite an immonulogical response (Topuzogullari *et al.*, 2013)

For the binary grafted catheters, the results of the [PVC-*g*-PEGMA]-*g*-AAc system resembled those of PVC-*g*-AAc, where the lower grafting percentages of AAc improved

the original catheter's cell viability. The [PVC-*g*-AAc]-*g*-PEGMA system did not show a significant improvement and it remained close to the original PVC cell viability range.

After 48 h, the cell viability of PVC dropped to a value of $73 \pm 4\%$, which is one of the lowest values recorded for all samples tested. Overall, although the cell viability of all samples decreased after 48 h, it remained above the value recorded for PVC. The one exception is the PVC-*g*-AAc(44%) catheter, which after 48 h had a cell viability of $69 \pm 2\%$; however, this catheter had already proven less cytocompatible at the 24 h mark and its cell viability did not change much after 24 h. From these results it can be gathered that the modified catheters are able to either maintain or improve upon the original catheter's cytocompatibility and they also retain it for prolonged periods of time.

Table 5.7: Cytocompatibility of PVC and modified catheters after 24 and 48 h exposure time

	Cytocompatibility	
	24 h	*48 h*
PVC	94 ± 7	73 ± 4
PVC-*g*-PEGMA(9%)	91 ± 3	81 ± 5
PVC-*g*-PEGMA(21%)	98 ± 6	89 ± 2
PVC-*g*-PEGMA(41%)	99 ± 1	83 ± 8
PVC-*g*-AAc(7%)	99 ± 11	83 ± 3
PVC-*g*-AAc(23%)	107 ± 6	90 ± 3
PVC-*g*-AAc(44%)	67 ± 5	69 ± 2
[PVC-*g*-PEGMA(11%)]-*g*-AAc(14%)	98 ± 16	92 ± 8
[PVC-*g*-PEGMA(15%)]-*g*-AAc(21%)	105 ± 6	85 ± 7
[PVC-*g*-AAc(11%)]-*g*-PEGMA(17%)	79 ± 8	72 ± 5
[PVC-*g*-AAc(14%)]-*g*-PEGMA(18%)	96 ± 4	78 ± 2
[PVC-*g*-AAc(18%)]-*g*-PEGMA(24%)	89 ± 16	84 ± 6

5.4 Drug loading and release studies

The uptake of the ciprofloxacin by different grafted catheters is shown in Fig. 5.32. Unlike PVC-*g*-PEGMA and PVC catheters, which did not load a significant amount of ciprofloxacin, catheters grafted with AAc were able to load better quantities of the drug, noting that as the AAc grafting percentage increased, so did the amount of ciprofloxacin that was loaded, with a PVC-*g*-AAc(36%) catheter loading 0.28 mg/g of ciprofloxacin in 48 h. Even catheters with as little as 7% AAc were able to load better amounts of the drug (0.13 g/mg) than PVC or PVC-*g*-PEGMA. The uptake of ciprofloxacin by the PVC-*g*-AAc catheters confirms that there is an interaction between the ciprofloxacin, a second generation fluoroquinolone with a secondary amine group (pKa = 6 to 8.8), and the ionized carboxylic acid groups of the PAAc.

In the case of the binary grafted catheters (although all the catheters had the ability to load the drug) the catheters that had PEGMA on the surface loaded the ciprofloxacin to a lesser extent than the PVC-*g*-AAc catheters, with a [PVC-*g*-AAc(15%)]-*g*-PEGMA(20%) catheter loading about 0.014 mg/g of ciprofloxacin, in comparison to the 0.23 mg/g loaded by PVC-*g*-AAc(15%). Increasing the AAc grafting percentage also increased the amount of drug loaded. The catheter with AAc grafted on its surface was able to load the drug much better than [PVC-*g*-AAc]-*g*-PEGMA catheters, but not as well as PVC-*g*-AAc. This difference in the single and binary grafted system is because, 1) there is a complexation between the poly(PEGMA) and PAAc chains which competes with the ionic interaction between the ciprofloxacin and PAAc, and 2) when PEGMA is primarily grafted on the surface it makes it difficult for the ciprofloxacin molecules to reach the ionized groups that are deeper within the polymer matrix, which is perhaps due to simple steric effects and/or PEG's inherent ability to prevent other molecules from attaching to its surface.
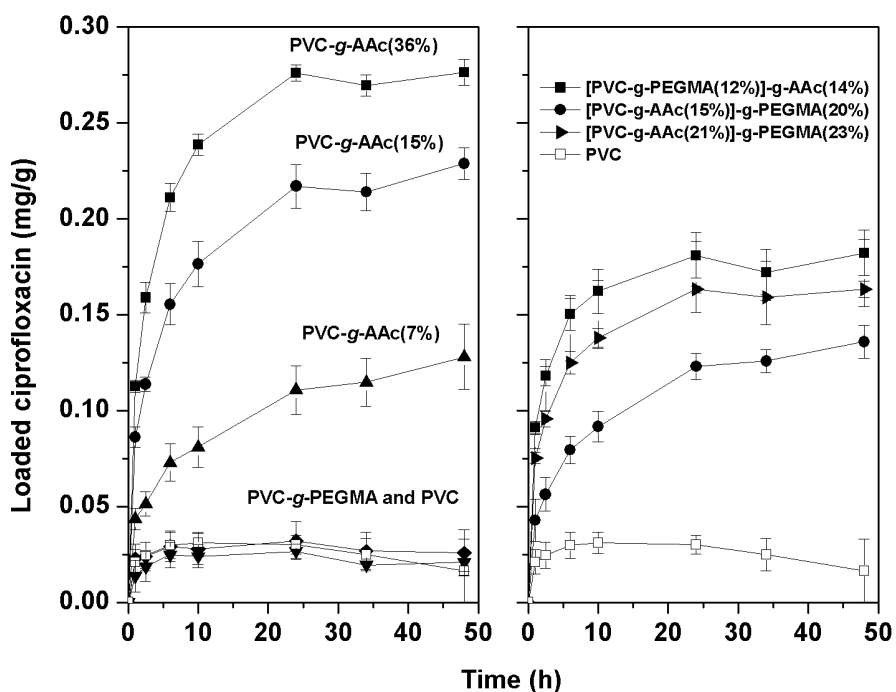
Figure 5.32: Ciprofloxacin loading profile for PVC, PVC-*g*-AAc, PVC-*g*-PEGMA, [PVC-*g*-PEGMA]-*g*-AAc, and [PVC-*g*-AAc]-*g*-PEGMA catheters in an aqueous ciprofloxacin solution.

A sustained drug release profile is observed when the swollen drug-loaded catheters are placed in the artificial urine release medium (pH 6) (Fig. 5.33). The PVC and PVC-*g*-PEGMA catheters released almost all of the drug that they had been able to load in almost 2 h. A similar release percentage was obtained for the binary grafted catheters;

however, these latter ones were able to load greater quantities of the drug. In 4 h, the PVC-*g*-AAc(36%) catheter only released about 50% of the drug it had initially absorbed because of the interactions between the amine groups of the ciprofloxacin and the carboxylic acid of the PAAc chains. The minimum inhibitory concentration (MIC) of ciprofloxacin against S. *aureus* and E. *coli* is 0.12-0.5 μg/mL and 0.004-0.015 μg/mL, respectively (Clinical & Institute, 2012). Therefore, if a 1 cm long piece of PVC-*g*-AAc(36%), with an approximate weight of 0.14 g, releases about 50% of the original drug loaded ($\sim$ 0.27 mg/g) in 4 h, meaning that it released about 0.019 mg of ciprofloxacin in the 5 mL of the release medium, it elutes ciprofloxacin amounts that fall above the MIC ranges for both E. *coli* and S. *aureus*. Even the PVC-*g*-AAc(7%), with a 90% release of the drug in 6 h, released $\sim$ 5 μg/mL of ciprofloxacin. Therefore, catheters of standard length (20-26 cm female; 40-45 cm male) will be able to release adequate amounts of the drug for prophylaxis.

This rapid release could prove advantageous because it has been studied that the attachment of bacteria to urinary catheters happens within the first hours after insertion, and the source of bacteria oftentimes comes from the patient's own skin (Jordan & Nicolle, 2014). One of the drawbacks of the observed 6 h sustained release of ciprofloxacin is that because there are several stages towards the development of a biofilm, for example it takes on average a catheterization period of 4 days for the risk of developing a CAUTI to become imminent (Barbadoro *et al.,* 2015), it would have been better to have a longer release profile. Nonetheless, PVC-*g*-AAc catheters did not release all of the ciprofloxacin they had loaded, meaning that the drug remains present in the catheter and could potentially prevent bacteria from attaching to the catheter's surface.
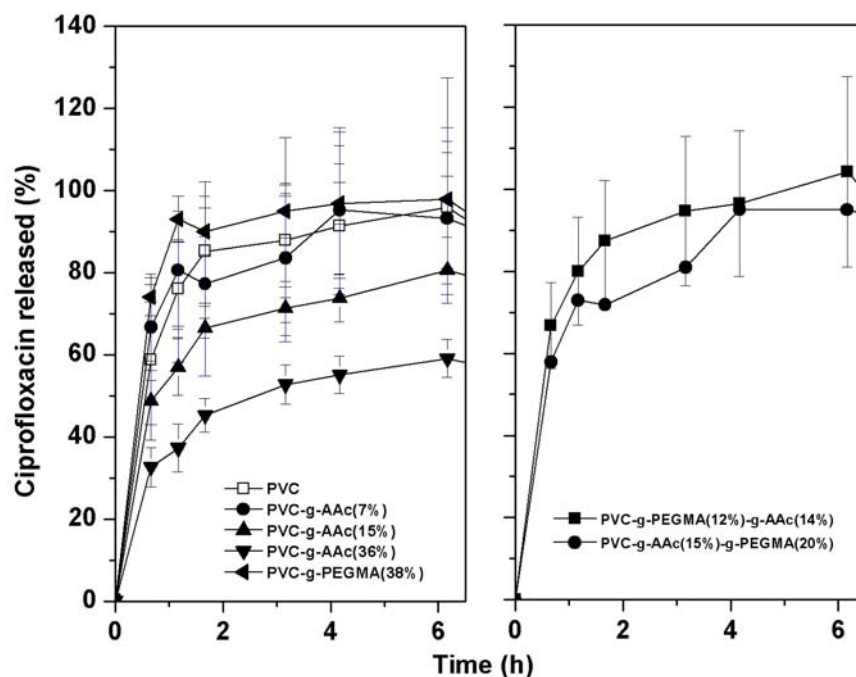
Figure 5.33: Ciprofloxacin controlled-release profile for PVC, PVC-*g*-AAc, PVC-*g*-PEGMA, [PVC-*g*-PEGMA]-*g*-AAc, and [PVC-*g*-AAc]-*g*-PEGMA catheters in an artificial urine medium at a pH of 6 and 37 °C.

5.5 Bacterial growth and adhesion

All of the drug-loaded catheters were able to prevent bacterial growth better than the original PVC catheter after a first and second challenge against freshly seeded bacteria (Table 5.8). However, none of the PVC-*g*-AAc catheters were able to prevent the growth of bacteria after a third challenge against *Escherichia coli*. Interestingly, even though they only loaded very small amounts of ciprofloxacin, PVC-*g*-PEGMA catheters prevented the growth of bacteria better than PVC-*g*-AAc catheters. This is perhaps because under dry conditions, the PVC-*g*-PEGMA catheters are able to better hold any drug that was *trapped* on the grafted PEGMA chains, which is not surprising given that PEG has been used to influence the pharmakocinetics of administered drugs because it can provide a shield for the drugs to have longer circulation times in the body (Know *et al.,* 2010). This is in comparison to PVC-*g*-AAc catheters, where perhaps because AAc grafts in bulk and it also swells significantly, under dry conditions most of the drug on its surface is quickly released and the rest of the drug deep inside the polymer matrix is unable to have an effect on the surrounding bacteria. This would also explain why the binary grafts were overall much better at preventing the growth of bacteria for both E. *coli* and S. *aureus*, as the greater amounts of loaded ciprofloxacin by the PAAc are better retained

62

by the PEGMA chains and thus allow the catheters to have antibacterial properties for prolonged periods.

Table 5.8: Inhibition rings against E. *coli* and S. *aureus* for pristine and modified PVC.

| | Diameter of inhibition rings (mm) | | | | | |
| | *Escherichia coli* | | | *Staphylococcus aureus* | | |
	1st challenge	2nd challenge	3rd challenge	1st challenge	2nd challenge	3rd challenge
PVC	10	0	0	10	0	-
PVC-*g*-PEGMA(38%)	30	17	9	20	15	-
PVC-*g*-PEGMA(20%)	26	10	11	17	6	-
PVC-*g*-PEGMA(10%)	28	5	5	10	0	-
PVC-*g*-AAc(36%)	25	15	0	17	0	-
PVC-*g*-AAc(15%)	19	17	0	21	8	-
PVC-*g*-AAc(7%)	26	12	0	16	0	-
[PVC-*g*-AAc(21%)]-*g*-PEGMA(23%)	27	16	14	17	0	-
[PVC-*g*-AAc(15%)]-*g*-PEGMA(20%)	25	16	9	15	13	-
[PVC-*g*-PEGMA(10%)]-*g*-AAc(15%)	31	20	21	20	13	-
[PVC-*g*-PEGMA(13%)]-*g*-AAc(15%)	30	27	12	18	15	-

The [PVC-*g*-PEGMA(10%)]-*g*-AAc(15%) catheter showed the greatest inhibition rings against both E. *coli* and S. *aureus* after every challenged to freshly seeded bacteria as illustrated in Fig. 5.34.
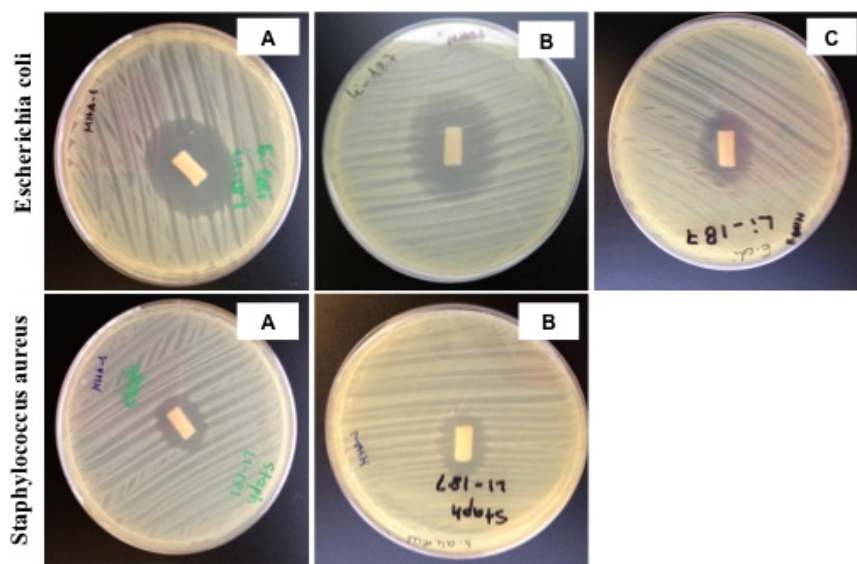
Figure 5.34: Bacteria growth-inhibition zones against *Escherichia coli* (top) and *Staphylococcus aureus* (bottom) after A) 24, B) 48 and possibly C) 72 h, each 24 h exposing the catheter to freshly seeded bacteria, for [PVC-*g*-PEGMA(10%)]-*g*-AAc(15%).

Because the attachment of bacteria on the surface of the catheter is the first step towards the development of a biofilm, drug-loaded catheters were submerged in a concentrated E. *coli* solution for 3 h in order to see if bacteria were able to attach to their surface (Fig. 5.35). All the catheters that had not been exposed to ciprofloxacin were not

able to prevent bacterial attachment. Furthermore, the only drug-loaded catheters that successfully prevented bacteria from attaching to their surface were the singly grafted PVC-*g*-AAc(36%) and PVC-*g*-PEGMA(20%) catheters. In the case of PVC-*g*-AAc(36%), because this catheter was able to load the greatest amount of drug ($\sim$ 0.27 mg/g) and it released only half of it in 3 h (Fig. 5.33) it was probably easier for it to shield against any bacteria that approached its surface for the chosen incubation period. In the case of the PVC-*g*-PEGMA(20%), there must be a synergetic effect between the small amounts of drug retained by the catheter and PEG's studied anti-biofouling properties that also allowed it to ward off any bacteria.

Even though by themselves PEGMA and AAc grafted catheters are able to prevent the adhesion of bacteria, the binary grafted catheters yielded similar results as PVC. Some possible reasons for this are that for example, the binary grafted catheters have a rougher surface where bacteria could more easily attach (Fig. 5.31). Furthermore, the binary grafted catheters were able to load less quantities of the drug and also quickly released it, similarly to PVC-*g*-AAc(7%). Another important factor that could explain why the binary grafted catheter could not prevent the attachment of bacteria is due to the complexation between the PAAc and poly(PEGMA) chains, which would inhibit PEG's mobility, which is an important factor that is believed to give PEG the ability to deflect the attachment of macromolecules.
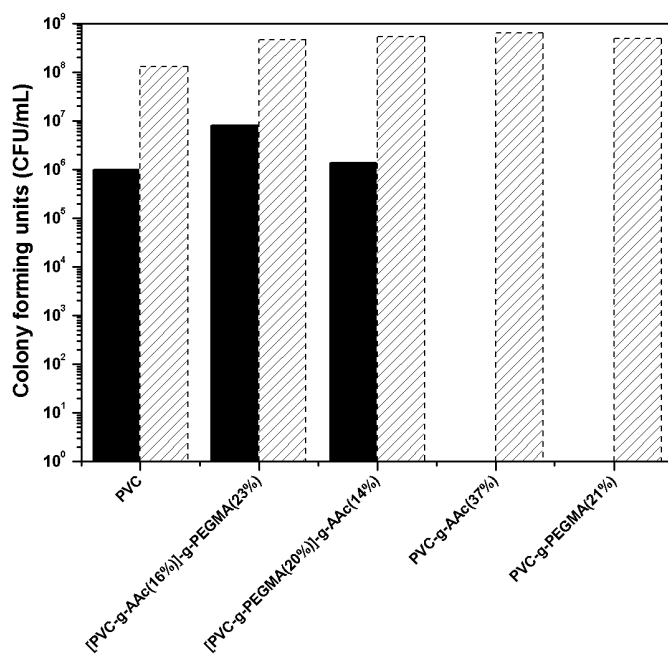
Figure 5.35: Bacterial adhesion test for catheters that had been exposed to water (shaded region) or a ciprofloxacin aqueous solution (black). The results are measured in CFUs taken from samples that had been placed in a concentrated *E. coli* solution for 3 h at 37 °C).

Chapter 6

Conclusions

In this work, the successful modification of catheters via grafting of AAc, PEGMA, or a combination of both compounds was accomplished. In the case of PVC-*g*-AAc, a wide range of grafting percentages (5-158%) was obtained using reaction times of 4 h and doses of up to 15 kGy. For PVC-*g*-PEGMA, the obtained grafting range fell between 10-25% and much longer reaction times, as well as irradiation doses, were needed. The binary grafted systems showed that the presence of either AAc or PEGMA on the surface of the catheter improved the grafting yield of the second compound and therefore lower irradiation doses and monomer concentrations were needed.

The modification of the catheters was confirmed through IR-spectroscopy, thermal analysis, SEM, and XPS. The IR analysis showed that in the binary grafted catheters the compound grafted during the second step was predominant on the surface, which was further confirmed by the XPS analysis. The XPS analysis also revealed that the grafting densities of the interior and outer surface of the catheter were similar, indicating that grafting was uniform throughout. The thermal analysis of the compounds showed that the modified catheters gained thermal stability, with AAc having a greater effect at providing this stability than PEGMA. Because the graft of AAc onto PVC was in bulk, the catheters had a more homogenous surface after grafting, which was observed in the SEM images. This was not the case for the PVC-*g*-PEGMA grafted catheters, where because PEGMA grafts primarily on the surface any catheter that had PEGMA also had a rougher surface. Although all the modified catheters were able to retain water, and those with AAc showed a swelling response to changes in pH, their lubricity did not improve.

From the biological analysis it was observed that for the prevention of bacterial adhesion, the singly-grafted catheters are preferred. Even catheters that were only grafted with PEGMA, and thus only loaded small quantities of ciprofloxacin (similar to pristine PVC), were able to prevent the growth of bacteria better than PVC-*g*-AAc catheters. In addition, PVC-*g*-PEGMA catheters were softer, as measured by a lower Young's modulus, which could prove advantageous in the industrial processes because PEGMA, in addition of acting as a biofouling agent, could play the role of the plasticizerer. Nonetheless,

because AAc is able to load greater quantities of the drug and does not release all of it within the first few hours, its role must not be undervalued. Furthermore, the presence of AAc on the surface of the catheter made it possible for PEGMA to be grafted using much lower radiation doses, thus preventing the catheter from degrading. It would be recommended for further studies to focus on catheters that are first grafted with less than 10% AAc, so that the catheter will not change much yet still have some ability to load slightly better quantities of the drug, and then between 10-20% PEGMA, because higher PEGMA grafting percentages lead to visibly rougher catheters.

Bibliography

1. Alcantar, N. A., Aydil, E. S. & Israelachvili, J. N. Polyethylen glycol-coated biocompatible surfaces. *Journal of Biomedical Materials Research* **51,** 343–351 (2000).

2. Arenas, E., Bucio, E., Burillo, G. & Lopez, G. P. Radiation grafting of poly(ethylene glycol) methacrylate onto poly(vinyl chloride) tubes. *Desinged Monomers and Polymers* **10,** 459–467 (2007).

3. Baccaro, S., Brunella, V., Cecilia, A. & Costa, L. Gamma irradiation of poly(vinyl chloride) for medical applications. *Nuclear Instruments and Methods in Physics Research B* **208,** 195–198 (2003).

4. Bank, B. L. & Brown, J. L. in *From natural and synthetic biomedical polymers* (eds Kumbar, S., Lurencin, C. T. & Deng, M.) (Elsevier Sciene, 2014).

5. Barbadoro, P. *et al. Catheter-associated urinary tract infection: role of the setting of catheter insertion* doi: 10.1016/j.ajic.2015.02.011. 2015.

6. Beloin, C., Renard, S., Ghigo, J. & Lebeaux, D. Novel approaches to combat bacterial biofilms. *Current Opinion in Pharmacology* **18,** 61–68 (2014).

7. Benarmer, S. *et al.* Radiation synthesis of chitosan beads grafted with acrylic acid for metal ions sorption. *Physics and Chemistry* **80,** 1391–1397 (2011).

8. Bhattacharya, A. & Misra, B. N. a. Grafting: a versatile means to modify polymers - techniques, factors, and applications. *Progress in Polymer Science* **29,** 767–814 (2004).

9. Biggin, H. C. in *Irradiation effects on polymers* (eds Clegg, D. W. & Collier, A. A.) (Elsevier Sciene, Essex, 1991).

10. Brooks, B. D., Brooks, A. E. & Grainger, W. D. in *Biomaterials associated infections: immunological aspects and antimicrobial strategies* (eds Moriarty, T. F., Zaat, S. A. J. & Busscher, H. J.) 455–483 (Springer, New York, NY, 2013).

11. Brooks, T. & Keevil, C. W. A simple artificial urine for the growth of urinary pathogens. *Letters in Applied Microbiology* **24,** 203–206 (1996).

12. Cadieux, P. & Carriveaue, R. in *Biomaterials and tissue engineering in urology* (eds Denstedt, J. & Atala, A.) 3–41 (Woodhead Publishing, 2009).

13. Chapiro, A. *Radiation chemistry of polymeric systems* (Interscience Publishers, 1962).

14. Chenoweth, C. E., Gould, C. V. & Saint, S. Diagnosis, management, and prevention of catheter-associated urinary tract infections. *Infectious Diseases Clinics of North America* **28,** 105–119 (2014).

15. Chenoweth, E. C. & Saint, S. Preventing catheter associated urinary tract infections in the intensive care unit. *Critical Care Clini* **29,** 19–32 (2013).

16. Chern, C. *Principles and Applications of Emulsion Polymerization* (Wiley, 2008).

17. Chopra, I. The increasing use of silver-based products as antimicrobial agents: a useful development or a cause for concern. *Journal of Antimicrobial Chemotherapy* **59,** 587–590 (2007).

18. Chutipongtanate, S. & Thongboonkerd, V. Systematic comparisons of artificial urine formulas for in vitro cellular study. *Analytical Biochemistry* **402,** 110–112 (2010).

19. Clinical & Institute, L. S. *Performance standards for antimicrobial susceptibility testing; twenty-second informational supplement* online. antimicrobianos.com.ar/ATB/wp-content/uploads/2012/11/M100S22E.pdf, 2012.

20. Costa, L., Brunella, V., Paganini, M. C., Baccaro, S. & Cecilia, A. Radical formation induced by gamma-radiation in poly(vinyl chloride) powerd. *Nuclear Instruments and Methods in Physics Research B* **215,** 471–178 (2004).

21. Danese, P. N. Antibiofilm approaches: prevention of catheter colonisation. *Chemistry and Biology* **9,** 873–880 (2002).

22. Davenport, K. & Keelye, F. X. Evidence for the use of silver-alloy-coated urethral catheters. *Journal of Hospital Infection* **60,** 298–303 (2005).

23. Dehn, R. W. & Asprey, D. P. *Essential clinical procedures* (Elsevier Health Sciences, 2013).

24. Desai, D. G., Liao, K. S., Cevallos, M. E. & Trautner, B. W. Silver or nitrofurazone impregnation of urinary catheters has a minimal effect on uropathogen adherence. *The Journal of Urology* **184,** 2565–2571 (2010).

25. DiTizio, V. *et al.* A liposomal hydrogel for the prevention of bacterial adhesion to catheters. *Biomaterials* **19,** 1877–1884 (1998).

26. Drobny, J. G. *Ionizing Radiation and Polymers* (Elsevier, Pennsylvania, 2013).

27. Ferraz, C. C., Varca, G. H. C., Ruiz, J., Lopes, P. S. & Mathor, M. B. Radiation-grafting of thermo- and pH responsie poly(N-vinylcaprolactam-co-acrylic acid) onto silicone rubber and polypropylene films for biomedical purposes. *Radiation Physics and Chemistry* **97,** 298–303 (2014).

28. Fisher, L. E. *et al.* Biomaterial modification of urinary catheters with antimicrobials to give long-term broadspectrum antibiofilm acivity. *Journal of Controlled Release* **202,** 57–64 (2015).

29. Fugaru, V., Bubueanu, G. & Tuta, C. Radiaton induced grafting of acrylic acid onto extruded polystyrene surface. *Radiation Physics and Chemistry* **81,** 1345–1348 (2012).

30. Glastrup, J. Degradation of polyethylene glycol. A study of the reaction mechanism in a model molecule: tetra ethylene glycol. *Polymer Degradation and Stability* **52,** 217–222 (1996).

31. Glinel, K., Thebault, P., Humblot, V., Pradier, C. M. & Jouenne, T. Antibacterial surfaces developed from bio-inspired approaches. *Acta Biomaterialia* **8,** 1670–1684 (2012).

32. Goddard, J. M. & Hotchkiss, J. M. Polymer surface modification for the attachment of bioactive compounds. *Progress in Polymer Science* **32,** 698–725 (2007).

33. Gonzales-Gomez, R., Ortega, A., Lazo, L. M. & Burillo, G. Retention of heavy metal ions on comb-type hydrogels base on acrylic acid and 4-vinylpyridine, synthesised by gamma radiation. *Physics and Chemistry* **102,** 117–123 (2014).

34. Griffith, D. P., Musher, D. M. & Itin, C. Urease: the preliminary cause of infection-induced urinary stones. *Current Opinion in Pharmacology* **18,** 61–68 (2014).

35. Gupta, B., Muzyyan, N., Saxena, S., Grover, N. & Alam, S. Preparation of ion exchange membranes by radiation grafting of acrylic acid on FEP films. *Radiation Physics and Chemistry* **77,** 42–48 (2008).

36. Gupta, B., Mishra, S. & Saxena, S. Preparation of thermosensitive membranes by radiation grafting of acrylic acid/N-isopropyl acrylamide binary mixture on PET fabric. *Radiation Physics and Chemistry* **77,** 553–560 (2008).

37. Hidzir, M. N., Hill, D. J. T., Martin, D. & Grondahl, L. Radiation-induced grafting of acrylic acid onto expanded poly(tetrafluoroethylene) membranes. *Polymer* **53,** 6063–6071 (2012).

38. Hien, H. Q., Phu, D. V., Duy, N. N. & Huy, H. T. Radiation grafting of acrylic acid onto partially deacetylated chitin for metal ion adsorbent. *Nuclear Instruments and Methods in Physics Research B* **236,** 606–610 (2005).

39. Hilbert, L. R., Bagge-Ravn, D., Kold, J. & Gram, L. Influence of surface roughness of stainless steel on microbial adhesion and corrosion resistance. *International biodeterioration and biodegradation* **52,** 175–185 (2003).

40. Hoffman, S. A. Stimuli-responsive polymers: biomedical application and challenges for clinical translation. *Advanced Drug Delivery Reviews* **65,** 10–16 (2013).

41. Holappa, S., Kantonen, L., Francoise, M. W. & Tehnhu, H. Self-complexation of poly(ethyelene oxide)-block-poly(methacrylic acid) studied by fluorescence spectroscopy. *Macromolecules* **37,** 7008–7018 (2004).

42. Honey, J. P., Rijo, J., Anju, A. & Anoop, K. R. Smart polymers for the controlled delivery of drugs - a concise review. *Acta Pharmaceutica Sinica B* **4,** 120–127 (2014).

43. Hosseinidoust, Z., Olsson, A. L. J. & Tufenkji, N. Going viral: designing bioactive surfaces with bacterophages. *Colloids and Surfaces B: bionterfaces* **124,** 2–16 (2014).

44. Howard, B. C. *E. coli in Motion* (Springer, New York, NY, 2003).

45. Hsu, L. C., Fang, J., Borca-Tasciuc, D. A., Worobo, R. W. & Carmen, I. M. Effect of micro- and nano scale topography on the adhesion of bacterial cells to solid surfaces. *Applied and Environmental Biology* **79,** 2703–2712 (2013).

46. Johnson, J. R., Johnston, B. D., Kuskowski, M. A. & Pitout, J. In vitro activity of available antimicrobial coated foley catheters against Escherichia coli, including strains resistant to extended spectrum cephalosporins. *Journal of Urology* **184,** 2572–2577 (2010).

47. Jordan, R. P. C. & Nicolle, L. E. in *Biofilms in infection and prevention control* (eds Percival, S., Williams, D., Cooper, T. & Randle, J.) (Elsevier, 2014).

48. Kato, K., Uchida, E., Kang, E., Uyuma, Y. & Ikada, Y. Polymer surface with graft chains. *Progress in Polymer Science* **28,** 209–259 (2003).

49. Kilonzo, M., Vale, L., Pickard, R., Lam, T. & N'Dow, J. Cost effectiveness of antimicrobial catheters for adults requiring short-term catheterisation in hospital. *European Urology* **66,** 615–618 (2014).

50. Kimono, H., Hashimoto, H., Nishimura, M., Monden, K. & Ono, N. Catheter-associated urinary tract infections: impact of catheter materials on their management. *International Journal of Antimicrobial Agents* **17,** 311–316 (2001).

51. Know, K., Hoogenboom, R., Fishcer, D. & Shuber, U. Poly(ethylene glycol) in drug delivery: pros and cons as well as potential alternatives. *Angewandte Chemie International Edition* **49,** 6288–6308 (2010).

52. Kowalczuk, D., Ginalska, G. & Golus, J. Characterization of the developed antimicrobial urological catheters. *International Journal of Pharmaceutics* **402,** 175–183 (2010).

53. Kubiak, K., Wilson, M. C. T., Mathia, T. G. & Carval, P. Wettability versus roughness of engineering surfaces. *Wear* **271** (2011).

54. Kuckling, D., Doering, A., Krahl, F. & Arndt, F. in *Polymers for Advanced Funtional Materials* (Elsevier, 2012).

55. Kumar, A., Srivastava, A., Gulaev, I. Y. & Mattiasson, B. Smart polymers: physical forms and bioengineering applications. *Progress in Polymer Science* **32,** 1205–1237 (2007).

56. Lebeax, D., Ghigo, J. & Beloin, C. Biofilm-related infections: bridging the gap between clinical management and fundamental aspects of recalcitrance toward antibiotics. *Microbiology and Molecular Biology Reviews* **78,** 510–543 (2014).

57. Li, X. *et al.* Preparation of super-hydrophobic poly(vinyl chloride) surface via solvent-nonsolvent coating. *Polymer* **47,** 506–509 (2006).

58. Lichter, J. A., Van Vliet, K. J. & Rubner, M. F. Desing of antibacterial surfaces and interfaces: polyelectrolyte multilayers as a multifunctional platform. *Macromolecules* **42,** 8573–8586 (2009).

59. Lim, K. *et al.* Development of a catheter functionalized by a polydopamine peptide coating with antimicrobial and antibiofilm properties. *Acta Biomaterialia* **15,** 127–138 (2015).

60. Matuschek, G., Milanov, N. & Kettrup, A. Thermoanalytical investigation for the recycling of PVC. *Thermochimica Acta* **361,** 77–84 (2000).

61. Maurer, J. J., Eustace, D. J. & Ratcliffe, C. T. Thermal characterization of poly(acrylic acid). *Macromolecules* **20,** 196–200 (1987).

62. Miller, A. A. Radiation chemistry of polyvinyl chloride. *Journal of Physical Chemistry* **63,** 1755–1759 (1959).

63. Mitik-Dineva, N., Wang, J., Stoddart, P. R., Crawford, R. J. & Ivanova, E. P. *Nanostructured surfaces control bacterial attachment* in *Nanoscience and nanotechnology* (2008), 25–29.

64. Mobley, H. L. T. & Warren, J. W. Urease-positive bacteriuria and obstruction of long-term urinary catheters. *Journal of Clinical Microbiology* **25,** 2216–2217 (1987).

65. Nho, Y. C. & Kwon, O. H. a. Blood compatibility of AAc, HEMA, and PEGMA-grafted cellulose film. *Radiation Physics and Chemistry* **66,** 299–307 (2003).

66. Nickel, J. C., Cristina, A. G. & Costerton, J. W. Electron microscopic study of an infected Foley catheter. *Canadian Journal of Surgery* **28,** 50–54 (1985).

67. Nowatzki, P. J. *et al.* Salicylic acid-releasing polyurethane acrylate polymers as anti-biofilm urological catheter coatings. *Acta Biomaterialia* **8,** 1869–1880 (2012).

68. Ortega, A., Alarcon, D., Munoz-Munoz, F., Fontecha-Garzon, G. & Burillo, G. Radiation grafting of pH-sensitive acrylic acid and 4-vinyl pyridine onto nylon-6 using one- and two-step methods. *Radiation Physics and Chemistry* **109,** 6–12 (2015).

69. Ortega-Reyes, F. in *Smart Polymers and their Applications* (eds Aguilar De Armas, M. R. & Roman, J. S.) (Woodhead Publishing, 2014).

70. Pasanphan, W., Rattanawongwiboon, T. & Rimdusit, P. Radiation-induced graft copolymerization of poly(ethylen glycol) monomethacrylate onto deoxycholate-chitosan nanoparticles as a drug carrier. *Radiation Physics and Chemistry* **94,** 199–204 (2014).

71. Peppas, A. N., Keys, B. K., Torres-Lugo, M. & Lowman, A. M. Poly(ethylene glycol)-containing hydrogels in drug delivery. *Journal of Controlled Release* **62,** 81–87 (1999).

72. Perera, M. C. S. & Hill, D. J. T. in *Polymer Handbook* (eds Brandrup, J. & Immergut, E. H.) 3rd (John Wiley and Sons, New York, NY, 1989).

73. Ramirez-Fuentes, Y. S., Bucio, E. & Burillo, G. Radiation-induces grafting of N-isopropylacrylamide and acrylic acid onto polypropylene films by two step method. *Nuclear Instruments and Methods in Physics Research* **265,** 183–186 (2007).

74. Ratgeber, S., Pakula, T., Will, A., Matyjaszewski, K. & Beers, K. On the shape of bottle-brush macromolecules: systematic variation of architectural parameters. *The Journal fo Chemical Physics* **122** (2005).

75. Ratner, D. B., Hoffman, S. A., Schoen, J. F. & Lemons, E. J. *Biomaterials Science: an introduction to materials medicine* (Academic Press, 2012).

76. Riley, D. K., Classen, D. C., Stevens, L. E. & Burke, J. P. A large randomized clinical trial of a silver-impregnated urinary catheter: lack of efficacy and staphylococcal superinfection. *American Journal of Medicine* **98,** 349–356 (1995).

77. Rupp, M. E. *et al.* Effect of silver-coated urinary catheters: efficacy, cost-effectiveness, and antimicrobial resistance. *American Journal of Infection Control* **32** (2004).

78. Saint, S. & Chenoweth, C. E. Biofilms and catheter-associated urinary tract infections. *Infectious Diseases Clinics of North America* **29,** 19–32 (2013).

79. Sastri, R. V. *Plastics in medical devices: properties, requirements and applications* 2nd ed. (William Andrew Applied Science Publishers, 2010).

80. Seddiki, O., Harnagea, L., Levesque, D., Mantovani, F. & Rosei, F. Evidence of antibacterial activity on titanium surfaces through nano textures. *Applied Surface Science* **308,** 275–284 (2014).

81. Soshami-Regev, G., Ko, M., Crowe, A. & Av-Gay, Y. Comparative efficacy of commercially available and emerging antimicrobial urinary catheters against bacteriuria caused by E. coli in vitro. *Journal of Urology* **78,** 334–339 (2011).

82. Soto, S. M. Importance of biofilms in urinary tract infections: new therapeutic approaches. *Advances in Biology* **2014,** 1–13 (2014).

83. Spinks, J. W. T. & Woods, R. J. *Introduction to radiation chemistry* 3rd ed. (Wiley-Interscience, 1990).

84. Stickler, D. & Feneley, R. in *Biomaterials associated infections: immunological aspects and antimicrobial strategies* (eds Moriarty, T. F., Zaat, S. A. J. & Busscher, H. J.) 455–483 (Springer, New York, NY, 2013).

85. Stoodley, L. H., Costerton, J. W. & Stoodley, P. Bacterial biofilms: from the natural environment to infectious diseases. *Microbiology* **2,** 94–108 (2004).

86. Tasaki, K. Poly(oxyethylene)-water interactions: a molecular dynamic study. *Journal of the American Chemical Society* **119,** 8459–8469 (1996).

87. Temenoff, J. S. & Mikos, A. G. *Biomaterials: the intersection of biology and materials science* (Pearson Prentice Hall, New Jersey, 2008).

88. Tenke, P. *et al.* European and Asian guidelines on management and prevention of catheter-associated urinary tract infections. *International Journal of Antimicrobial Agents* **31S,** S68–S78 (2008).

89. Topuzogullari, M. *et al.* Conjugation, characterization and toxicity of lipophosphoglycan-polyacrylic acid conjugate for vaccination against leishmaniasis. *Journal of Biomedical Science* **20,** 35 (2013).

90. Williams, D. F. *The Williams dictionary of biomaterials* (Liverpool University Press, 1999).

91. Yang, C. *et al.* Water dispersible polytetrafluoroethylene microparticles prepared by grafting of poly(acrylic acid). *Physics and Chemistry* **103,** 103–107 (2014).

92. Ye, Q. & Zhou, F. in *Antifouling surfaces and materials, from land to marine environment* (ed Zhou, F.) (Springer, Berlin, 2015).

93. Yu, H., Huang, J. & Chang, P. R. in *Cellulose-Based Graft Copolymers* (ed Thakur, K. V.) 497–518 (CRC Press, 2015).

94. Zygoura, D. P., Paleologos, E. K. & Kontaminas, M. G. Migration levels of PVC plasticisers: effect of ionizising radiation treatment. *Food Chemistry* **128,** 106–113 (2011).

Singly and binary grafted poly(vinyl chloride) urinary catheters that elute ciprofloxacin and prevent bacteria adhesion

Luisa Islas [a], Carmen Alvarez-Lorenzo [b,*], Beatriz Magariños [c], Angel Concheiro [b], Luis Felipe del Castillo [d], Guillermina Burillo [a,**]

[a] Departamento de Química de Radiaciones y Radioquímica, Instituto de Ciencias Nucleares, Universidad Nacional Autónoma de México, Ciudad Universitaria, 04510 México D.F., Mexico
[b] Departamento de Farmacia y Tecnología Farmacéutica, Facultad de Farmacia, Universidad de Santiago de Compostela, 15782 Santiago de Compostela, Spain
[c] Departamento de Microbiología y Parasitología, Facultad de Biología CIBUS, Universidad de Santiago de Compostela, 15782 Santiago de Compostela, Spain
[d] Instituto de Materiales, Universidad Nacional Autónoma de México, Ciudad Universitaria, 04510 México D.F., Mexico

ABSTRACT

Acrylic acid (AAc) and poly(ethylene glycol) methacrylate (PEGMA) were singly and dually grafted onto poly(vinyl chloride) (PVC) urinary catheters with the aim of preventing biofouling by endowing the catheters with the ability to load and release antimicrobial agents and to avoid bacteria adhesion. The polymers were grafted applying an oxidative pre-irradiation (^{60}Co source) method in two steps. Grafting percentage and kinetics were evaluated by varying the absorbed pre-irradiation dose, reaction time, monomer concentration, and reaction temperature. Catheters with grafting percentages ranging from 8 to 207% were characterized regarding thermal stability, surface hydrophilicity, mechanical properties, swelling, and lubricity. The modified catheters proved to have better compatibility with fibroblast cells than PVC after long exposure times. Furthermore, grafted catheters were able to load ciprofloxacin and sustained its release in urine medium for several hours. Ciprofloxacin-loaded catheters inhibited the growth of *Escherichia coli* and *Staphylococcus aureus* in the catheter surroundings and prevented bacteria adhesion.

© 2015 Elsevier B.V. All rights reserved.

1. Introduction

Nearly 20% of hospitalized patients require at a certain stage a urinary catheter (Stickler, 2008). Despite their value in the management of a variety of diseases and conditions, the use of this and other types of catheters is not exempt of risks (Public Health Agency of Canada, 2013; Greene et al., 1998). Worldwide, health care-associated infections affect 30% of the patients in intensive care units (World Health Organization, 2011). Infections associated to urinary catheters represent 95% of the total urinary tract infections (UTIs) and account for 70% of health care-associated infections (Chenoweth et al., 2014; Nicolle, 2014). Patient morbidity and health costs have prompted the search of novel ways to prevent them (Chenoweth et al., 2014).

Catheter associated UTIs (CAUTIs) can be caused by a variety of microorganisms, prominently *Pseudomonas aeruginosa*, *Enterococcus faecalis*, *Escherichia coli*, *Proteus mirabilis* and *Staphylococcus aureus*, among others, that ascend the urethra and reach the bladder by forming a biofilm on the inner and outer surface of the catheter (Nicolle, 2014; Stickler, 2008). Once the bacteria anchor to the surface of the medical device and the biofilm has developed, their eradication becomes difficult as they show an increased tolerance to antibiotics and it takes longer for any biocide to penetrate the biofilm structure (Costerton et al., 1999; Denise, 2002; Donland, 2002; Tenke et al., 2006). In addition, certain bacteria in the biofilm (e.g., *P. mirabilis*) produce urease, an enzyme that yields enhanced amounts of free ammonia, which in turn increases the pH and favors the precipitation of minerals (struvite and apatite) that cause catheter blockages (Stickler, 2008). A blocked catheter may become too abrasive for the urethra and the bladder mucosa, causing additional problems (Tenke et al., 2006).

Commonly, the therapy for patients that develop a CAUTI involves the removal/replacement of the catheter and systemic treatment with antibiotics for a prolonged time, which may cause

collateral effects. Thus, prophylaxis has gained an increasing attention. In addition to the still not fully explored potential of biological weapons (specific bacteriophages and bacterial strains) (Hosseinidoust et al., 2014), chemical surface modification of catheters offers a wide range of possibilities for preparing anti-biofouling materials (Shah et al., 2013). Approaches to prevent biofilm formation can be classified into three large groups: (i) anti-adhesion surfaces, mainly through changes in the charge or hydrophilicity of the material to avoid attachment of micro-organisms; (ii) contact-killing surfaces, via functionalization with components that have biocidal moieties; and (iii) biocide-leaching materials, which release antimicrobial agents to the close surroundings of the catheter (Alvarez-Lorenzo and Concheiro, 2013; Lichter et al., 2009). Several polymers have been grafted onto implantable materials to accomplish any of these purposes. For example, poly(ethylene glycol) (PEG), along with its derivatives, has been shown to prevent bacterial and protein adhesion both in vitro and in vivo(Kingshott et al., 2003; Saldarriaga-Fernandez et al., 2010). Grafting of poly(acrylic acid) (PAA), a pH-responsive polymer (Aguilar et al., 2007), has been shown to be suitable both (i) to endow a material's surface with pH-responsive immobiliza-tion/release of different therapeutic substances through changes in swelling or affinity, and (ii) to tune the overall surface charge of the material in order to regulate bacterial adhesion (Asadinezhad et al., 2010; Garcia-Vargas et al., 2014; Gasparrini et al., 1980; Gratzl et al., 2014; Ping et al., 2011).

In the present work, poly(vinyl chloride) (PVC) urinary catheters were modified with poly(ethylene glycol) methacrylate (PEGMA) and acrylic acid (AAc), using an ionizing radiation source of ^{60}Co, to endow the catheters with dual abilities: prevention of bacterial adhesion and release of antimicrobial agents (e.g., ciprofloxacin), which may have synergic effects on the avoidance of bacteria biofilms. It has been previously observed that pre-incubation of urinary silicone latex catheters with a concentrated ciprofloxacin solution (0.05–0.10 mg/mL) caused a 99% reduction in the number of adherent *P. aeruginosa* (Reid et al., 1994). Moreover, ciprofloxacin concentrations even below the minimum inhibitory concentration (MIC) have been shown effective at reducing adherence, which could avoid potential problems of resistance during short-term low-dosage therapy. Nevertheless, most materials used to prepare indwelling medical devices (as is the case of PVC) have no sufficient affinity for ciprofloxacin and cannot uptake prophylactic doses. Grafting of AAc may provide the required affinity. Mono and binary grafted materials were prepared through the oxidizing pre-irradiation method in order to elucidate the role that PEGMA and PAAc may play on the catheter performance. Compared to other grafting methods, advantages of using ionizing radiation include absence of chemical initiating agents and catalysts, high reproducibility, and convenience for scaling up (Drobny, 2013; Pande et al., 1995). Grafting percentage and kinetics were investigated by varying the temperature, absorbed pre-irradiation dose, reaction time, and monomer or polymer concentrations. Water was chosen as the sole reaction medium for all AAc and PEGMA grafting experiments because PVC catheters contain plasticizers, which are known to leach in the presence of organic solvents (Zygoura et al., 2010). The modified catheters were then characterized regarding cytocompatibility, lubricity, loading and release of ciprofloxacin, and inhibition of bacterial growth and adhesion.

2. Experimental

2.1. Materials

PVC urinary catheters (diameter 3 mm, thickness 0.5 mm; Biçakcilar, Turkey) were cut into 2 cm pieces and washed in methanol for 24 h, exchanging the medium after 3, 6, and 18 h. The catheter pieces were dried in a vacuum desiccator at room temperature for 24 h, and then in a vacuum oven at 38 °C for 6 h. Acrylic acid (AAc) and poly(ethylene glycol) methacrylate (PEGMA, M_n 360) were from Sigma–Aldrich (St. Louis, MO, USA) and distilled before using. For the artificial urine medium, urea, creatinine, ammonium chloride, and sodium citrate were from Sigma–Aldrich (Madrid, Spain); calcium chloride from Scharlau (Barcelona, Spain); potassium chloride, magnesium sulfate hepta-hydrate, and sodium chloride from Panreac (Barcelona, Spain); and sodium phosphate monobasic hydrate and sodium phosphate dibasic dihydrate were from Merck (Madrid, Spain). Ciprofloxacin HCl Ph. Eur. was from Fagron Iberica (Barcelona, Spain). Agar technical was from Biolife (Milano, Italy). The cell proliferation kit (MTT) was from Roche (Germany). Fetal bovine serum (FBS), Dulbecco's Modified Eagle Medium F12Ham (DMEM F12Ham) and antibiotic solution (penicillin 10,000 units/mL and streptomycin 10.00 μg/mL) were from Invitrogen Corporation (Carlsbad, CA, USA).

2.2. Grafting of AAc or PEGMA onto PVC catheter (PVC-g-AAc or PVC-g-PEGMA)

Pieces of PVC catheters (2 cm) were placed inside open glass-ampoules and irradiated with a ^{60}Co gamma-ray ionizing radiation source (GammaBeam 651 PT from Nordion Co., Canada). Then, an AAc (10, 30 or 50% v/v) or PEGMA (14% v/v) aqueous solution (5 mL) was added to the glass ampoules, which were bubbled with argon for 10 min and sealed. For AAc grafting, the glass ampoule was placed in an iced water bath (5 °C) while it was being bubbled to prevent any homopolymerization. After air removal, the sealed glass ampoules were placed in a hot water bath at a set temperature for time periods ranging from 1 to 4 h. Afterwards, the catheters were washed with distilled water (minimum 48 h) to remove any non-grafted homopolymer and unreacted monomer. Finally, the catheters were dried under vacuum at 38 °C. The grafting percentage was calculated as follows,

$$G(\%) = \left(\frac{W_f - W_o}{W_o} \right) \times 100 \tag{1}$$

where W_f is the weight of the grafted catheter, and W_o is the initial weight of the dry catheter.

2.3. Grafting of AAc onto PVC-g-PEGMA and of PEGMA onto PVC-g-AAc

For the binary graft, the aforementioned process was repeated by exposing PVC-*g*-AAc and PVC-*g*-PEGMA pieces to γ-ray radiation, followed by immersion into an aqueous PEGMA or AAc solution, respectively, bubbled with argon and then heated. The grafting percentage was calculated using Eq. (1), W_o being the weight of the formerly grafted PVC-*g*-AAc or PVC-*g*-PEGMA catheter.

2.4. Physical and physicochemical characterization

A PerkinElmer Spectrum 100 spectrometer (PerkinElmer Cetus Instruments, Norwalk, CT) was used to record the FTIR-ATR spectra of the pristine and modified catheters. Thermal decomposition was evaluated in a TGA Q50 (TA Instruments, New Castle, DE, USA) under a nitrogen atmosphere for a temperature range between 35 °C and 800 °C.

A DSA 100 (Krüss GmbH, Hamburg, Germany) was used to measure the surface water contact angle. The modified catheters were first swollen in distilled water for 24 h, and then opened by cutting through one of their sides (parallel to the length). The opened catheters were flattened by placing them in-between two

clean glass slides (clamped), and dried in a vacuum oven for 8 h at 40 °C. The contact angle was measured immediately after the water droplet touched the surface of the catheter and 30 s later. All measurements were repeated 5 times at different surface points. Mechanical properties of pristine and grafted catheters (flattened as above; 3×1 cm) were analyzed using a DMA Q800 (TA Instruments, New Castle, DE, USA) in air at 28 °C.

Lubricity of 6-cm long catheter pieces (previously wetted for 30 s or swollen for 4 h in water) was measured using a texture analyzer (TA.XT plus, Stable Micro Systems, Surrey, UK). Each catheter piece was screwed to a bolt fixed to a cylindrical aluminum probe (Ref. P/20) and lowered at 5 mm/s into agar (1% w/v in purified water) to a depth of 20 mm. The sample remained inside the agar for 120 s and then it was removed at 5 mm/s (Jones et al., 2001). The forces required to insert and to withdraw each catheter into/from agar were recorded. All experiments were carried out in triplicate at 20 °C. Agar medium was prepared by dispersing 10 g of agar in 1 L of boiled water, which was maintained under mechanical stirring (300 rpm) at 60 °C for 60 min, and then poured into plastic containers (125 mL capacity) and stored for 48 h at 5 °C. Agar containers were removed from the fridge 2 h before the texture tests.

The surface roughness of the samples was analyzed using an ambient scanning electron microscope (Zeiss EVOL515, Madrid, Spain), at magnifications of 100, 300, 500, and $1000\times$.

2.5. Equilibrium swelling time and critical pH

Dried modified catheters were immersed in distilled water at 18 °C for 15 min, and then they were removed, gently padded with a paper towel, weighted and placed back in water. The process was repeated every 15 min up to an hour and then every 30 min, until a constant swelling weight was obtained. The percent of swelling was calculated using the following equation,

$$S(\%) = \left[\frac{(W_s - W_d)}{W_d} \right] \times 100 \qquad (2)$$

where W_d and W_s represent the weights of dried and swelled catheter, respectively. Swelling in artificial urine was measured using the same protocol. Artificial urine was prepared by adapting two different formulas (Brooks and Keevil, 1996; Chutipongtanate and Thongboonkerd, 2010) as follows: urea 170 mM, creatinine 7 mM, $Na_3C_6H_5O_7$ 2 mM, NaCl 90 mM, $MgSO_4$ 2 mM, $NaHCO_3$ 2 mM, Na_2SO_4 10 mM, NaH_2PO_4 3.6 mM, Na_2HPO_4 0.4 mM, NH_4Cl 15 mM, and $CaCl$ 2.5 mM in purified water (MilliQ®, Millipore, Madrid, Spain). The pH was adjusted to 6 with a 0.1 M HCl solution.

The pH critical point was determined by placing the catheters in buffer solutions of pH ranging from 2.5 to 12, for a period of 24 h at 20 °C. The buffer solutions were prepared mixing a 0.2 M boric acid/0.05 M citric acid aq. solution with a 0.1 M trisodium phosphate dodecahydrate aq. solution, at various proportions.

2.6. Cytocompatibility

Tests were conducted in vitro using BALB 3T3 mouse fibroblast clone A31 cells (ATCC® CCl-163™; Manassas, VA, USA). The catheters (3×1 mm rectangular strips) were previously washed for 48 h in 20 mL of sterile phosphate buffer saline solution pH 7.4, then in purified water for 24 h, and finally dried for 30 h at 40 °C. Afterwards, they were UV irradiated for 2 min and left in 300 μL of culture medium (DMEM F12 Ham supplemented with 10% FBS and 1% of the antibiotic solution) at 37 °C for 24 h. 100 μL of the medium that had been in contact with the samples were poured onto 100 μL of a BALB/3T3 cell suspension (200,000 cell/mL) in DMEM F12Ham supplemented with 10% FBS and 1% of an antibiotic solution, and seeded in 96-well plates. The plates were incubated

during 24 or 48 h (37 °C, 5% CO_2, 90% RH). Afterwards, the culture medium was replaced with 100 μL of fresh medium, and 10 μL of the reagent 1 of the MTT kit were added. Next steps and cell viability estimation were carried out as described by Garcia-Vargas et al. (2014).

2.7. Ciprofloxacin loading

Pieces (1 cm long) of pristine and grafted catheters were placed in 5 mL of ciprofloxacin aqueous solution (0.012 mg/mL; protected from light), and the absorbance at 271 nm was monitored for 48 h. The amount of drug loaded was calculated from the difference between the initial and final concentrations of ciprofloxacin in the loading medium. The experiments were carried out in triplicate.

2.8. Ciprofloxacin release

Ciprofloxacin-loaded catheter pieces were taken out of the drug solution and gently padded with adsorbing paper to remove any excess solution. They were then placed in 5 mL of artificial urine at 37 °C under constant magnetic agitation and protected from light for 48 h. Samples of the release medium were taken at regular time intervals to measure the absorbance at 273 nm, and immediately returned to the corresponding vials.

2.9. Microbiological tests

Non-loaded and ciprofloxacin-loaded catheters were challenged against *S. aureus* (ATCC 25923) and *E. coli* (ATCC 11229), and inhibition zones and bacteria adhesion were recorded. For the inhibition growth tests, the sample piece (1 cm in length) was placed in a Petri dish containing Müeller-Hinton agar that had been seeded with either *S. aureus* or *E. coli*. The plates were kept at 37 °C for 24 h and then assessed for inhibition zones. The samples that displayed activity against the bacteria were then transferred to a new plate (with freshly seeded bacteria), and the process was repeated again for a third time if the samples continued to exhibit antimicrobial activity (Garcia-Vargas et al., 2014).

For bacterial adhesion tests, catheter pieces (1 cm in length) were immersed in either water or ciprofloxacin solution (0.012 mg/mL) and autoclaved for 20 min at 120 °C. The catheters were then left in their respective medium until tested (maximum for 5 days). *E. coli* was cultured in trypticase soy agar (TSA) at 37 °C for 24 h. The catheter pieces were then transferred to vials containing 2 mL of *E. coli* solution in trypticase soy broth (TSB; 8×10^8 CFU/mL) and cultured at 37 °C for 3 h under static conditions. After incubation, the catheters were washed three times with phosphate buffer (PBS) solution to remove any non-adhered bacteria, and then placed in 2 mL of a sterile PBS and sonicated with a Bronson Sonifier 250 for 5 min to suspend adhered bacteria. The suspensions were then spread on TSA plates, and the CFUs were measured after 24 h of incubation at 37 °C (Garcia-Vargas et al., 2014).

3. Results and discussion

3.1. Mono and binary grafting

Functionalization of PVC was carried out by applying a pre-irradiation method in the presence of air, which led to the formation of peroxides and hydroperoxides suitable for grafting of AAc or PEGMA in a second step. This approach minimizes the homopolymerization of the monomer in the reaction medium. Pre-irradiation doses of 5–15 kGy were chosen to minimize the degradation of the PVC backbone (Rakita and Foure, 1987). The catheters were initially grafted solely with AAc (Fig. S1, Supporting

information). In general, the grafting percentage increased with the reaction time and the dose rate (Fig. S1a). For a 10 kGy pre-irradiation dose, the grafting percentage leveled off after 1 h, staying within the 50–65% range, and then increased again after 4 h attaining a maximum of 133%. For a pre-irradiation dose of 15 kGy, the maximum grafting percentage was 158% at a reaction time of 4 h. Lower pre-irradiation doses led to a slower grafting of the monomer onto the PVC backbone.

As the amount of grafted AAc increased, the catheters grew in size, suggesting that the grafting happened in both surface and bulk. The increase in surface area of the catheters was proportional to the AAc grafting percentage (Fig. S1b). A large change in dimensions and other physical parameters may not be desirable for the manufacturing of the catheters. Therefore, for the present application low AAc grafting levels (below 50%) were chosen for subsequent experiments.

Once the PVC-g-AAc graft kinetics was characterized, PEGMA was grafted onto either PVC or PVC-g-AAc catheters. In a first trial, the catheters were pre-irradiated with a dose of 60 kGy in order to evaluate the maximum grafting yield of the procedure (despite potential degradation of the substrate). PEGMA grafting onto PVC reached 10% at 5 h and a maximum of 26% after 24 h (Fig. 1a), which is in agreement with the literature (Arenas et al., 2007). For PVC-g-AAc, the grafting of PEGMA occurred faster and to a greater extent (Fig. 1a), with a maximum PEGMA grafting of 56% after 10 h. PAAc on the surface of the PVC-g-AAc catheter allowed the creation of a higher number of active sites suitable for grafting initiation. Furthermore, the PVC-g-AAc catheter swelled in water, which

facilitated the diffusion of PEGMA into the catheter. Nevertheless, for catheters with more than 20% AAc graft, the percentage of PEGMA grafted onto PVC-g-AAc reached a plateau (Fig. 1b) despite that the catheters swelled more as the AAc content was greater. This finding suggests that PEGMA grafting mainly occurs at the surface, and not within the swollen catheter. As expected from previous experiments, at this working pre-irradiation dose (60 kGy) the catheter turned an orange color after being heated, indicating degradation due to conjugated bonds formed in the PVC backbone with release of HCl. To avoid this problem, subsequent experiments were carried out with lower pre-irradiation doses: 10 and 40 kGy. Pre-irradiation at 40 kGy led to similar grafting percentages than those recorded for samples pre-irradiated at 60 kGy probably due to a saturation of the substrate with peroxides and hydroperoxides (Fig. 1a). As the irradiation dose decreased more, PEGMA grafting onto PVC-g-AAc(10%) diminished due to a lower concentration of radicals. Nonetheless, even with a pre-irradiation dose of 10 kGy, PEGMA could be successfully grafted up to a maximum of 20% in 4 h. Altogether, by using a pre-irradiation dose of 10 kGy to graft PEGMA, the catheter was irradiated with a total dose of 15 kGy (5 kGy to graft AAc) minimizing PVC degradation.

The binary graft was also prepared in the opposite sequence; namely, PEGMA was first grafted to PVC and then AAc was grafted to PVC-g-PEGMA in order to study the effect that PEGMA may have on the AAc grafting. As can be seen in Fig. 2, when PEGMA was present, the graft percentage of AAc increased dramatically; in one hour, the AAc grafting was 8% onto PVC and 81% onto PVC-g-PEGMA(10%) for a pre-irradiation dose as low as 5 kGy and a fixed AAc concentration of 50% (v/v) in the reaction medium. The curve for grafting AAc onto PVC-g-PEGMA(10%) reached a maximum in 2 h. Catheters with such high graft percentages notably increased their size, the edges were deformed, and the whole catheter was hardened. Further kinetic studies for grafting of AAc onto PVC-g-PEGMA were conducted by varying the monomer (AAc) concentration (Fig. 2). Decreasing AAc concentration from 50 to 30% (v/v) in water, the grafting increased even more, leading to a maximum of 169% AAc grafted after 4 h. This finding can be explained as a decrease in the likelihood of homopolymerization due to a lower monomer concentration in the reaction medium, which in turn favored grafting. The grafting percentage was lower when AAc concentration in the reaction medium was 10% (v/v): 14% grafting was attained in one hour, and this value did not increase beyond this time.
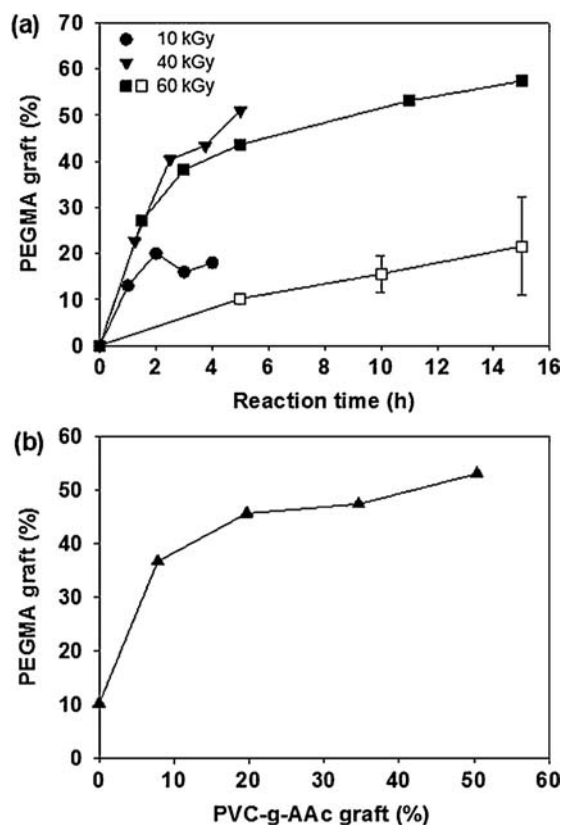
Fig. 1. (a) PEGMA grafting onto PVC (□) and PVC-g-AAc(27%) (■) that received a pre-irradiation dose of 60 kGy, and onto PVC-g-AAc(10%) that received a pre-irradiation dose of 40 (▼) or 10 (●) kGy, as a function of reaction time; and (b) PEGMA grafting onto PVC-g-AAc (pre-irradiation dose 60 kGy) as a function of the percentage of AAc previously grafted, for a reaction time of 5 h. In all cases, the reaction temperature was 70 °C and the PEGMA concentration in the reaction medium (water) was 14% (v/v).
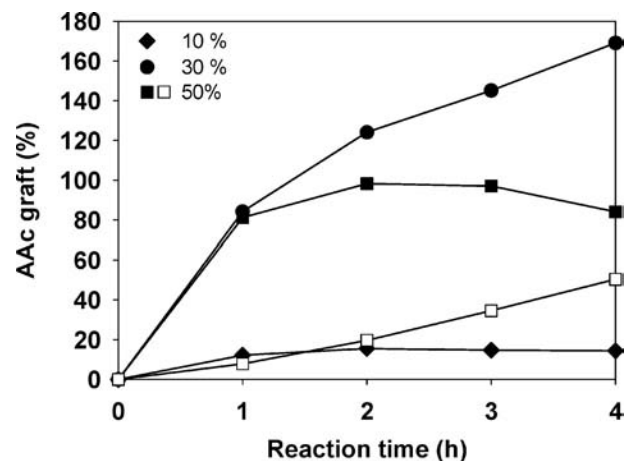
Fig. 2. Grafting percentage of AAc onto PVC-g-PEGMA(10%) when the monomer concentration in the reaction medium was 10% (◆), 30% (●), and 50% (■) (v/v); and onto PVC (□) when the monomer concentration was 50% (v/v). The pre-irradiation dose was 5 kGy and the reaction temperature 80 °C.

3.2. Physical and physicochemical characterization

ATR-FTIR spectrum of unmodified PVC showed the typical C—H stretch peaks, symmetric and asymmetric, at 2962, 2932, 2875 and 2862 cm^{-1}, and an ester C=O stretch peak at 1724 cm^{-1} attributed to the plasticizer, which is typically an phthalate as confirmed by another prominent peak at 1260 cm^{-1} attributed to the C—O ester stretch (Fig. S2, Supporting information). For [PVC-g-PEGMA]-g-AAc, the spectrum resembled that of PAAc, where a prominent and broad O—H peak that extends from around 2750 cm^{-1} to 3500 cm^{-1} was visible, alongside the typical C—H stretch bands in between (2952 cm^{-1} and 2912 cm^{-1}). The peak at 1702 cm^{-1} corresponded to the carboxylic acid. Other peaks, also seen in PVC-g-AAc, belonged to C—OH bending (1452 cm^{-1}) and C—O stretching (1246 cm^{-1}). In the case of a [PVC-g-AAc]-g-PEGMA catheter, the ATR-FTIR spectrum showed a characteristic broad peak at 3450–3475 cm^{-1} indicating the presence of alcohol groups (OH stretch), a peak at 1726 cm^{-1} belonging to the C=O ester stretch, and a prominent peak at 1106 cm^{-1} due to the C—OH stretch. These peaks are characteristic of PEGMA. In sum, ATR-FTIR spectra of the binary grafts indicate that the polymer (PEGMA) or the monomer (AAc) that was grafted during the second step is predominant at the surface of the catheter (at least up to the depth that can be analyzed by the apparatus).

Regarding the thermal stability of PVC catheters, the first weight drop occurred at around 200 °C due to the de-chlorination process (Fig. S3, Supporting information). Grafting of either AAc or PEGMA slightly increased the temperature required for a 10% weight loss (about 254 °C compared to 244 °C for pristine PVC catheters) as loss of chlorine becomes more difficult. The char residue was 0% for PVC and increased for the grafted catheters, with 6% char residue for PVC-g-PEGMA(27%) and 8% char residue for PVC-g-AAc(58%). Binary grafted catheters showed better thermal stability, with a 10% weight loss temperature of 280 °C for [PVC-g-AAc(20%)]-g-PEGMA(93%) with 6% char residue, and of 300 °C for [PVC-g-AAc(46%)]-g-PEGMA(27%) with a 30% char residue (Fig. S3b). For the binary system, increasing AAc grafting percentage made the catheters more thermally stable (compared to a similar increase in PEGMA grafting percentage).

Water contact angle values were recorded immediately after drop deposition and 30 s later (Table 1). Catheters grafted with PEGMA (either singly or as final binary component) showed initially greater contact angles, but after 30 s the values decreased below those of pristine PVC. This behavior is typical of PEG-functionalized materials since the polymer modifies its conformation when wetted, and the hydrophobic regions of the polymer initially exposed to air move to allow the most hydrophilic ones entering into contact with water (dos Santos et al., 2009). Interestingly, [PVC-g-PEGMA]-g-AAc catheters remained hydrophobic after 30 s, which can be related to the strong hydrogen bonding between PEGMA and AAc (Yokoyama and Yusa, 2013). For

PVC-g-AAc catheters, the surface contact angle decreased more as grafted AAc increased, as expected from the hydrophilic nature of AAc. The surface of dried catheters was visibly rougher when grafted with PEGMA or the binary graft, while it became smoother with the AAc graft (Fig. S4, Supporting information). The surface roughness can also explain the increase in water contact angle as previously observed for a wide variety of engineered materials (Kubiak et al., 2011).

3.3. Equilibrium swelling time and critical pH

PVC did not swell in water. Swelling of PVC-g-AAc increased with AAc% content; namely, 7%, 15%, 25%, 36% and 49% AAc grafted led to 3.5%, 12%, 21%, 25% and 51% swelling, respectively, in 2.5 h (data partially shown in Fig. 3). Grafting of PEGMA, also endowed PVC with swelling capability although at lower extent; PVC-g-PEGMA 11, 20 and 38% swelled 8.3, 11.4 and 19.6%, respectively. When PEGMA was grafted to PVC-g-AAc catheters, or AAc to PVC-g-PEGMA, the equilibrium swelling time was somehow longer

Table 1
Water contact angle (degrees) for grafted catheters measured at 20 °C and two different times.

Catheter	Contact angle	
	0 s	30 s
PVC	99 ± 2	98 ± 3
PVC-g-AAc(20%)	86 ± 1	87 ± 1
PVC-g-AAc(59%)	81 ± 5	78 ± 1
PVC-g-PEGMA(16%)	106 ± 7	87 ± 9
PVC-g-PEGMA(41%)	114 ± 4	84 ± 2
[PVC-g-AAc(7%)]-g-PEGMA(21%)	94 ± 5	88 ± 3
[PVC-g-AAc(7%)]-g-PEGMA(40%)	102 ± 5	65 ± 4
[PVC-g-PEGMA(13%)]-g-AAc(12%)	99 ± 3	97 ± 2
[PVC-g-PEGMA(13%)]-g-AAc(84%)	94 ± 5	90 ± 3
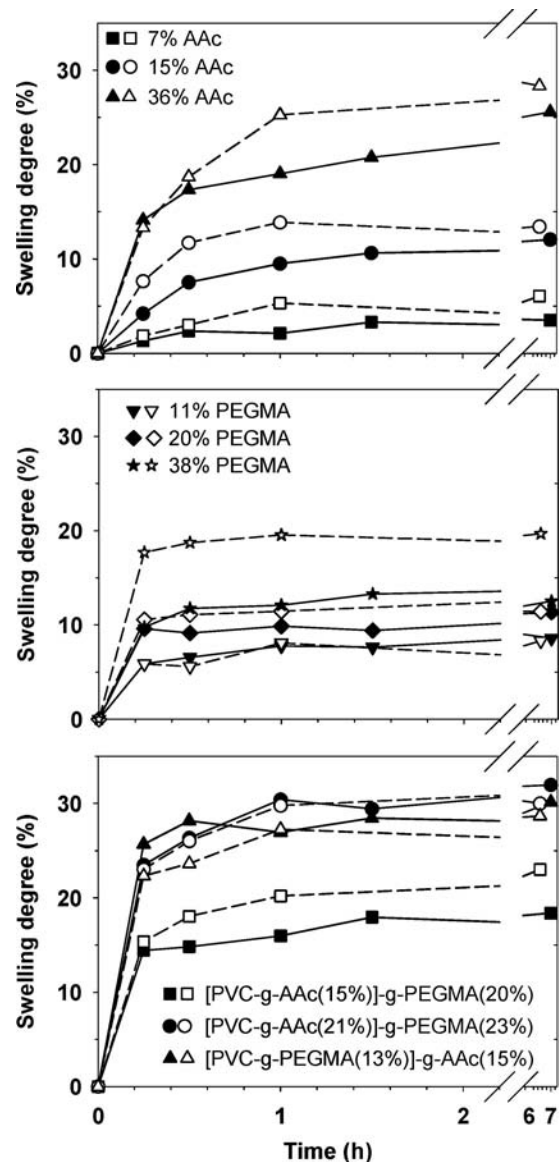
Fig. 3. Degree of swelling in water (open symbols, dotted lines) and artificial urine (solid symbols, continuous lines) of various PVC-g-AAc, PVC-g-PEGMA, [PVC-g-AAc]-g-PEGMA and [PVC-g-PEGMA]-g-AAc catheters prepared with the grafting percentages indicated in the plots.

(up to 5 h). This finding can be related to hydrogen bonding formation between PEGMA and PAAc chains, which delays water uptake (Kim and Peppas, 2003). The swelling of grafted catheters was also evaluated in artificial urine (pH 6). Overall, the catheters showed a slightly lower degree of swelling in urine than in water, which can be attributed to the salting out effect that the ions may exert on the PAAc chains (Fig. 3). Additionally, owing to carboxylic groups with pK_a 4.74, the catheters with grafted AAc (as little as 11%) showed a typical pH-dependent swelling (Fig. S5, Supporting information). The critical pH for PVC-g-AAc catheters (covering a wide interval of content in AAc) remained fairly constant in the 7–8 range; the shift in the critical pH compared to the pK_a of the monomer is characteristic of homopolymer chains, where the vicinity of other AAc mers makes deprotonization more difficult (Mayo-Pedrosa et al., 2008; Yoo et al., 2004). Even binary grafted catheters with higher content in PEGMA than in AAc displayed a critical pH, although an increased percentage in PEGMA shifted the critical pH towards lower values (ca. 5.7).

3.4. Mechanical properties

The Young's modulus for PVC catheter was found to be 18 MPa, which is in agreement with published literature (Jones et al., 2001; Sastri, 2014). The modulus decreased to 10 MPa for PVC-g-PEGMA (16%) catheters (Fig. 4), which is not uncommon since PEG performs as a plasticizer due to its below zero Tg value (Graham, 1992; Vieira et al., 2011). The opposite happened when AAc was grafted; a catheter with 25% AAc had a Young's modulus of 64 MPa, due to the relatively high Tg of PAAc (approx. 110 °C). For the binary grafts, catheters initially grafted with AAc and then with PEGMA showed a Young's modulus (12 MPa) in between that of PVC and that of PVC-g-PEGMA(16%). Conversely, when PEGMA was grafted first and then AAc, the Young's modulus increased to 150 MPa, which was the highest Young's modulus recorded. This behavior suggests that for the binary graft, the polymer that is grafted in the last step, i.e., the one exposed to the surface, is the one that has more influence upon the final elastic behavior of the material.

Lubricity was estimated from measurements of the force required to insert and to remove the catheters from agar containers using a texture analyzer. Agar matrix (1% w/w) has been proposed as a suitable model that mimics the wet environment of urethra mucosa (Jones et al., 2001). Catheters were tested immediately after soaking in water for 30 s or 4 h (Fig. 5). Low forces were required to insert pristine PVC catheters in the agar matrix (0.11–0.14 N) and also to remove them (0.03–0.05 N). The values recorded
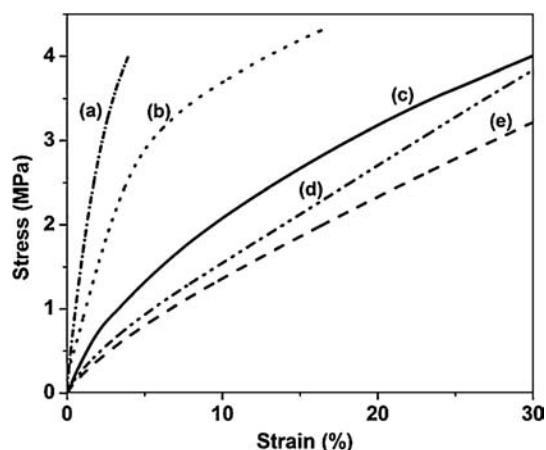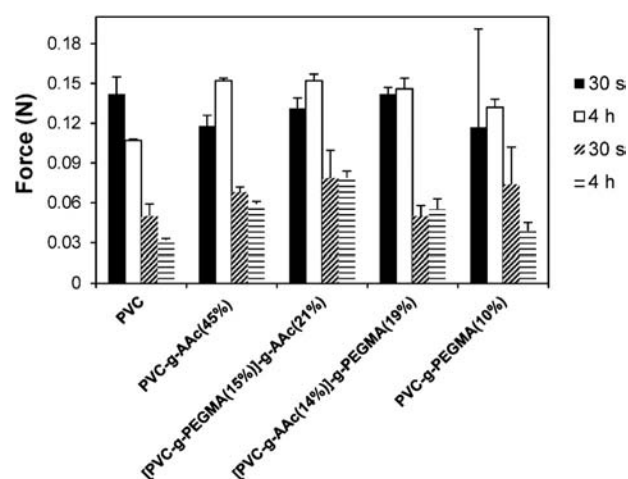
Fig. 5. Force required to insert (black and white) and remove (shaded regions) pristine and grafted PVC catheters from an agar gel at a constant rate of 5 mm/s, after being soaked in water for 30 s or 4 h.

were lower than those previously reported for other PVC catheters (Jones et al., 2001), which may be related to the polishing of catheters surface tested in the present work (see SEM images in Fig. S4). Grafting did not significantly alter the lubricity, although grafted catheters that were swollen in water for 4 h required slightly greater force to be inserted, probably due to the roughness of their surface. Swollen PVC-g-AAc(45%) and [PVC-g-PEGMA (15%)]-g-AAc(21%) catheters required the greatest amount of force to be removed from agar (Fig. 5), which could be a result of hydrogen bonding with agar. This finding is in agreement with previous reports on lubricity of commercially available coated catheters, which showed that the coating may not improve very much the insertion due to the concomitance of several features: increased contact area between the substrate and the wet catheter (due to roughness and swelling) and, in some cases, loss of rigidity (rigid catheters are easier to insert) (Jones et al., 2001). In our case, PAAc is a well-known bio-adhesive polymer and interactions with agar cannot be discarded since agar (as mucin) possesses acid groups suitable for hydrogen bonding with AAc groups (Blanco-Fernández et al., 2011). Nevertheless, this detrimental effect was quantitatively of poor relevance.

3.5. Cytocompatibility

As expected, grafted catheters showed an excellent compatibility with fibroblasts (Table S1, Supporting information). During the first 24 h of incubation, the cell viability remained in the 90–107% range, except for the catheter with the highest content in AAc, PVC-g-AAc(44%), which showed 67% cell viability. These results are in agreement with previous reports on biocompatibility of AAc-grafted materials (Ahmad et al., 2014; Garcia-Vargas et al., 2014). Overall, catheters grafted with PEGMA showed the highest cytocompatibility even after 48 h of exposure. Among the binary grafted catheters, [PVC-g-PEGMA]-g-AAc catheters proved to have slightly better cell viability than [PVC-g-AAc]-g-PEGMA. Although a slight decrease in cell viability was observed after 48 h, all grafted catheters showed similar or even better cytocompatibility than the pristine PVC ones.

3.6. Ciprofloxacin loading and release

Pristine PVC catheters exhibited very low affinity for ciprofloxacin (0.025 mg loaded/g). As AAc grafting percentage increased, a higher amount of ciprofloxacin was loaded due to a greater density

Fig. 4. Stress vs. strain curves for (a) [PVC-g-PEGMA(12%)]-g-AAc(26%), (b) PVC-g-AAc(25%), (c) PVC, (d) [PVC-g-AAc(12%)]-g-PEGMA(26%), and (e) PVC-g-PEGMA (16%) at 28 °C.
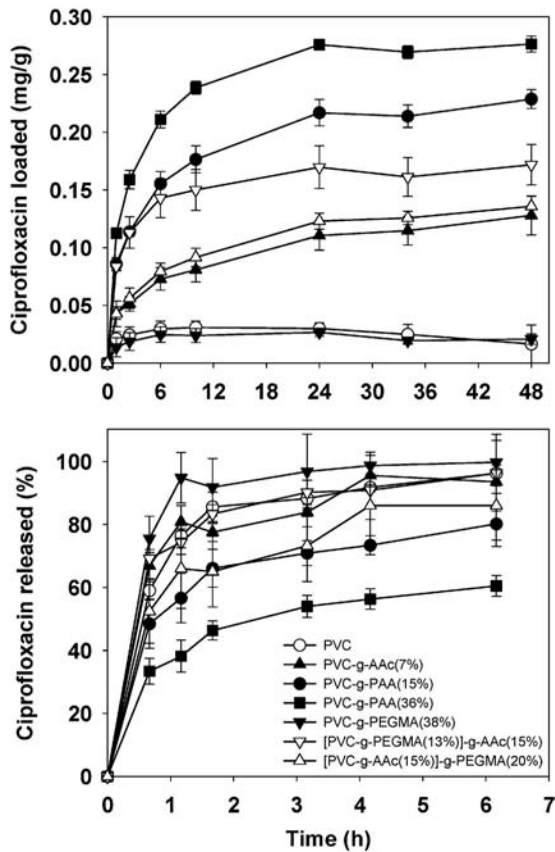
Fig. 6. Ciprofloxacin loading and release profiles recorded for pristine and grafted PVC catheters. Loading was carried out by soaking in a ciprofloxacin aqueous solution (0.012 mg/mL) at room temperature, while release profiles were recorded in an artificial urine medium (pH 6) at 37 °C.

of functional groups available to interact with the drug. In water, this second-generation fluoroquinolone exhibits a positive charge (as the amine groups are protonated). Thus, conditioning the catheters in PBS (pH 7.4) before exposing them to the drug solution made the carboxylic acid groups of the grafted PAAc to be in salt form and thus easier to dissociate, which in turn facilitated ionic interactions with the drug. Grafting of AAc as low as 7% led to 0.11 mg of ciprofloxacin loaded per gram of catheter. Grafting of PEGMA slightly improved ciprofloxacin uptake compared to PVC, in spite the surface of the catheters being swollen (Fig. 6). This finding is explained by the typical inertness of PEG chains to bind to other molecules. Binary grafted catheters were able to absorb ciprofloxacin better than PVC, but the amounts of ciprofloxacin loaded remained below the levels that were achieved by PVC-g-

AAc catheters. The drug uptake was similar disregarding whether the catheter had AAc or PEGMA on the surface of the binary graft. Total amounts loaded are summarized in Table 2.

Release studies were carried out in artificial urine fluid in order to mimic the medium in which the catheters would have to perform. Ciprofloxacin-loaded PVC and PVC-g-PEGMA released the small amount of the drug that had been loaded in less than one hour (Fig. 6). The grafted catheters that loaded more amount of drug showed more sustained release profiles. PVC-g-AAc with grafting percentages of 15 and 36% controlled the release for several hours, and similar results were recorded for [PVC-g-AAc]-g-PEGMA binary grafts. [PVC-g-PEGMA]-g-AAc catheters exhibited an intermediate release rate. In all cases, an important burst release was observed due to the attenuation of the electrostatic interactions of the drug with the grafted polymer in the presence of urine ions. Competitive binding of ions with the acrylic acid groups is responsible for the triggering of the release. Nevertheless, the length and entanglement of the grafted chains oppose to the diffusion of free drug and, therefore, the catheters with higher grafting percentages released more slowly. It has been previously reported that bacteria colonization rapidly occurs in the few first hours after implantation and, therefore, prophylaxis of CAUTIs require a fast release of an important amount of antimicrobial agent followed by more sustained release profiles for maintenance of therapeutic doses (Kwok et al., 1999). It should be noted that, in the case of the grafted catheters, 1-cm long piece in 5 mL urine medium provided in 2 h a drug concentration well above the ciprofloxacin MIC of *E. coli* (0.004–0.015 μg/mL) and *S. aureus* (0.12–0.50 μg/mL) (Clinical and Laboratory Standards Institute, 2012). Therefore, catheters of standard length (20–26 cm female; 40–45 cm male) could provide in few minutes a high local concentration of ciprofloxacin.

3.7. Microbiological tests

The functionalized, ciprofloxacin-loaded catheters were able to inhibit the growth of both Gram-positive (*S. aureus*) and Gram-negative (*E. coli*) bacteria, and large inhibition zones were observed after an incubation period of 24 h (Table 2). As expected from the MIC values, inhibition zones were larger in the plates seeded with *E. coli* than with *S. aureus*. In fact, the tested ciprofloxacin-loaded grafted catheters successfully performed against a second challenge with *E. coli*. PVC-g-PEGMA and [PVC-g-PEGMA]-g-AAc catheters were also able to inhibit the growth of *E. coli* even after being exposed to a freshly seeded culture for a third time. This behavior can be related to the slower discharge of the drug from the binary grafts when tested in vitro using agar plates, compared to the release tests carried out under sink conditions (as described above). In fact, it has been previously reported that drug release

Table 2
Amounts of ciprofloxacin loaded by the catheters and diameter of inhibition zones caused by the grafted catheters in *E. coli* and *S. aureus* cultures after the first, second, and third exposure to freshly seeded bacteria cultures.

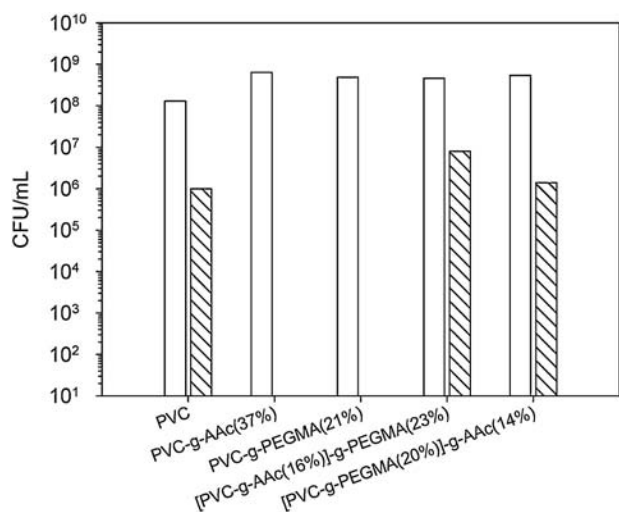| Catheter	Ciprofloxacin loaded (mg/g)	*E.coli* inhibition zone (cm)			*S. aureus* inhibition zone (cm)	
		1st challenge	2nd challenge	3rd challenge	1st challenge	2nd challenge
PVC	0.025 (0.005)	10	0	0	10	0
PVC-g-PEGMA(10%)	0.025 (0.008)	28	5	5	10	0
PVC-g-PEGMA(20%)	0.025 (0.009)	26	10	11	17	6
PVC-g-PEGMA(38%)	0.026 (0.009)	30	17	9	20	15
PVC-g-AAc(7%)	0.13 (0.02)	26	12	0	16	0
PVC-g-AAc(15%)	0.23 (0.01)	19	17	0	21	8
PVC-g-AAc(36%)	0.28 (0.01)	25	15	0	17	0
[PVC-g-AAc(15%)]-g-PEGMA(20%)	0.13 (0.01)	25	16	9	15	13
[PVC-g-AAc(21%)]-g-PEGMA(23%)	0.17 (0.01)	27	16	14	17	0
[PVC-g-PEGMA(12%)]-g-AAc(14%)	0.18 (0.01)	31	20	21	20	13
[PVC-g-PEGMA(13%)]-g-AAc(15%)	0.17 (0.02)	30	27	12	18	15
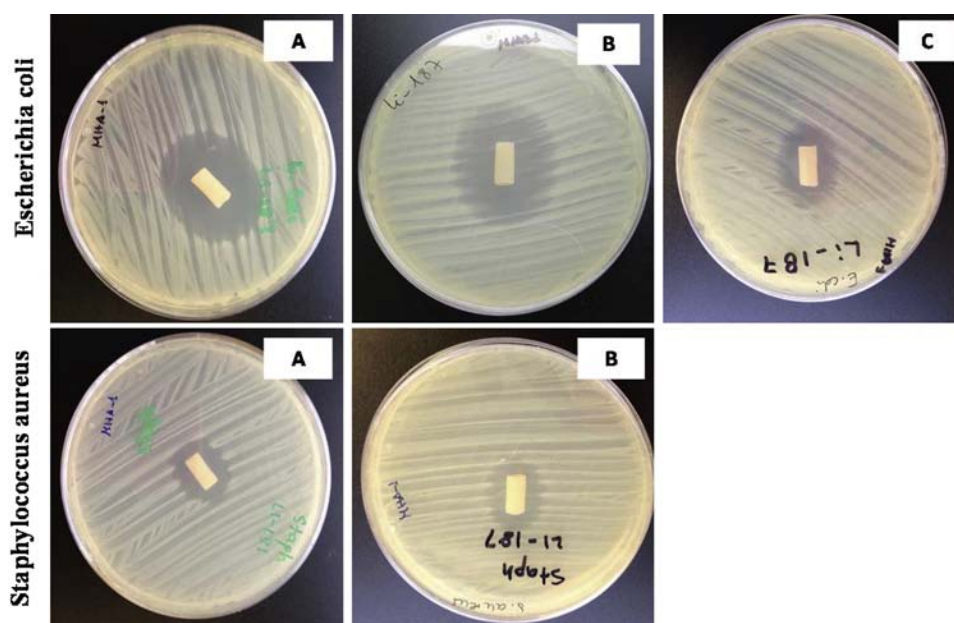
Fig. 7. Inhibition zones caused by a ciprofloxacin-loaded [PVC-*g*-PEGMA(10%)]-*g*-AAc(15%) catheter against *Escherichia coli* (top) and *Staphylococcus aureus* (bottom) after (A) the first, (B) the second, and (C) the third challenge to freshly seeded bacteria for 24 h of incubation at 37 °C.

rates from polymeric platforms recorded under sink conditions in aqueous medium are usually much higher than those achieved when the platform is implanted in the body, which can be better mimicked recording diffusion in agar plates (Casalini et al., 2012).

As an example, the inhibition zones caused by [PVC-*g*-PEGMA (10%)]-*g*-AAc(15%) catheter are shown in Fig. 7. For PVC-*g*-PEGMA catheters, as the grafting percentage of PEGMA increased, the diameters of the inhibition zones were larger. The PVC-*g*-AAc catheters led to inhibition zones slightly smaller than all the other catheters, and they were not able to inhibit bacterial growth in the third challenge against *E. coli*, and the second challenge against *S. aureus* (Table 2).

A second microbiological test was carried out to assess whether the grafting of PEGMA and PAAc, and the subsequent loading of ciprofloxacin, could prevent bacteria adhesion (a first step for the biofilm formation) onto the catheters when a small piece was immersed in a highly contaminated medium. After 3 h incubation, polymer grafting itself did not prevent *E. coli* adhesion, and the bacteria CFUs were similar for both pristine and grafted PVC catheters (Fig. 8). Presoaking in ciprofloxacin aqueous solution decreased nearly two orders of magnitude the number of CFUs onto pristine PVC and binary grafts. More relevantly, catheters grafted with either AAc or PEGMA and loaded with ciprofloxacin completely prevented bacteria adhesion. It should be noted that the binary grafted catheters can load and release ciprofloxacin similarly to PVC-*g*-AAc catheters, although in lower quantities. Thus, bacteria adhesion onto binary catheters could be related to their rougher surface (Fig. S4, Supporting information), due to the double grafting, which may provide more binding points for the attachment of bacteria. Interestingly, the small amount of ciprofloxacin loaded by PVC-*g*-PEGMA (21%) may have a synergic effect with the low biofouling PEG surface. PVC-*g*-AAc catheters load and quickly release a high amount of ciprofloxacin, which could explain why at the chosen exposure time of 3 h these catheters were very effective at preventing bacterial adhesion.

4. Conclusions

PVC urinary catheters can be grafted with AAc and/or PEGMA covering a wide range of grafting percentages. Importantly, the gamma pre-irradiation doses should be kept as low as possible in order to avoid damage of the catheter bulk. Similarly, the grafting percentage should not exceed in total 50% in order to prevent changes in size that could interfere with the primary use of the catheters. In the binary grafts, the polymer grafted in the second step seems to determine water wettability and Young's modulus. Overall, effect of grafting on these properties has minor practical repercussions. Oppositely, grafting of AAc notably favors the loading of ciprofloxacin and both singly and binary grafted catheters containing AAc are able to uptake therapeutically useful amounts of the antimicrobial agent, as confirmed in the in vitro microbiological tests. Catheters grafted with PEGMA, although less efficient regarding ciprofloxacin loading, also lead to remarkable inhibition of bacteria growth and adhesion, which can be attributed to synergic antibiofouling effects of PEG and ciprofloxacin. In summary, tuning the relative proportions and the total

Fig. 8. Results of *E. coli* adhesion tests for PVC, PVC-*g*-PEGMA, PVC-*g*-AAc, [PVC-*g*-PEGMA]-*g*-AAc, and [PVC-*g*-AAc]-*g*-PEGMA catheters that were previously swollen in either water (white) or in a ciprofloxacin aqueous solution (shaded), after an exposure time of 3 h at 37 °C.

amount of AAc and PEGMA grafted onto PVC may open novel possibility for the design of ciprofloxacin-eluting urinary catheters that minimize the risk of CAUTIs.

Acknowledgments

Appendix A. Supplementary data

Supplementary data associated with this article can be found, in the online version, at http://dx.doi.org/10.1016/j.ijpharm.2015.04.036.

References

Aguilar, M.R., Elvira, C., Gallardo, A., Vazquez, B., San Roman, J., 2007. Smart polymers and their applications as biomaterials. In: Ashammakhi, M., Reis, R.L., Chiellini, E. (Eds.), Topicsin Tissue Engineering, vol. 3. University of Oulu, Finland, pp. 1–27.

Ahmad, N., Amin, M.C.I.M., Mahali, S.M., Ismail, I., Chuang, V.T.G., 2014. Biocompatible and mucoadhesive bacterial cellulose-g-poly(acrylic acid) hydrogels for oral protein delivery. Mol. Pharm. 11, 4130–4142.

Alvarez-Lorenzo, C., Concheiro, A., 2013. Drug/medical device combination products with stimuli-responsive eluting surface. In: Alvarez-Lorenzo, C., Concheiro, A. (Eds.), Smart Materials for Drug Delivery, vol. 2. Royal Society of Chemistry, Cambridge, pp. 313–348.

Arenas, E., Bucio, E., Burillo, G., Lopez, G.P., 2007. Radiation grafting of poly(ethylene glycol) methacrylate onto poly(vinyl chloride) tubes. Des. Monomers Polym. 10, 459–467.

Asadinezhad, A., Novák, I., Lehocký, M., Sedlařík, V., Vesel, A., Junkar, I., Sáha, P., Chodák, I., 2010. An in vitro bacterial adhesion assessment of surface-modified medical-grade PVC. Colloids Surf. B: Biointerfaces 77, 246–256.

Blanco-Fernández, B., López-Viota, M., Concheiro, A., Alvarez-Lorenzo, C., 2011. Synergistic performance of cyclodextrin-agar hydrogels for ciprofloxacin delivery and antimicrobial effect. Carbohydr. Polym. 85, 765–774.

Brooks, T., Keevil, C.W., 1996. A simple artificial urine for the growth of urinary pathogens. Lett. Appl. Microbiol. 24, 203–206.

Casalini, T., Masi, M., Perale, G., 2012. Drug eluting sutures: a model for in vivo estimations. Int. J. Pharm. 429, 148–157.

Chenoweth, C.E., Gould, C.V., Saint, S., 2014. Diagnosis, management, and prevention of catheter-associated urinary tract infections. Infect. Dis. Clin. North Am. 28, 105–119.

Chutipongtanate, S., Thongboonkerd, V., 2010. Systematic comparisons of artificial urine formulas for in vitro cellular study. Anal. Biochem. 402, 110–112.

Costerton, J.W., Stewart, P.S., Greenberg, E.P., 1999. Bacterial biofilms: a common cause of persistent infections. Science 284, 1318–1322.

Clinical and Laboratory Standards Institute, 2012. Performance standards for antimicrobial susceptibility testing; 22nd information supplement. CLSI document M100-S22. Pennsylvania, USA.

Denise, N.P., 2002. Antibiofilm approaches: prevention of catheter colonization. Chem. Biol. 9, 873–880.

Drobny, J.G., 2013. Ionizing Radiation and Polymers: Principles, Technology, and Applications. Elsevier, United States.

Donland, R.M., 2002. Biofilms: microbial life on surfaces. Emerg. Infect. Dis. 8, 881–890.

dos Santos, J.F.R., Alvarez-Lorenzo, C., Silva, M., Balsa, L., Couceiro, J., Torres-Labandeira, J.J., Concheiro, A., 2009. Soft contact lenses functionalized with pendant cyclodextrins for controlled drug delivery. Biomaterials 30, 1348–1355.

Garcia-Vargas, M., Gonzalez-Chomon, C., Magariños, B., Concheiro, A., Alvarez-Lorenzo, C., Bucio, E., 2014. Acrylic polymer-grafted polypropylene sutures for covalent immobilization or reversible adsorption of vancomycin. Int. J. Pharm 461, 286–295.

Gasparrini, G., Carenza, M., Palma, G., 1980. Some investigations on the radiation-induced grafting of acrylic acid onto poly(vinyl chloride). J. Polym. Sci. 18, 29–33.

Graham, N.B., 1992. Poly(ethylene glycol) gels and drug delivery. In: Harri, J.M. (Ed.), Poly(Ethylene Glycol) Chemistry: Biotechnical and Biomedical Applications. Springer Science and Media, New York.

Gratzl, G., Paulik, C., Hild, S., Guggenbichler, J.P., Lackner, M., 2014. Antimicrobial activity of poly(acrylic acid) block copolymers. Mater. Sci. Eng. C38, 94–100.

Greene, M.T., Fakih, M.G., Fowler, K.E., Meddings, J., Ratz, D., Safdar, N., Olmsted, R.N., Saint, S., 1998. Regional variation in urinary catheter use and catheter-associated urinary tract infection: results from a national collaborative. Infect. Control Hosp. Epidemiol. 35, S99–S106.

Hosseinidoust, Z., Olsson, A.L.J., Tufenkji, N., 2014. Going viral: designing bioactive surfaces with bacteriophage. Colloids Surf. B: Biointerfaces 124, 2–16.

Jones, D.S., Gravin, C.P., Gorman, S.P., 2001. Design of a simulated urethra model for the quantitative assessment of urinary catheter lubricity. J. Mater. Sci. Mater. Med. 12, 15–21.

Kim, B., Peppas, A.N., 2003. Analysis of molecular interactions in poly(methacrylic acid-g-ethylene glycol) hydrogels. Polymer 44, 3701–3707.

Kingshott, P., Wei, J., Bagge-Ravn, D., Gadegaard, N., Gram, L., 2003. Covalent attachment of poly(ethylene glycol) to surfaces, critical for reducing bacterial adhesion. Langmuir 19, 6912–6921.

Kubiak, K.J., Wilson, M.C.T., Mathia, T.G., Carval, P.h., 2011. Wettability versus roughness of engineering surfaces. Wear 271, 523–528.

Kwok, C.S., Horbett, T.A., Ratner, B.D., 1999. Design of infection-resistant antibiotic releasing polymers- II: controlled release of antibiotics through a plasma deposited thin film barrier. J. Control. Release 62, 301–311.

Lichter, J.A., Van Vliet, K.J., Rubner, M.F., 2009. Design of antibacterial surfaces and interfaces: polyelectrolyte multilayers as a multifunctional platform. Macromolecules 42, 8573–8586.

Mayo-Pedrosa, M., Cachafeiro-Andrade, N., Alvarez-Lorenzo, C., Martinez-Pacheco, R., Concheiro, A., 2008. In situ photopolymerization-coated pellets for pH-dependent drug delivery. Eur. Polym. J. 44, 2629–2638.

Nicolle, L.E., 2014. Urinary catheter-associated infections. Infec. Dis. Clinic. North Am. 26, 13–27.

Pande, C.S., Single, S., Gupta, N., 1995. Functionalization of poly(vinyl chloride) through radiation-induced grafting. J. Appl. Polym. Sci. 58, 1735–1739.

Ping, X., Wang, M., Ge, X., 2011. Surface modification of poly(ethylene terephthalate) (PET) film by gamma-ray induced grafting of poly(acrylic acid) and its application in antibacterial hybrid film. Radiat. Phys. Chem. 80, 567–572.

Public Health Agency of Canada, 2013. Report on the state of public health in Canada: healthcare-associated infections. http://publichealth.gc.ca/CPHOReport, (accessed 03.15.).

Rakita, P.E., Foure, M., 1987. Gamma radiation stabilization of PVC. J. Vinyl Technol. 6, 73–76.

Reid, G., Sharma, S., Advikolanu, K., Tieszer, C., Martin, R.A., Bruce, A.W., 1994. Effects of ciprofloxacin, norfloxacin, and ofloxacin on in vitroadhesion and survival of *Pseudomonas aeruginosa* AK1 on urinary catheters. Antimicrob. Agents Chemother. 38, 1490–1495.

Saldarriaga-Fernandez, I.C., van der Mei, H.C., Metzger, S., Grainger, D.W., Engelsman, A.F., Nejadnik, M.R., Busscher, H.J., 2010. In vitro and in vivo comparisons of staphylococcal biofilm formation on a cross-linked poly (ethylene glycol)-based polymer coating. Acta Biomater. 6, 1119–1124.

Sastri, R.V., 2014. Commodity thermoplastics: polyvinyl chloride, polyolefins, and polystyrene, In: Sastri, V.R. (Ed.), Plastics in Medical Devices. 2nd edition Elsevier, pp. 73–120.

Shah, S.R., Tatara, A.M., D'souza, R.N., Mikos, A.G., Kasper, F.K., 2013. Evolving strategies for preventing biofilm on implantable materials. Mater. Today 16, 177–182.

Stickler, D.J., 2008. Bacterial biofilms in patients with indwelling urinary catheters. Nat. Rev. Urol. 5, 598–608.

Tenke, P., Kovacs, B., Jackel, M., Nagy, E., 2006. The role of biofilm infection in urology. World J. Urol. 24, 13–20.

Vieira, M.G.A., da Silva, M.A., dos Santos, L.O., Beppu, M.M., 2011. Natural-based plasticizers and biopolymer films: a review. Eur. Polym. J. 47, 254–263.

World Health Organization, 2011. Report on the burden of endemic health care-associated infection worldwide.

Yokoyama, Y., Yusa, S., 2013. Water-soluble complexes formed from hydrogen bonding interactions between a poly(ethylene glycol)-containing triblock copolymer and poly(methacrylic acid). Polym. J. 45, 985–992.

Yoo, M.K., Seok, W.K., Sung, Y.K., 2004. Characterization of stimuli-sensitive polymers for biomedical applications. Macromol. Symp. 207, 173–186.

Zygoura, D.P., Paleologos, K.E., Kontominas, M.G., 2010. Migration levels of PVC plasticisers: effect of ionizing radiation treatment. Food Chem. 128, 106–113.

Appendix A

Ciprofloxacin

Ciprofloxacin is a second generation fluoroquinolone antibiotic that has a stronger activity against gram-negative bacteria than gram-positive bacteria. The drug is commonly used to treat different infections, including those of the urinary tract. The antibacterial properties of ciprofloxacin are due to an interference in the copying and transcription of the bacteria's DNA, which prevents them from developing and duplicating, ultimately leading to their death.

The ciprofloxacin structure is the following:
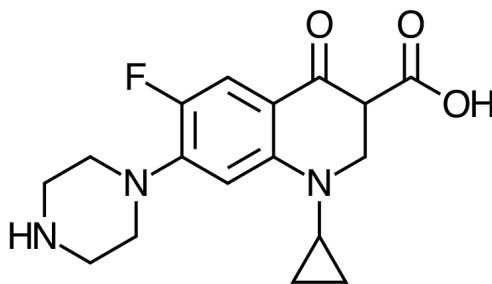
Figure A.1: Ciprofloxacin structure

[1] Masadeh, M. M. et al., *Current Therapeutic Research* 77 (2014), pp 14-17.

Appendix B

UV-VIS Validation

Validation of UV-VIS spectrophotometer for ciprofloxacin in water.

Validation for the UV spectrometry calibration curve of Ciprofloxacin in water

Concentration (mg/mL)	Absorbance (276 nm)	Calculated concentration using the callibration curve (Xp)	Xp average	Percent recovery	Media	Standard deviation	Variation coefficient(%)
0.00029	0.18708	0.000348374					
0.00029	0.21115	0.000326191	0.0003	110.1923	0.1960	0.0132	6.7134
0.00029	0.18989	0.000284108					
0.00058	0.23998	0.000504182					
0.00058	0.293685	0.000558579	0.0005	93.8718	0.2771	0.0322	11.6276
0.00058	0.29768	0.000570608					
0.00087	0.343865	0.000810158					
0.00087	0.3999035	0.000857651	0.0008	97.0309	0.3840	0.0350	9.1240
0.00087	0.408325	0.000864697					
0.00116	0.4499	0.001122467					
0.00116	0.505075	0.001153776	0.0011	98.9258	0.4923	0.0376	7.6451
0.00116	0.521825	0.001166374					
0.00145	0.58909	0.001532428					
0.00145	0.60481	0.001434593	0.0015	101.7369	0.6085	0.0216	3.5448
0.00145	0.631745	0.001458536					
0.00174	0.678635	0.001796168					
0.00174	0.707575	0.001723941	0.0018	100.8475	0.7085	0.0303	4.2754
0.00174	0.739195	0.001744133					
0.00203	0.770665	0.002067227					
0.00203	0.817035	0.00203214	0.0020	100.8814	0.8133	0.0409	5.0244
0.00203	0.85213	0.002044308					
0.00232	0.854255	0.002313428					
0.00232	0.929765	0.002349547	0.0023	100.3009	0.9130	0.0525	5.7454
0.00232	0.95509	0.00231797					
0.00261	0.952335	0.002602306					
0.00261	1.03615	0.002649088	0.0026	100.7995	1.0217	0.0634	6.2076
0.00261	1.0767	0.002641204					
0.0029	1.0377	0.002853735					
0.0029	1.11215	0.002863076	0.0029	98.5682	1.1028	0.0526	4.7737
0.0029	1.1585	0.002858624					

Figure B.1: Validation of UV-VIS spectrophotometer for ciprofloxacin in water.

Appendix C

UV-VIS Validation

Validation of spectrometric method: ciprofloxacin in artificial urine.

Validation for the UV spectrometry calibration curve of Ciprofloxacin in artificial urine (pH = 6)

Concentration (mg/mL)	Absorbance (276 nm)	Calculated concentration using the callibration curve (Xp)	Xp average	Percent recovery	Media	Standard deviation	Variation coefficient(%)
0.001	0.1226	0.001077885					
0.001	0.13408	0.00107064	0.001051395	105.1394797	0.129986667	0.006409535	4.930916939
0.001	0.13328	0.00100566					
0.002	0.21336	0.001950577					
0.002	0.22633	0.001971959	0.001929761	96.48803317	0.219896667	0.006485617	2.94939324
0.002	0.22	0.001866746					
0.003	0.33962	0.003164615					
0.003	0.32565	0.002942355	0.00299478	99.82600798	0.329016667	0.009384414	2.852261096
0.003	0.32178	0.002877371					
0.004	0.42247	0.00396125					
0.004	0.42935	0.003955545	0.003973324	99.33310116	0.428993333	0.006352514	1.480795491
0.004	0.43516	0.004003177					
0.005	0.52649	0.004961442					
0.005	0.53513	0.004989057	0.004991443	99.82886844	0.53319	0.005971231	1.119906793
0.005	0.53795	0.005023831					
0.006	0.63171	0.005973173					
0.006	0.64174	0.006030679	0.006045834	100.7639066	0.641056667	0.009024424	1.407742051
0.006	0.64972	0.006133651					
0.007	0.73609	0.006976827					
0.007	0.74415	0.007031265	0.007063466	100.9066563	0.74519	0.00966207	1.296591496
0.007	0.75533	0.007182306					
0.008	0.84959	0.008068173					
0.008	0.84841	0.008049927	0.008115129	101.4391086	0.852856667	0.006705948	0.786292453
0.008	0.86057	0.008227286					
0.009	0.94736	0.009008269					
0.009	0.94662	0.009009477	0.009076316	100.8479518	0.951213333	0.007324379	0.77000386
0.009	0.95966	0.0092112					
0.01	1.0475	0.009971154					
0.01	1.0431	0.009952125	0.009798376	97.98376258	1.025503333	0.00311127	0.303389539
0.01	0.98591	0.00947185					

Figure C.1: Validation of UV-VIS spectrophotometer for ciprofloxacin in artificial urine.